

## INFORMATION TO USERS

This manuscript has been reproduced from the microfilm master. UMI films the text directly from the original or copy submitted. Thus, some thesis and dissertation copies are in typewriter face, while others may be from any type of computer printer.

**The quality of this reproduction is dependent upon the quality of the copy submitted.** Broken or indistinct print, colored or poor quality illustrations and photographs, print bleedthrough, substandard margins, and improper alignment can adversely affect reproduction.

In the unlikely event that the author did not send UMI a complete manuscript and there are missing pages, these will be noted. Also, if unauthorized copyright material had to be removed, a note will indicate the deletion.

Oversize materials (e.g., maps, drawings, charts) are reproduced by sectioning the original, beginning at the upper left-hand corner and continuing from left to right in equal sections with small overlaps.

ProQuest Information and Learning  
300 North Zeeb Road, Ann Arbor, MI 48106-1346 USA  
800-521-0600

**UMI<sup>®</sup>**

Vertical line on the left side of the page.

Vertical line on the right side of the page.

ELUCIDATION OF STEREOCHEMISTRY

BY N.M.R. SPECTROSCOPY

by

CÉSAR REYES ZAMORA

This thesis is submitted in partial fulfillment of the  
requirements for the degree of

DOCTOR OF PHILOSOPHY

at the

Department of Chemistry, University of Ottawa

SEPTEMBER 1968



César Reyes Zamora  
Candidate

---

R.R. Fraser  
Professor of Chemistry  
Research Director

UMI Number: DC52502

### INFORMATION TO USERS

The quality of this reproduction is dependent upon the quality of the copy submitted. Broken or indistinct print, colored or poor quality illustrations and photographs, print bleed-through, substandard margins, and improper alignment can adversely affect reproduction.

In the unlikely event that the author did not send a complete manuscript and there are missing pages, these will be noted. Also, if unauthorized copyright material had to be removed, a note will indicate the deletion.

**UMI<sup>®</sup>**

---

UMI Microform DC52502  
Copyright 2007 by ProQuest LLC  
All rights reserved. This microform edition is protected against  
unauthorized copying under Title 17, United States Code.

---

ProQuest LLC  
789 East Eisenhower Parkway  
P.O. Box 1346  
Ann Arbor, MI 48106-1346

PREFACE

Considerable confusion arose concerning the configuration and conformation of several 2,3-disubstituted 1,4-dioxanes mainly because of misinterpretation of their n.m.r. spectra. In this thesis, a detailed analysis of the spectra of five of these compounds is reported and the configuration and conformation of the compounds have been unambiguously determined.

Dr. R.R. Fraser and P. Hanbury found a difference in the value of the vicinal coupling constants  $J_{AX}$  and  $J_{BX}$  in the  $ABX_3$  absorption of the trifluoroethoxy group at the 2-position of tetrahydropyran. Two other trifluoroethoxy compounds were synthesized and their spectra analyzed in an attempt to determine the origin of this non-equivalence.

The Hammett relationship has been widely used to study the effect of substituents on the chemical shift of protons. In this work, we have studied the effect of substituents on the chemical shift of the methylene group in para-substituted benzyl phenyl sulfides, sulfoxides and sulfones.

ACKNOWLEDGEMENTS

The author wishes to thank Dr. R.R. Fraser who promoted the present investigation and guided the research and the University of Ottawa for the opportunity to engage in graduate studies.

The author also wishes to thank Mrs. J. Kirkwood for typing the thesis.

Special thanks are due to my colleagues and friends who made my stay here both memorable and pleasant.

TABLE OF CONTENTS

	<u>Page No.</u>
Preface	i
Acknowledgements	ii
Table of Contents	iii
List of Tables	vi
List of Figures	vii
Abstract	x

INTRODUCTION

1. Analysis of n.m.r. spectra	1
2. Classification of n.m.r. spectra	7
3. Solution of the eigenvalue problem and analysis of the n.m.r. spectra	9
4. Solution of the $A_2B_2$ type of spectra	11
5. Analysis of the $ABX_q$ type of spectra	21
6. Conformational analysis by n.m.r. spectroscopy	32
7. Magnetic non-equivalence	37
8. Correlation of chemical shifts with the electronic properties of the molecule	43
9. Studies applied to systems containing the sulfide, sulfoxide and sulfone groups	54

EXPERIMENTAL

1. Preparation of <u>cis</u> -2,3-Dichloro-1,4-dioxane	60
2. Preparation of <u>cis</u> -2,3-Diphenyl 1,4-dioxane	60

TABLE OF CONTENTS (continued)

	<u>Page No.</u>
3. Preparation of Naphthodioxane	60
4. Preparation of 4a,8a-Dimethoxy-4a,8a-dihydro-1,4-benzodioxan	62
5. Preparation of 4a,8a-Dimethoxy-4a,5,6,7,8,8a,hexahydro-1,4-benzodioxan	62
6. Preparation of 2,3-Dihydrofuran	62
7. Preparation of 2,2,2-Trifluoroethyl-2-Tetrahydrofuranyl ether	63
8. Preparation of tetrahydrothiapyran	63
9. Preparation of tetrahydrothiapyran-1-oxide	63
10. Preparation of 2,3-Dihydrothiapyran	64
11. Preparation of 2,2,2-Trifluoroethyl-2-tetrahydrothiapyranyl ether	64
12. Preparation of p-Aminobenzyl phenyl sulfide	65
13. Preparation of p-Aminobenzyl phenyl sulfoxides	65
14. Preparation of p-Aminobenzyl phenyl sulfone	66
15. Preparation of partially deuterated p-nitrobenzyl phenyl sulfoxide	66
16. Preparation of partially deuterated p-aminobenzyl phenyl sulfoxide	66

RESULTS AND DISCUSSION

1. Determination of the configuration and conformation of 2,3-Dichloro-1,4-dioxane, m.p. 52 <sup>o</sup>	69
2. Determination of the configuration and conformation of 2,3-Diphenyl-1,4-dioxane, m.p. 136 <sup>o</sup>	77

TABLE OF CONTENTS (continued)

	<u>Page No.</u>
3. Determination of the configuration and conformation of Naphthodioxane	82
4. Determination of the configuration and conformation of 4a,8a-Dimethoxy-4a-8a-dihydro-1,4-benzodioxan; and 4a,8a-Dimethoxy-4a,5,6,7,8a-hexahydro-1,4-benzodioxan	87
5. Study of the non-equivalence of $J_{AX}$ and $J_{BX}$ in 2-(2,2,2-trifluoroethoxy)-tetrahydropyran	94
6. Effects of substituents on the chemical shift of benzylic protons	109
CLAIMS FOR ORIGINAL WORK	122
BIBLIOGRAPHY	123

LIST OF TABLES

<u>Table No.</u>		<u>Page No.</u>
1.	Basic symmetry functions for two equivalent nuclei	5
2.	Basic functions and complete matrix of Hamiltonian $\mathcal{H}$ for four nuclei $A_2B_2$	16
3.	Explicit expression for energies and wave functions for four nuclei $A_2B_2$	17
4.	Energies and intensities of A transitions for four nuclei $A_2B_2$	18
5.	AB wave functions and energy levels for given X in $ABX_q$ systems	24
6.	Transition energies and intensities for two nuclei AB for given X in $ABX_q$ systems	27
7.	X-transitions ( $x \rightarrow x+1$ ) for $ABX_q$ systems with $F_z(AB)=0$	28
8.	Coupling Constants and chemical shifts obtained in the analysis of compounds containing the 1,4-dioxane system	73
9.	Coupling constants and chemical shifts in compounds with the $ABX_3$ absorption pattern	95
10.	Variation with temperature of the n.m.r. parameters of 2(2,2,2-trifluoroethoxy)-tetrahydropyran	100
11.	Rho values of substituent chemical shift-Hammett plots for a series of compounds containing the p-substituted benzyl group	112
12.	Tau values for the methylene protons in para-substituted benzyl phenyl sulfoxides	117
13.	Variation of the $\rho$ value with the solvent of the methylene group in 6-substituted phthalides	119

LIST OF FIGURES

<u>Figure No.</u>		<u>Page No.</u>
1.	Classification of some typical molecules	8
2.	Some typical $A_2B_2$ type of molecules	13
3.	Schematic form of A spectrum with $J \gg J' > 0, J_B \gg J_A > 0.$	19
4.	Term diagram and calculated spectrum for the system ABX	30
5.	The chair form of <u>trans</u> -2,3-dichloro-1,4- dioxane showing the four protons whose coupling constants have been determined	35
6.	Three stable conformations in 1,1,1,2-tetra- substituted ethane	40
7.	Three stable conformations in substituted benzyl phenyl sulfoxide	58
8.	The low field half of the $-OCH_2CH_2O-$ absorption of compound II: (a) the experimental spectrum; (b) the calculated spectrum	72
9.	The four considered representations for 2,3- dichloro-1,4-dioxane, m.p. $52^\circ$	75
10.	The chair form of 1,3-dioxane showing the four protons whose coupling constants have been determined.	76
11.	The partial n.m.r. spectrum of <u>trans</u> -2,3-diphenyl- 1,4-dioxane (III) measured in $CDCl_3$	79
12.	The partial n.m.r. spectrum of <u>cis</u> -2,3-diphenyl- 1,4-dioxane (IV) measured in $CDCl_3$	80
13.	The n.m.r. spectrum of Naphthodioxane (V) measured in $CDCl_3$	83
14.	Chair-chair conformations for Naphthodioxane (V)	85

LIST OF FIGURES (continued)

<u>Figure No.</u>		<u>Page No.</u>
15.	The temperature dependence of $A_2B_2$ absorption pattern in the n.m.r. spectrum of naphthodioxane	86
16.	The n.m.r. spectrum of 4a,8a-dimethoxy-4a,8a-dihydro-1,4-benzodioxan (VII)	89
17.	(a) The possible conformation for <u>trans</u> -4a,8a-dimethoxy-4a,8a-dihydro-1,4-benzodioxan (b) The possible conformations for <u>cis</u> -4a,8a-dimethoxy-4a,8a-dihydro-1,4-benzodioxan	90
18.	The low-field half of the $OCH_2CH_2O$ absorption of compound VII: (a) the experimental spectrum; (b) the spectrum calculated from the parameters of assignment A; and (c) the spectrum calculated from the parameters of assignment B	92
19.	The most favorable conformation of 2(2,2,2-trifluoroethoxy)-tetrahydropyran	98
20.	The n.m.r. spectrum of 2,2,2-trifluoroethyl-2-tetrahydrofuranylether (X)	102
21.	The n.m.r. spectrum of 2,2,2-trifluoroethyl-2-tetrahydrothiapyranylether (XI)	103
22.	The n.m.r. spectrum of the diastereomeric methylene protons in 2,2,2-trifluoroethyl-2-tetrahydrofuranylether (X); (a) experimental; (b) calculated	104
23.	The n.m.r. spectrum of the diastereomeric methylene protons in 2,2,2-trifluoroethyl-2-tetrahydrothiapyranylether (XI); (a) experimental; (b) calculated	105
24.	Example of the splittings resulting from coupling of an $ABX_3$ group	106

LIST OF FIGURES (continued)

<u>Figure No.</u>		<u>Page No.</u>
25.	The n.m.r. spectrum of p-nitrobenzyl phenyl sulfoxide	110
26.	(a) Non-irradiated and irradiated n.m.r. spectra of the methylene group in the partially deuterated p-nitrobenzyl phenyl sulfoxide.	
	(b) Non-irradiated and irradiated n.m.r. spectra of the methylene group in the partially deuterated p-aminobenzyl phenyl sulfoxide	113
27.	A Hammett plot of the benzylic proton shifts of <u>para</u> -substituted benzyl phenyl sulfoxides	115

ABSTRACT

The analysis of the n.m.r. spectra of a series of substituted 1,4-dioxanes showed the following configurations and conformations for the compounds: 2,3-dichloro-1,4-dioxane m.p. 52°, 2,3-diphenyl-1,4-dioxane m.p. 132° and naphtodioxane have the cis configuration and at room temperature are rapidly interconverting between chair conformations; 4a,8a-dimethoxy-4a,8a-dihydro-1,4-benzodioxan and 4a,8a-dimethoxy-4a,5,6,7,8,8a-hexahydro-1,4-benzodioxan have the trans configuration with a rigid chair conformation.

Non-equivalence in the vicinal coupling constants  $J_{AX}$  and  $J_{BX}$  were found for 2,2,2-trifluoroethyl-2-tetrahydrofuranylether and 2,2,2-trifluoroethyl-2-tetrahydrofuranylether and 2,2,2-trifluoroethyl-2-tetrahydrothiapyranylether as found previously for 2,2,2-trifluoroethyl-2-tetrahydropyranylether by Dr. R.R. Fraser and P. Hanbury. No definite conclusion regarding the origin of this non-equivalence could be drawn from the results.

Linear Hammett plots were obtained in a study of the effect of substituents on the chemical shift of the methylene protons in para-substituted benzyl phenyl sulfides, sulfoxides and sulfones. It has been found that the protons in the methylene group are affected very differently by the substituent in each series.

The causes for this variation have been examined and it is proposed that the effect is conformational. In the conformation in which a C-H bond is parallel to the adjacent p-orbital of the benzene ring, that C-H proton will experience the maximum substituent effect.

## INTRODUCTION

### 1. Analysis of n.m.r. spectra.

Nuclear magnetic resonance arises as a result of transitions between the energy levels of a nuclear magnetic dipole in a static magnetic field. These transitions occur between discrete energy levels. The observation of nuclear magnetic resonance requires the presence of an external alternating magnetic field of suitable frequency to induce the transitions between the states.

When nuclear magnetic resonance signals were first observed, it was found that this "nuclear Zeeman effect" could be explained by the simple equation:

$$h \nu_0 = \frac{g \mu H_0}{I} \quad (1)$$

where:

$h$  = Planck's constant

$\nu_0$  = the resonance or Larmor frequency

$g$  = the nuclear  $g$  factor

$\mu$  = the magnetic moment of the nucleus

$I$  = the nuclear spin

$H_0$  = the strength of the external magnetic field.

With better resolution it became possible to recognize differences in the shielding of the external magnetic field by the electrons of atoms of identical species in different chemical environments.

In this way, the  $i$ th nucleus does not "see"  $H_0$  but  $H_i$  given by:

$$H_i = H_0 (1 - \sigma_i) \quad (2)$$

where  $\sigma_i$  is the dimensionless nuclear shielding parameter.

Later, it was found that the signals in high resolution n.m.r. are accompanied by a fine structure that arises from interactions between magnetically active nuclei in molecules. This fine structure is of extreme importance in determining the structure of molecules and gives valuable information concerning bond angles, hybridization of atoms and other characteristics of bonds in molecules.

A complete description of the spectrum, therefore, requires the introduction of a spin Hamiltonian operator, which is given by

$$\mathcal{H} = -\hbar \sum_i \gamma_i H_i I_{zi} + h \sum_{i < j} J_{ij} I_i \cdot I_j \quad (3)$$

In the first term of the above equation, which yields the chemical shift,  $\gamma_i$  is the magnetogyric ratio of nucleus  $i$ ,  $H_i = H_0(1 - \sigma)$ , and  $I_{zi}$  is the component of  $I_i$  along  $H_0$ . The second term, in which  $J_{ij}$  is the coupling constant between nuclei  $i$  and  $j$  (in c.p.s.), describes the spin-spin interaction. This form of the Hamiltonian is justified ultimately by its success in accounting in detail for the numbers, positions, and intensities of resonance lines in high resolution n.m.r. spectra.

If the system contains  $p$  nuclei (of spin  $1/2$ ), there will be a total of  $2^p$  possible spin states. The simplest set of functions describing this many-spin system would be the  $2^p$  basic product functions

such as:

$$\psi_n = \alpha(1) \beta(2) \alpha(3) \dots \alpha(p) \quad (4)$$

where  $\alpha(1)$  and  $\beta(2)$  denote the fact that nuclei 1 and 2 are in spin states corresponding to  $m=1/2$  and  $m=-1/2$  respectively.

Matrix elements of the Hamiltonian  $\mathcal{H}$  (equation 3) between the various possible spin wave functions are calculated, and the energy eigenvalues  $E_n$  are obtained by solution of the secular equation

$$| H_{mn} - E \delta_{mn} | = 0 \quad (5)$$

$\delta_{mn}$  is the delta function and is unity for  $m=n$  and zero for  $m \neq n$ . The eigenfunctions for the problem are then taken as linear combinations of the basis functions,

$$\phi_q = \sum_m a_{qm} \psi_m \quad (6)$$

values of  $a_{qm}$  are obtained from the solution of the set of linear equations

$$\sum_m H_{mn} a_{qm} = E_q a_{qm} \quad (7)$$

and the normalization condition

$$\sum_m a_{qm}^* a_{qm} = 1 \quad (8)$$

The secular equation 5 is of order  $2^p$  but it can be factorized into a number of equations of lower order if we classify the basic functions  $\psi_n = \alpha(1) \beta(2) \dots \alpha(p)$  according to the expectation value of the total spin component in the z direction

$$F_z = \sum_i I_z(i) \quad (9)$$

All the product functions  $\psi_n$  are eigenfunctions of this operator, that is, each corresponds to a definite value of  $F_z$ .

Further factorization of the secular equation can be carried out if more than one species of nuclei are involved (i.e. of different elements) or if the chemical shifts are large relative to the coupling constants.

If the nuclear species are X, Y, ... , the total spin component  $F_z$  is made up from contributions from each type:

$$F_z = F_z(X) + F_z(Y) + \dots \quad (10)$$

The basic product functions are eigenfunctions of  $F_z(X)$ ,  $F_z(Y)$ , ... and to a good approximation mixing occurs only between product functions which correspond to the same values of each of  $F_z(X)$ ,  $F_z(Y)$  .... (1)

The secular equation 5 can be further factorized by use of the symmetry properties of the molecule we are studying. This is based on the fact that the energy of the system does not change by an interchange of the nuclei in an equivalent set. In a symmetrical molecule, equivalent nuclei are those which can be interchanged by the application of symmetry operations such as rotations and reflections.

The set of basic product functions 4 could form an irreducible representation of the symmetry transformation of the nuclear assembly. However, these basic product functions will not always belong to irreducible representation of the symmetry group. For example, in a set of two equivalent nuclei, the symmetry operation which interchanges them will transform the product function  $\alpha(1) \beta(2)$  into  $\beta(1) \alpha(2)$ . It is possible, however, to construct a new set of basic functions which do belong to irreducible representation by taking certain linear combination of the simple products as 6. The condition 8 should also be fulfilled.

Table 1 lists the set of basic symmetry functions for the set of two nuclei; s and a stand for symmetrical and antisymmetrical. The suffix corresponds to the value of  $F_z$ .

Table 1		
SPIN FUNCTION	SPIN COMPONENT $F_z$	DESIGNATION
$\alpha \alpha$	1	$S_1$
$(\alpha\beta + \beta\alpha) / \sqrt{2}$	0	$S_0$
$(\alpha\beta - \beta\alpha) / \sqrt{2}$	0	$a_0$
$\beta\beta$	-1	$S_{-1}$

Table 1. Basic symmetry functions for two equivalent nuclei.

The factorization of the secular equation arises because there are no matrix elements of the Hamiltonian belonging to different irreducible representations.

The difference between the different energy levels  $E_n$  calculated from the equation 5 after factorization will give us the energy associated with the transition. The line with a frequency  $\nu_{mn}$  for a transition from the state  $\phi_m$  of energy  $E_m$  to the state  $\phi_n$  with energy  $E_n$  is given by the Bohr frequency condition

$$\nu_{mn} = (E_m - E_n) / h \quad (11)$$

The intensity of the transition between states m and n is proportional to

$$| \langle \phi_m | \sum_i \gamma_i I_x(i) | \phi_n \rangle |^2 \quad (12)$$

where  $I_x$  is the component of I along the x-axis.

An important selection rule is that transitions can occur only between states for which

$$\Delta F_z = \pm 1 \quad (13)$$

The x-component of the nuclear moment  $\gamma_i I_x(i)$  is also a totally symmetric operator with respect to permutations, so it will have no matrix elements between functions of different symmetry. As a result, transitions between states of different symmetry will be forbidden. This important selection rule leads to a considerable reduction in the number of lines observed in the spectrum of a symmetrical molecule (2-3).

2. Classification of n.m.r. spectra.

It is usual and convenient to divide nuclear magnetic resonance spectra into types according to the classification of Bernstein, Pople and Schneider (4).

The first nucleus, i.e. that with the highest spin coupling, is always denoted by A and the other nuclei by a subsequent letter from the beginning of the alphabet (B....) if  $J_{AB}$  is comparable in magnitude to  $\nu_0 \delta_{AB}$ . A letter from the middle of the alphabet (K....) is used when  $J_{AK}$  is approximately one order of magnitude smaller than  $\nu_0 \delta_{AK}$ . A letter from the end of the alphabet (X....) is used if  $J_{AX}$  is two or more orders of magnitude smaller than  $\nu_0 \delta_{AX}$ . Fig. 1 shows various examples.

In the case of  $A_2B_2$  systems, it should be noted that notations such as  $A'_2B'_2$  or  $AA'BB'$  are also used in order to indicate that the nuclei are not magnetically equivalent. However, the usual notations  $A_2B_2$  and  $A_2X_2$  will be used in the present work. There is no danger of confusion, since there are very few systems of the  $A_2B_2$  type with magnetically equivalent nuclei. Two rare examples are cyclopropene and difluoromethane which may be denoted by  $A_2^*B_2^*$  or  $A_2^*X_2^*$  (5).

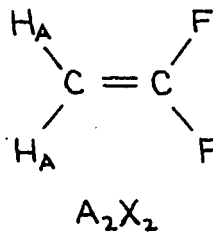
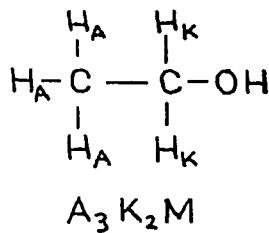
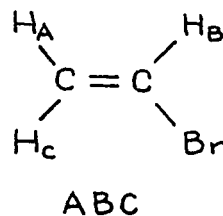
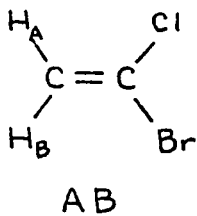
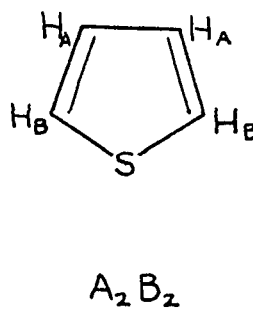
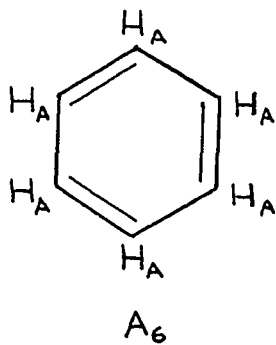
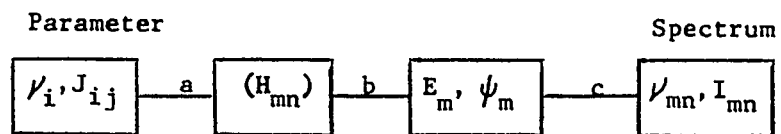


Figure 1 - Classifications of some typical molecules.

3. Solution of the eigenvalue problem and analysis of the n.m.r. spectra.

The entire calculations of nuclear magnetic resonance spectra have been programmed for electronic computers. The course of the calculation is shown in the following scheme (6),



where the step a denotes the calculation of the complete energy matrix,  $H_{mn}$  being equal to  $\psi_m \mathcal{H} \psi_n$ ; step b denotes reduction to the diagonal form by solution of the eigenvalue problem and step c denotes calculation of the frequencies and intensities of the allowed transitions.

The values of the parameters  $\nu_i$  and  $J_{ij}$  are inserted in the Hamiltonian operator (equation 3). The desired eigenvalues  $E_m$  and eigenfunctions  $\psi_m$  that satisfy equation 5 must then be calculated in the usual manner by means of secular equations, i.e. the energy matrix  $H_{mn}$  is calculated with a set of starting functions and brought into the diagonal form by a unitary transformation. The diagonal elements are then the desired eigenvalues, and the transformation matrix consists of the eigenvectors that link the eigenfunctions with the starting functions.

In the analysis of an experimental spectrum, one determines the numerical values of the chemical shifts  $\nu_0 \delta_{i,j}$  and the spin coupling constants  $J_{ij}$  from the observed position of the lines in the spectrum.

As a way to check these parameters, one calculates the theoretical spectrum corresponding to this given set of parameters. The above scheme should now be followed from right to left. This is possible for steps a and c, but there is no simple solution for the inversion of step b. Various methods have been devised for the solution of this problem in the analysis of complex spectra. Dischler in a recent paper reviews some of the methods and compares them using  $A_2B_2$  types of spectra. (6)

In the analysis of the n.m.r. spectra after classification of the spectrum into one of the types defined in section 2, a trial assignment of the lines with the corresponding theoretical transitions is done. From this assignment, an estimate of the coupling constants and chemical shifts is made. An approximate value of these parameters can also be obtained from a search in the literature for structurally similar compounds whose analyses have been previously carried out. These approximate values are then used in the computer calculation of the theoretical spectra as mentioned before.

If a trial and error method is employed, the same calculation is repeated using different values for the parameters until good agreement is obtained between the experimental and calculated spectra. The same calculation can also be made using an iteration method. The agreement was of the order of 0.2 c.p.s. in our work.

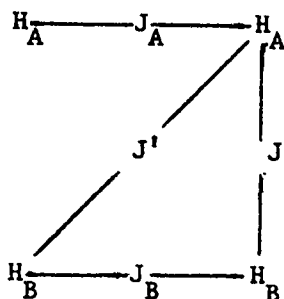
In order to confirm the results of the analysis, the spectrum can also be taken at a higher magnetic field and in this way by a change in the chemical shift, the position of the transition lines are also changed. The theoretical calculations are then repeated using the same value for the coupling constants but changing the value for the chemical shifts. A similar change can often be obtained by a change in solvent.

Other experimental techniques used as aids in the analysis of spectra are isotopic substitution and double irradiation (3).

#### 4. Solution of the $A_2B_2$ Type of Spectra.

A system containing four magnetically non-equivalent nuclei forming two different pairs of symmetrically equivalent nuclei separated from each other by a chemical shift which is of the same order of magnitude as the coupling constants involved is described as an  $A_2B_2$  system. If the two pairs are of different species, or have a large chemical shift, this would be referred to as  $A_2X_2$ . Many examples of this system have been investigated and they include disubstituted aromatic compounds, thiophene, furan, monosubstituted piridines, 1,2-disubstituted ethanes and disubstituted cyclohexadienes as indicated in Fig. 2.

In general, there are four different coupling constants as shown:



For the solution of the secular equation, it is convenient to define new quantities:

$$K = J_A + J_B$$

$$L = J - J'$$

$$M = J_A - J_B$$

$$N = J + J'$$

The basic functions will be chosen as symmetry functions which are either symmetrical (s) or antisymmetrical (a) with respect to reflection in the plane of symmetry.

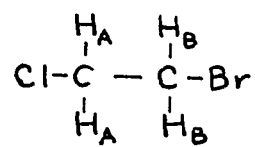
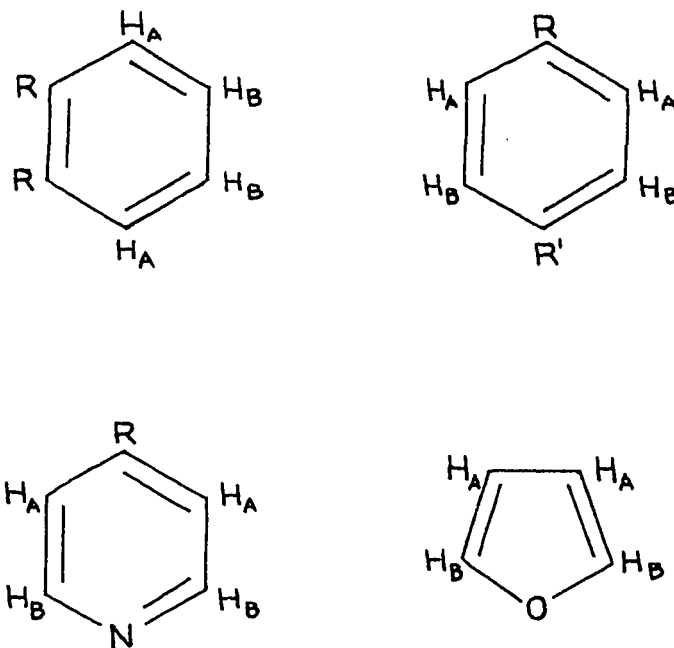


Figure 2 - Some typical A<sub>2</sub>B<sub>2</sub> type molecules.

The appropriate matrix elements of the Hamiltonian are presented in Table 2. The 16 x 16 matrix representing the Hamiltonian for the system can be factorized into two 1x1, five 2x2 and one 4x4 submatrices. Although one can calculate the roots of the five 2x2 secular determinants and express them in explicit algebraic form, the 4x4 sub-determinant cannot be solved in this way. Therefore, the only explicit expressions for the eigenvalues and eigenfunctions for the system are those shown on Table 3(1).

A consequence of this is that one cannot have explicit expressions for six of the allowed transitions and their relative intensities are not available.

Table 4 lists the transitions frequencies and relative intensities for all the other transitions. Altogether, there are 28 transitions, four of them being combination transitions corresponding to the change of spin of three or four nuclei simultaneously. This type of transition is always weak and can be neglected. Moreover, the A region of the spectrum will always be a mirror image of the B part and consequently only the twelve A transitions need be considered (1).

There are certain general trends in the  $A_2B_2$  type of spectra that should be considered before attempting the detailed analysis.

From the matrix elements in Table 2, one can see that substitution of  $-L$  for  $L$  does not alter the secular equation and substitution of  $-M$  for  $M$  simply interchanges the labeling of energy levels in the antisymmetric set, so the spectrum does not provide information on the signs of  $L$  and  $M$ . Similarly, changing  $K$  to  $-K$  simply shifts by a constant amount all the antisymmetric energy levels, and the associated transitions ( 9 to 12 in Table 4 ) among these levels are not altered. On the other hand, both  $N$  and  $K$  appear in the  $4 \times 4$  matrix ( $s_0$  functions in Table 2) such that replacement of either  $N$  by  $-N$  or  $K$  by  $-K$  displaces these symmetric levels and affects the appearance of the  $A_2B_2$  spectra in the same way for either sign change. It is for these reasons that the  $A_2B_2$  spectrum is sensitive to the relative signs of  $K$  and  $N$ , but not of either  $M$  or  $L$  with respect to  $K$  and  $N$ . Because of this, even though an  $A_2B_2$  spectrum can be analyzed completely to give the absolute values of  $K, N, L$  and  $M$  and the sign of  $K$  relative to  $N$ , from which  $J_A$ ,  $J_B$  and  $J$  and  $J'$  and the three relative signs of the four constants can be obtained,  $J_A$  still cannot be differentiated from  $J_B$  nor  $J$  from  $J'$ , this is in spite of the fact that the relative magnitudes and signs of the  $J$ 's do affect the appearance of the spectrum as discussed by Gutowsky and co-workers (7-8).

In practice, the correct assignments of the coupling constants including relative signs, can often be made by comparison with coupling constants obtained from the spectra of similarly substituted compounds for which the assignments are unambiguous.

Table 2. Basic Functions and Complete Matrix of Hamiltonian for Four Nuclei A,B,2,2.

Function	A	B	Diagonal matrix elements *	Off-diagonal matrix elements
s <sub>2</sub>	$\alpha\alpha$	$\alpha\alpha$	$\nu_A + \nu_B + \frac{1}{2}N$	
1s <sub>1</sub> 2s <sub>1</sub>	$2^{-\frac{1}{2}}(\alpha\beta + \beta\alpha)$ $\alpha\alpha$	$2^{-\frac{1}{2}}(\alpha\beta + \beta\alpha)$	$\nu_B$ $\nu_A$	$(1s_1   \mathcal{H}   2s_1) = \frac{1}{2}N$
1s <sub>0</sub> 2s <sub>0</sub> 3s <sub>0</sub> 4s <sub>0</sub>	$\beta\beta$ $\alpha\alpha$ $2^{-\frac{1}{2}}(\alpha\beta - \beta\alpha)$ $2^{-\frac{1}{2}}(\alpha\beta + \beta\alpha)$	$\alpha\alpha$ $\beta\beta$ $2^{-\frac{1}{2}}(\alpha\beta - \beta\alpha)$ $2^{-\frac{1}{2}}(\alpha\beta + \beta\alpha)$	$-\nu_A + \nu_B - \frac{1}{2}N$ $\nu_A - \nu_B - \frac{1}{2}N$ $-\frac{1}{2}K$ 0	$(1s_0   \mathcal{H}   2s_0) = 0$ ( $2s_0   \mathcal{H}   3s_0$ ) = $\frac{1}{2}L$ $(1s_0   \mathcal{H}   3s_0) = \frac{1}{2}L$ ( $2s_0   \mathcal{H}   4s_0$ ) = $\frac{1}{2}N$ $(1s_0   \mathcal{H}   4s_0) = \frac{1}{2}N$ ( $3s_0   \mathcal{H}   4s_0$ ) = $-\frac{1}{2}L$
1s <sub>-1</sub> 2s <sub>-1</sub>	$2^{-\frac{1}{2}}(\alpha\beta + \beta\alpha)$ $\beta\beta$	$2^{-\frac{1}{2}}(\alpha\beta + \beta\alpha)$	$-\nu_B$ $-\nu_A$	$(1s_{-1}   \mathcal{H}   2s_{-1}) = \frac{1}{2}N$
s <sub>-2</sub>	$\beta\beta$	$\beta\beta$	$-\nu_A - \nu_B + \frac{1}{2}N$	
1a <sub>1</sub> 2a <sub>1</sub>	$2^{-\frac{1}{2}}(\alpha\beta - \beta\alpha)$ $\alpha\alpha$	$2^{-\frac{1}{2}}(\alpha\beta - \beta\alpha)$	$\nu_B - \frac{1}{2}K - \frac{1}{2}N$ $\nu_A$	$(1a_1   \mathcal{H}   2a_1) = -\frac{1}{2}L$
1a <sub>0</sub> 2a <sub>0</sub>	$2^{-\frac{1}{2}}(\alpha\beta + \beta\alpha)$ $2^{-\frac{1}{2}}(\alpha\beta - \beta\alpha)$	$2^{-\frac{1}{2}}(\alpha\beta - \beta\alpha)$ $2^{-\frac{1}{2}}(\alpha\beta + \beta\alpha)$	$-\frac{1}{2}K + \frac{1}{2}M$ $-\frac{1}{2}K - \frac{1}{2}M$	$(1a_0   \mathcal{H}   2a_0) = -\frac{1}{2}L$
1a <sub>-1</sub> 2a <sub>-1</sub>	$2^{-\frac{1}{2}}(\alpha\beta - \beta\alpha)$ $\beta\beta$	$2^{-\frac{1}{2}}(\alpha\beta - \beta\alpha)$	$-\nu_B - \frac{1}{2}K - \frac{1}{2}M$ $-\nu_A$	$(1a_{-1}   \mathcal{H}   2a_{-1}) = -\frac{1}{2}L$

\* For convenience,  $\frac{1}{2}K$  is subtracted from all diagonal matrix elements. This makes no difference in calculating transition energies.

Table 3. Explicit Expression for Energies and Wave Functions for Four Nuclei  $A_2B_2$ .

State	Energy	Wave function
$s_2$	$V_A + V_B + \frac{1}{2}N$	$s_2$
$1s_1$	$\frac{1}{2}(V_A + V_B) - \frac{1}{2}[(\nu_0\delta)^2 + N^2]^{\frac{1}{2}}$	$(1s_1) \cos \phi - (2s_1) \sin \phi$
$2s_1$	$\frac{1}{2}(V_A + V_B) + \frac{1}{2}[(\nu_0\delta)^2 + N^2]^{\frac{1}{2}}$	$(1s_1) \sin \phi + (2s_1) \cos \phi$
$1s_{-1}$	$-\frac{1}{2}(V_A + V_B) + \frac{1}{2}[(\nu_0\delta)^2 + N^2]^{\frac{1}{2}}$	$(1s_{-1}) \cos \phi + (2s_{-1}) \sin \phi$
$2s_{-1}$	$-\frac{1}{2}(V_A + V_B) - \frac{1}{2}[(\nu_0\delta)^2 + N^2]^{\frac{1}{2}}$	$-(1s_{-1}) \sin \phi + (2s_{-1}) \cos \phi$
$s_{-2}$	$-(V_A + V_B) + \frac{1}{2}N$	$s_{-2}$
$1a_1$	$\frac{1}{2}(V_A + V_B) - \frac{1}{2}K - \frac{1}{2}[(\nu_0\delta + M)^2 + L^2]^{\frac{1}{2}}$	$(1a_1) \cos \psi_+ + (2a_1) \sin \psi_+$
$2a_1$	$\frac{1}{2}(V_A + V_B) - \frac{1}{2}K + \frac{1}{2}[(\nu_0\delta + M)^2 + L^2]^{\frac{1}{2}}$	$-(1a_1) \sin \psi_+ + (2a_1) \cos \psi_+$
$1a_0$	$-\frac{1}{2}K + \frac{1}{2}(M^2 + L^2)^{\frac{1}{2}}$	$(1a_0) \cos \theta_a - (2a_0) \sin \theta_a$
$2a_0$	$-\frac{1}{2}K - \frac{1}{2}(M^2 + L^2)^{\frac{1}{2}}$	$(1a_0) \sin \theta_a + (2a_0) \cos \theta_a$
$1a_{-1}$	$-\frac{1}{2}(V_A + V_B) - \frac{1}{2}K + \frac{1}{2}[(\nu_0\delta - M)^2 + L^2]^{\frac{1}{2}}$	$(1a_{-1}) \cos \psi_- - (2a_{-1}) \sin \psi_-$
$2a_{-1}$	$-\frac{1}{2}(V_A + V_B) - \frac{1}{2}K - \frac{1}{2}[(\nu_0\delta - M)^2 + L^2]^{\frac{1}{2}}$	$(1a_{-1}) \sin \psi_- + (2a_{-1}) \cos \psi_-$

Table 4. Energies and Intensities of A Transitions for Four Nuclei  $A_2B_2$ .

Transition	Energy relative to $\frac{1}{2}(\nu_A + \nu_B)$	Intensity
1. $1s'_1 \rightarrow s_2$	$\frac{1}{2}N + \frac{1}{2}[(\nu_0\delta)^2 + N^2]^{\frac{1}{2}}$	$1 - \sin 2\phi$
2. $1s'_0 \rightarrow 1s_1$	$-\frac{1}{2}N + \frac{1}{2}[(\nu_0\delta)^2 + N^2]^{\frac{1}{2}}$	$1 + \sin 2\phi$
3. $s_{-2} \rightarrow 1s'_1$		
4. $1s'_{-1} \rightarrow 2s'_0$		
5. $3s'_0 \rightarrow 2s'_1$		
6. $2s'_{-1} \rightarrow 4s'_0$		
7. $4s'_0 \rightarrow 2s'_1$		
8. $2s'_{-1} \rightarrow 3s'_0$		
9. $2a'_0 \rightarrow 2a'_1$	$\frac{1}{2}[(\nu_0\delta + M)^2 + L^2]^{\frac{1}{2}} + \frac{1}{2}(M^2 + L^2)^{\frac{1}{2}}$	$\sin^2(\theta_a - \psi_+)$
10. $2a'_{-1} \rightarrow 1a'_0$	$\frac{1}{2}[(\nu_0\delta - M)^2 + L^2]^{\frac{1}{2}} + \frac{1}{2}(M^2 + L^2)^{\frac{1}{2}}$	$\cos^2(\theta_a + \psi_-)$
11. $1a'_0 \rightarrow 2a'_1$	$\frac{1}{2}[(\nu_0\delta + M)^2 + L^2]^{\frac{1}{2}} - \frac{1}{2}(M^2 + L^2)^{\frac{1}{2}}$	$\cos^2(\theta_a - \psi_+)$
12. $2a'_{-1} \rightarrow 2a'_0$	$\frac{1}{2}[(\nu_0\delta - M)^2 + L^2]^{\frac{1}{2}} - \frac{1}{2}(M^2 + L^2)^{\frac{1}{2}}$	$\sin^2(\theta_a + \psi_-)$

The complex relationship between the form of an  $A_2B_2$  spectrum and the chemical shift and coupling constant parameters makes the analysis of a spectrum of this type very difficult. Because of this several methods of analysis have been adopted.

Several approximations can be made to simplify the solution of the secular equation and the assignment of the lines. For example, one important class of  $A_2B_2$  spectra occurs in molecules where the four nuclei are so arranged that one of the pairs is more strongly coupled than another as is the case in ortho disubstituted benzenes. In this system, it probably holds that  $J \gg J' > 0$  and  $J_B \gg J_A \geq 0$ . The numbering of transitions for the A portion of the spectrum is shown in Figure 3.

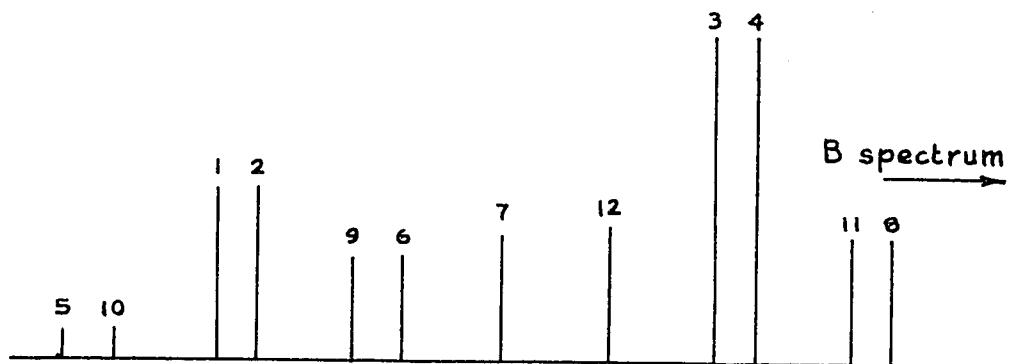


Figure 3. Schematic form of A spectrum with

$$J \gg J' > 0, J_B \gg J_A > 0.$$

As the chemical shift decreases, this spectrum becomes modified in a characteristic manner. The part which is closest to the B spectrum increases further in intensity at the expense of the outer components. In fact, the signals 5 and 10 may become so weak that they are practically unobservable.

The pairs of transitions 1,2 and 3,4 increase their separations as do transitions 9,6 and 7,12. It is possible for the bands of the outermost pair of transitions 11,8 to overlap the corresponding B part of the spectrum, but the more intense bands for transitions 3,4 never cross the bands for the corresponding B transitions (9).

In the analysis of the spectrum of the type shown in Fig. 3, one can assign the intense transitions 1,2 and 3,4 fairly easily. Lines 1 and 3 can then be manipulated to find the chemical shift of the A nucleus and the parameter  $N = J_A + J_B$

$$N = \nu_1 - \nu_3$$
$$\{(\nu_0 \delta)^2 + N^2\}^{\frac{1}{2}} = \nu_1 + \nu_3$$

and lines 9 and 11 can be used to find two of the other parameters,

$$(M^2 + L^2)^{\frac{1}{2}} = \nu_9 - \nu_{11}$$
$$\{(\nu_0 \delta + M)^2 + L^2\}^{\frac{1}{2}} = \nu_9 + \nu_{11}$$

A value of K can be obtained from transitions 6 and 7 by an indirect process involving trial and error fitting or by means of the Dischler rule (10).

If values for K, L, M and N are known, then the complete set of spectral parameters for the molecule can be found.

### 5. Analysis of the ABX<sub>q</sub> Type of Spectra.

This system corresponds to the case in which only two of the total q+2 nuclei are strongly coupled compared with their chemical shift, the others being well separated from each other.

Complete analysis of different types of ABX<sub>q</sub> spectra for q=1,2,3 have been carried out by different authors (4,11-14). Pople and Schaeffer have considered also the more general case ABR<sub>p</sub>X<sub>q</sub> where p and q are any small integers (15).

The spin Hamiltonian (in cycles per second) for an ABX<sub>q</sub> can be written

$$\mathcal{H} = \nu_A I_z(A) + \nu_B I_z(B) + \nu_X F_z(X) + J_{AB} I(A) \cdot I(B) + \\ + F(X) \cdot [J_{AX} I(A) + J_{BX} I(B)]$$

where  $\nu_A$ ,  $\nu_B$  and  $\nu_X$ , the Larmor precession frequencies of A, B and X nuclei are:

$$\begin{aligned} \nu_A &= \gamma \mathbb{H}_0 (1 - \sigma_A) / 2\pi \\ \nu_B &= \gamma \mathbb{H}_0 (1 - \sigma_X) / 2\pi \\ \nu_X &= \gamma \mathbb{H}_0 (1 - \sigma_X) / 2\pi \end{aligned}$$

and  $H_0$  is the applied static field.

$F(X)$  has been written for the total spin of all the X-nuclei

$$F(X) = \sum_{i=1}^q I(X_i)$$

The fact that all X nuclei have the same coupling constants and the same chemical shift means that only the total X spin is significant. The spectrum is independent of  $J_{XX}$  which can be made equal to zero.

The total component in the z-direction,

$$F_z = I_z(A) + I_z(B) + F_z(X)$$

is a good quantum number, that is, there is no mixing between spin functions with different values of  $F_z$ . The X-spin component plays an important part in the theory and for convenience is written as x (15).

The Hamiltonian can be written then

$$\begin{aligned} \mathcal{H} = & \left[ \nu_A + xJ_{AX} \right] I_z(A) + \left[ \nu_B + xJ_{BX} \right] I_z(B) + \\ & + x \nu_X + J_{AB} I(A) \cdot I(B) \end{aligned}$$

This Hamiltonian depends now on the X nuclei only through the z-component of the X spin. This has important consequences in simplifying the spectrum, for the point of view of the A and B nuclei, coupling with the X nuclei is merely equivalent to the experience of

an additional magnetic field in the z-direction and leads to new 'effective Larmor frequencies' depending on x

$$\nu_A^*(x) = \nu_A + x J_{AX}$$

$$\nu_B^*(x) = \nu_B + x J_{BX}$$

The Hamiltonian can now be solved for the AB spin functions for a given x. This differs from the theory of an isolated AB pair only by replacing the Larmor frequencies  $\nu_A$  and  $\nu_B$  by the 'effective frequencies'  $\nu_A^*$  and  $\nu_B^*$ , so that there are four functions and energies, as given in Table 5 (15).

The quantities  $\theta_x$  and  $C_x$  in Table 5 are both functions of the X spin component x and are given by

$$C_x \cos 2\theta_x = \frac{1}{2} (\nu_A^* - \nu_B^*)$$

$$C_x \sin 2\theta_x = \frac{1}{2} J_{AB}$$

so that

$$C_x = +\frac{1}{2} \left\{ (\nu_A^* - \nu_B^*)^2 + J_{AB}^2 \right\}^{\frac{1}{2}}$$

Table 5

	WAVE FUNCTION	ENERGY
1 <sub>x</sub>	$\alpha \alpha$	$\frac{1}{2} \nu_A^*(x) + \frac{1}{2} \nu_B^*(x) + x \nu_X + \frac{1}{2} J_{AB}$
2 <sub>x</sub>	$(\alpha\beta) \cos \theta_x + (\beta\alpha) \sin \theta_x$	$C_x + x \nu_X - \frac{1}{2} J_{AB}$
3 <sub>x</sub>	$-(\alpha\beta) \sin \theta_x + (\beta\alpha) \cos \theta_x$	$- C_x + x \nu_X - \frac{1}{2} J_{AB}$
4 <sub>x</sub>	$\beta \beta$	$-\frac{1}{2} \nu_A^*(x) - \frac{1}{2} \nu_B^*(x) + x \nu_X + \frac{1}{2} J_{AB}$

Table 5. AB wave functions and energy levels for given x in ABX<sub>q</sub> systems.

$$C_x = +\frac{1}{2} \left\{ \left[ (\nu_A - \nu_B) + x(J_{AX} - J_{BX}) \right]^2 + J_{AB}^2 \right\}^{\frac{1}{2}}$$

For each value of  $x$ , there is only one set of AB functions, but for each value of  $x$ , there may be several corresponding X functions. Thus, if there are two X-nuclei ( $q=2$ ), there is only one X-function corresponding to  $x=1$  or  $x=-1$  ( $\alpha\alpha$  or  $\beta\beta$ ), but there are two functions  $(\alpha\beta + \beta\alpha)/\sqrt{2}$  and  $(\alpha\beta - \beta\alpha)/\sqrt{2}$  for  $x=0$ .

Turning now to selection rules and the spectra that will actually be observed, one can consider AB and X transitions in turn. For the AB pair of nuclei, the selection rule is  $\Delta F_z(AB) = \pm 1$ ,  $x = 0$ . Since  $x$  is the only way in which X nuclei appear in the Hamiltonian, all AB transitions take place without any change in the spin arrangement of the X-nuclei. This means that the AB part of an  $ABX_q$  spectrum consists of a number of simple AB spectra for each possible value of  $x$ . The relative intensity of each such AB sub-spectrum will be determined by the number of X states associated with the corresponding value of  $x$ , and it will be written  $n_q(x)$ . For  $ABX_3$  spectrum, for example, there will be 1,3,3,1 functions for  $x = 3/2, 1/2, -1/2$  and  $-3/2$ . In general,

$$n_q(x) = \frac{q!}{(\frac{1}{2}q - x)! (\frac{1}{2}q + x)!}$$

The transition energies and intensities for each AB sub-spectrum are now easily obtained and are given in Table 6.

The X transitions are treated in a similar way. The selection rules are now  $\Delta x = \pm 1$ ,  $F_z(AB) = 0$  so that in any x-transition the total z-component of the AB spin is unchanged. But this can only take the values +1, 0 and -1. If  $F_z(AB) = +1$ , the AB wave function must be  $\alpha\alpha$  before and after the transition, so that the z-spin component of the X-nuclei is changed by  $\pm 1$  in the presence of the  $\alpha\alpha$  configuration of A and B. The A and B nuclei again give an effective field at the X nuclei and the energy of the transition is clearly  $\nu_X + 1/2 (J_{AX} + J_{BX})$ . Similarly if  $F_z(AB) = -1$ , the only AB configuration is  $\beta\beta$  and the corresponding X transitions have energies  $\nu_X - 1/2 (J_{AX} + J_{BX})$ . This accounts for half of the possible AB states, so that half of the intensity of the X-spectrum will be concentrated in a simple doublet with separation equal to  $(J_{AX} + J_{BX})$ . These will be the strongest pair of lines in the X spectrum and are usually picked out quite easily (15).

The remaining X transitions occur with zero resultant z-spin in the AB set ( $F_z(AB)=0$ ) and are rather more complicated since the mixing of AB functions themselves is a function of x and is changed by the transition. Table 5 shows that there will be four transitions in which x changes to x + 1, the energies and intensities of which are given in Table 7.

Table 6

TRANSITION	ENERGY	RELATIVE INTENSITY
$3_x \rightarrow 1_x$	$\frac{1}{2} \nu_A^* (x) + \frac{1}{2} \nu_B^* (x) + C_x + \frac{1}{2} J_{AB}$	$n_q(x) \{1 - \sin 2\theta_x\}$
$4_x \rightarrow 2_x$	$\frac{1}{2} \nu_A^* (x) + \frac{1}{2} \nu_B^* (x) + C_x - \frac{1}{2} J_{AB}$	$n_q(x) \{1 + \sin 2\theta_x\}$
$2_x \rightarrow 1_x$	$\frac{1}{2} \nu_A^* (x) + \frac{1}{2} \nu_B^* (n) - C_x + \frac{1}{2} J_{AB}$	$n_q(x) \{1 + \sin 2\theta_x\}$
$4_x \rightarrow 3_x$	$\frac{1}{2} \nu_A^* (x) + \frac{1}{2} \nu_B^* (x) - C_x - \frac{1}{2} J_{AB}$	$n_q(x) \{1 - \sin 2\theta_x\}$

Table 6. Transition energies and intensities for two nuclei AB for given x in ABX<sub>q</sub> systems.

Table 7

TRANSITION	ENERGY	RELATIVE INTENSITY
$3_x \rightarrow 2_x + 1$	$\nu_X + C_{x+1} + C_x$	$n_q(x \rightarrow x + 1) \sin^2 [\theta_{x+1} - \theta_x]$
$2_x \rightarrow 2_x + 1$	$\nu_X + C_{x+1} - C_x$	$n_q(x \rightarrow x + 1) \cos^2 [\theta_{x+1} - \theta_x]$
$3_x \rightarrow 3_x + 1$	$\nu_X - C_{x+1} + C_x$	$n_q(x \rightarrow x + 1) \cos^2 [\theta_{x+1} - \theta_x]$
$2_x \rightarrow 3_x + 1$	$\nu_X - C_{x+1} - C_x$	$n_q(x \rightarrow x + 1) \sin^2 [\theta_{x+1} - \theta_x]$

Table 7. X-transitions ( $x \rightarrow x+1$ ) for ABX<sub>q</sub> systems with

$$F_z(AB) = 0.$$

Apart from the factor due to the mixing of AB functions, the intensity is also proportional to the number of X transitions in which the z-component of the spin changes from  $x$  to  $x + 1$  (in the absence of the AB system) which we shall write  $N_q(x \rightarrow x + 1)$ . For  $ABX_3$ , for example, there are three transitions corresponding to  $-3/2, -1/2$  ( $\beta\beta\beta \rightarrow \alpha\beta\beta, \beta\beta\beta \rightarrow \beta\alpha\beta, \beta\beta\beta \rightarrow \beta\beta\alpha$ ) six corresponding to  $-1/2 \rightarrow +1/2$  ( $\alpha\beta\beta \rightarrow \alpha\beta\alpha, \alpha\beta\beta \rightarrow \alpha\alpha\beta, \beta\alpha\beta \rightarrow \beta\alpha\alpha, \beta\alpha\beta \rightarrow \alpha\alpha\beta, \beta\beta\alpha \rightarrow \beta\alpha\alpha, \beta\beta\alpha \rightarrow \alpha\beta\alpha$ ) and three corresponding to  $+1/2 \rightarrow +3/2$  ( $\beta\alpha\alpha \rightarrow \alpha\alpha\alpha, \alpha\beta\alpha \rightarrow \alpha\alpha\alpha, \alpha\alpha\beta \rightarrow \alpha\alpha\alpha$ ). In general,

$$N_q(x \rightarrow x + 1) = \frac{q!}{(1/2 q + x)! (1/2 q - x - 1)!}$$

All the above discussion can be exemplified by the analysis of a simple spectrum of the ABX type. In Fig. 4, a term diagram and a calculated spectrum for the system is shown. In the figure, transitions 1-4 occur when there is no change in the spin states of the X nuclei and transitions 5-10 when there is no change in the spin states of the AB nuclei. The 'effective Larmor frequencies' depend on the coupling constants with the X nucleus in the following manner:

Subgroup  $x = +1/2$

$$\nu_A^I = \nu_A^*(\frac{1}{2}) = \nu_A + \frac{1}{2} J_{AX}; \nu_B^I = \nu_B^*(\frac{1}{2}) = \nu_B + \frac{1}{2} J_{BX}$$

Subgroup  $x = -1/2$

$$\nu_A^{II} = \nu_A^*(\frac{1}{2}) = \nu_A - \frac{1}{2} J_{AX}; \nu_B^{II} = \nu_B^*(\frac{1}{2}) = \nu_B - \frac{1}{2} J_{BX}$$

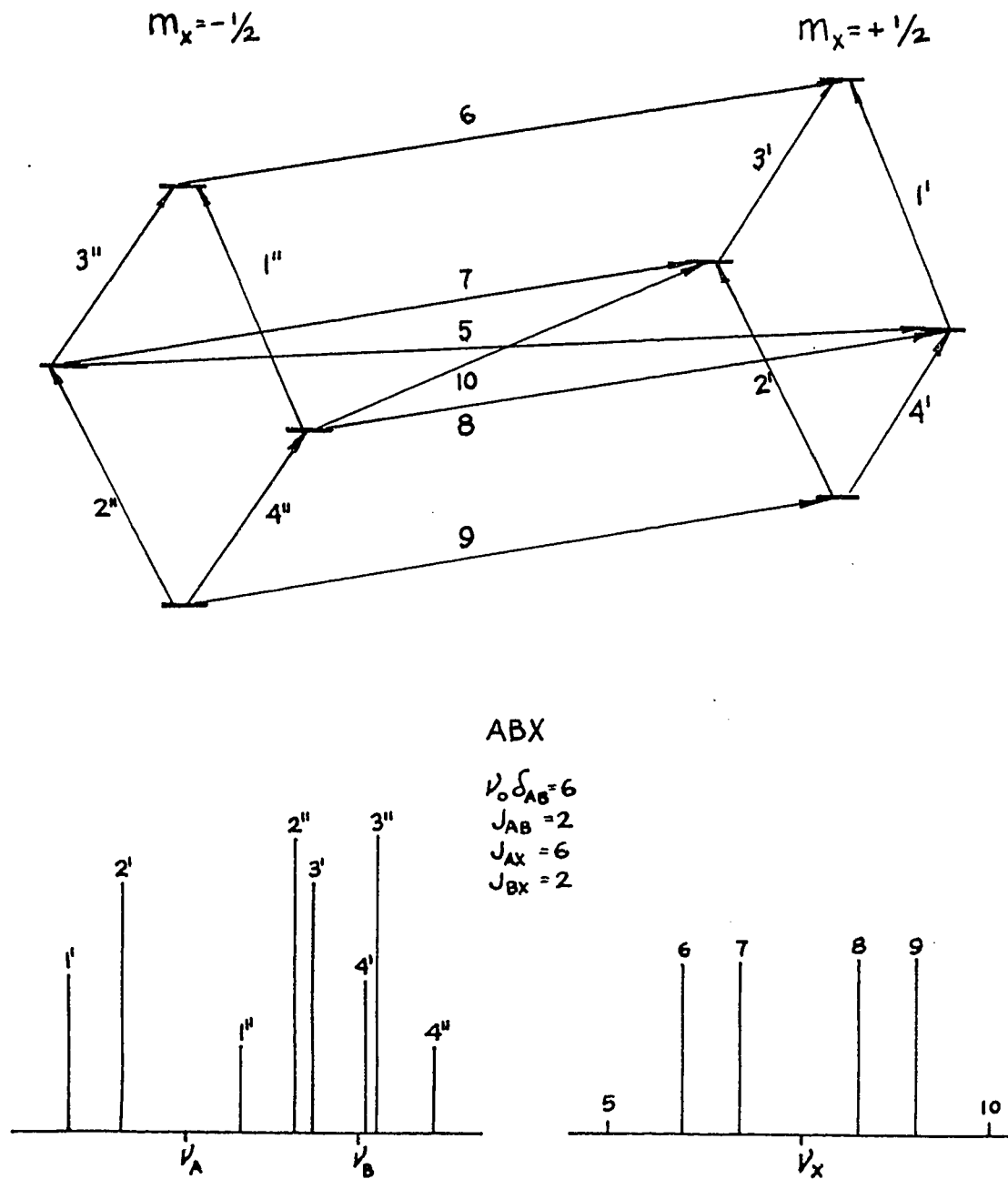


Figure 4. Term diagram and calculated spectrum for the system ABX.

In the analysis of the ABX spectrum, all the parameters can be found from the two AB subspectra. The defining equations are:

$$|J_{AB}| = f_1' - f_2' = f_3' - f_4' = f_1'' - f_2'' = f_3'' - f_4''$$

$$\Delta\nu_{AB} = \frac{1}{2} (D' + D'')$$

$$J_{AX} = f_o' - f_o'' + \frac{1}{2}(D' - D'')$$

$$J_{BX} = f_o' - f_o'' - \frac{1}{2}(D' - D'')$$

The symbols used have the following meanings:

$$D' = \nu_A' - \nu_B' = + \sqrt{(f_1' - f_4')(f_2' - f_3')}$$

$$D'' = \nu_A'' - \nu_B'' = + \sqrt{(f_1'' - f_4'')(f_2'' - f_3'')}$$

$$f_o' = \frac{1}{2} (\nu_A' + \nu_B') = \frac{1}{2}(f_1' + f_4') = \frac{1}{2}(f_2' + f_3')$$

$$f_o'' = \frac{1}{2} (\nu_A'' + \nu_B'') = \frac{1}{2}(f_1'' + f_4'') = \frac{1}{2}(f_2'' + f_3'')$$

The resonance lines of the X nucleus permit the calculation of two additional quantities:

$$J_{AX} + J_{BX} = f_6 - f_9$$

$$J_{AX} - J_{BX} = \frac{1}{2 \Delta\nu_{AB}} (f_5 - f_{10})(f_7 - f_8)$$

Whereas the spectrum is affected only by the magnitude of the coupling parameter  $J_{AB}$ , the relative signs of  $J_{AX}$  and  $J_{BX}$  affect the frequencies and intensities throughout the spectrum (6).

6. Conformational analysis by nuclear magnetic resonance spectroscopy.

In a flexible molecule, individual groups of atoms can take up different positions in relation to each other. The different arrangements of the atoms in the molecule are known as the conformations of the molecule. In most cases, only a very small amount of energy is required in order to move a flexible molecule from one conformation to another and for this reason, very often one is dealing with a mixture in which many conformations may be in equilibrium with each other. For example, cyclohexane possesses two favorable conformations which corresponds to the two chair forms. These two forms can interconvert, but a relatively high energy (about 11 kcal/mole) is required to overcome the torsional rigidity and also to change the bond angles in passing through the intermediate states. During the interconversion, cyclohexane passes through an energy minimum (of about 5.0 kcal/mole) known as the twist (or skew) form which is, however, above the energy level of the two chair forms. Smaller energy maxima (about 5.5 kcal/mole) above the twist form correspond to the boat forms of the molecule. At room temperature, the thermal energy is high enough to overcome the energy barrier for the interconversion which occurs with a high frequency, but at low temperatures the interconversion of the two forms is almost completely prevented (16).

Two types of protons can be distinguished in cyclohexane. Six are perpendicular to the plane of the ring (axial) and six are more or less parallel to it (equatorial). When one conformation changes into the other, these protons exchange their positions. When, by some means, the conformation of the cyclohexane molecule is fixed, one can distinguish in the n.m.r. spectrum the two types of protons absorbing at different fields. In substituted cyclohexanes, if the substituent is much more electronegative than the methylene group, the diamagnetic shielding of the proton on  $C_1$  will be decreased, and its signal will appear at lower field. For this reason, the  $\alpha$  proton signals are particularly useful in conformational analysis.

Using n.m.r. spectroscopy, one can resort to several methods for the determination of conformations. These different methods have been recently summarized (17).

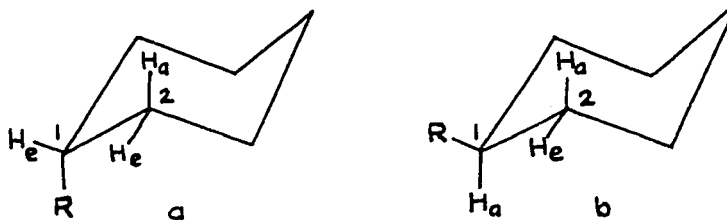
In our work, the method of average coupling constants has been used. This method is based on the Karplus relation

$$J_{AB} = C_1 + C_2 \cos \varphi + C_3 \cos 2\varphi$$

in which  $J_{AB}$  is the vicinal coupling constant between the AB protons,  $C_1$ ,  $C_2$  and  $C_3$  are constants and  $\varphi$  is the dihedral angle between the planes, formed by the  $H_A$  and  $H_B$  protons and the C-C bond (18,19).

The constants  $C_1$ ,  $C_2$  and  $C_3$  depend on the system under consideration. The coupling constants also vary with the electronegativity of the substituent and with the size of the ring in cyclic olefins (20-26).

The value of the vicinal coupling constant will be maximum when the dihedral angle  $\varphi$  is  $180^\circ$  or when  $J_{AB} = J_{\text{axial-axial}}$  and will have a lower value when  $\varphi$  is  $60^\circ$  or  $J_{AB} = J_{\text{axial-equat.}}$  or  $J_{\text{equat-equat.}}$ . This is found to be the case in all compounds studied. The theory also requires  $J_{ae} = J_{ea} = J_{ee}$  since the dihedral angle is  $60^\circ$  in each instances. However, this expectation is not fulfilled. Many experimental measurements have shown that it is not possible to equate  $J_{ea}$  either with  $J_{ae}$  or  $J_{ee}$  (27-29). For instance, it has been found that in the systems:



$J_{e1-a2}$  in a is, in general, lower than  $J_{a1e2}$  in b. One example of this case is reported by Bhacca and William on the coupling constants of a number of hydroxy and acetoxy steroids. The cis coupling constant  $J_{e1-a2}$  (values 2.5-3.2 c.p.s.) with the substituent in the equatorial position (Fig.b).

Other examples are found in the isomeric 4-tert-butyl-cyclohexanols and derived acetates of Anet (27), and in the isomeric 3,5-di-tert-butylcyclohexanols and 2,5-dialkylcyclohexanols of Feltkamp and Franklin (30, 31).

One explanation for this phenomenon is the assumption of a ring deformation by the introduction of an axial substituent (31).

Whenever  $J_{ee}$  or  $J_{ea}$  can be measured, the electronegative group is in the axial position, and owing to the non-bonding interactions with the neighboring protons, the ring is deformed. This deformation is only slight when the electronegative group is in the equatorial position. The angles corresponding to  $J_{ae}$ ,  $J_{ea}$  and  $J_{ee}$  are, therefore, different.

In contrast, Booth (32) has noted that in  $J_{ea}$  the electronegative substituent is coplanar with one of the protons which participates in the coupling. He suggested this as the reason for  $J_{ea}$  being smaller than  $J_{ae}$  without discussing the possible reasons for this difference.

Support for Booth's explanation is provided by the analysis of the n.m.r. spectrum of trans-2,3-dichloro-1,4-dioxane (Fig.5).

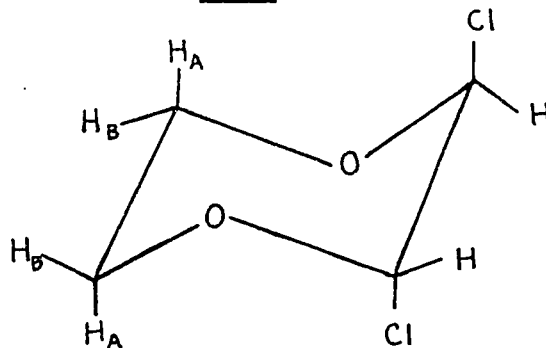


Figure 5. The chair form of trans-2,3-dichloro-1,4-dioxane showing the four protons whose coupling constants have been determined.

Jung (33) has found that  $J_A^{vic} = 12.37$ ,  $J_B^{vic} = .59$  and  $J_{AB}^{vic} = 3.28$  c.p.s. Altona and Romers (34) investigated the structure of the compound by X-ray analysis and found that the angles O-C<sub>5</sub>-C<sub>6</sub> and C<sub>5</sub>-C<sub>6</sub>-O were equal to 111.2° and that the bond length C<sub>5</sub>-C<sub>6</sub> was 1.50Å° not very different from the normal values (109.60 and 1.55Å°). The large differences between the coupling constants  $J_B^{vic}$  and  $J_{AB}^{vic}$  cannot be properly explained by distortions in the ring. However, considering Booth's arguments, both H<sub>B</sub> protons have a trans co-planar arrangement with the ring oxygens and, therefore, the value of  $J_B^{vic}$  should be low. In  $J_{AB}^{vic}$ , there is only one proton involved in this arrangement, and therefore, its value should be closer to the expected value of 3.1 c.p.s. according to the Karplus relationship.

In the mobile cyclohexane system, it is possible to determine the position of the conformational equilibrium from the average coupling constants if the coupling constants are known in equations

$$J_{aa}^{ee} = xJ_{aa} + (1-x)J_{ee}$$

$$J^{ea} = xJ_{ae} + (1-x)J_{ea}$$

The coupling constants  $J_{aa}$ ,  $J_{ee}$ ,  $J_{ae}$  and  $J_{ea}$  should be known beforehand. They can be estimated from previously studied model compounds whose structures are similar to the one that is being studied. Alternatively, data can be obtained from low temperature studies of model molecules in a frozen conformation, or from molecules which possess a bulky "anchoring" group.

#### 7. Magnetic non-equivalence.

By definition, two nuclei are magnetically non-equivalent when they have different chemical shifts and/or they are coupled to different extents with other nuclei in the molecule. Nuclei that are chemically non-equivalent are generally magnetically non-equivalent. Exceptions do exist, for example, the two hydrogens in the amide group which have different spatial environment. In this example, magnetic non-equivalence exists only if rapid re-orientation about the C-N bond is absent. Nuclei which interchange their position in a molecule upon the application of a

symmetry operation are symmetrically equivalent, but they are not of necessity magnetically equivalent as in 1,1-difluoroethylene. Here the molecule has two pairs of symmetrically equivalent nuclei, but neither pair is magnetically equivalent because  $J_{HF}^{cis} \neq J_{HF}^{trans}$ . However, in 1,1-difluoroallene, both pairs of nuclei are magnetically equivalent because the two nuclei in each pair have the same chemical shift; each hydrogen nucleus couples to each of the fluorine nuclei to the same extent.

Conversely, nuclei which are chemically equivalent are generally magnetically equivalent. The common, but erroneous, supposition that two protons on a  $CH_2$  group are always chemically equivalent led to a great deal of surprise amongst chemists when magnetic non-equivalence of geminal nuclei was first reported by Finegold. Since then, magnetic non-equivalence of geminal nuclei has been reported in a vast number of molecules (35-40). From these data, one has observed that magnetic non-equivalence frequently occurs in, but is not restricted to the  $R-CH_2-C^*-R'R''R'''$  type of molecule.

First of all, the asterisked carbon need not be asymmetric in the usual sense. If one of the R-stroke groups is  $R-CH_2-$ , the methylene hydrogens may be still magnetically non-equivalent and the geminal pair need not be bonded directly to the source of asymmetry, but may be separated from it by a group such as  $-COO-$ ,  $-CH_2-$ , or  $-O-$ . Other structural sources of asymmetry such as sulfoxides, phosphines, biphenyl etc. also give rise to non-equivalence of geminal nuclei.

Two basic types of potential asymmetry have been recognized as the cause of non-equivalence. They are 1) conformational and 2) intrinsic. Gutowsky (41) has suggested that one possible way to show the contribution of "intrinsic asymmetry" to magnetic non-equivalence is to measure the non-equivalence at room temperature where interconversion of the different conformers is rapid but conformers are unequally populated and at higher temperatures where the conformers will approach equal distribution.

The non-equivalence should decrease with an increase in temperature until equal population of rotamers is achieved. At this temperature, the non-equivalence would be a measure of the intrinsic asymmetry contribution to the non-equivalence. Gutowsky (41) thus obtained a value of 6.7 c.p.s. for the intrinsic asymmetry contribution to the non-equivalence for  $\text{CF}_2\text{Br-CFBrCl}$ .

Raban (42) has measured the contribution of intrinsic asymmetry to non-equivalence in the same molecule using a low temperature method, and found a value of 5 c.p.s. At low temperature, the individual spectra of each rotamer shown in Fig. 6 can be observed. We can see from the figure that the environment of  $\text{H}_A$  in the first conformer is very similar to that of  $\text{H}_B$  in the third, and the same occurs that the environment of  $\text{H}_B$  in the first conformer is very similar to the environment of  $\text{H}_A$  in the second and  $\text{H}_B$  in the second is similar to  $\text{H}_A$  in the third.

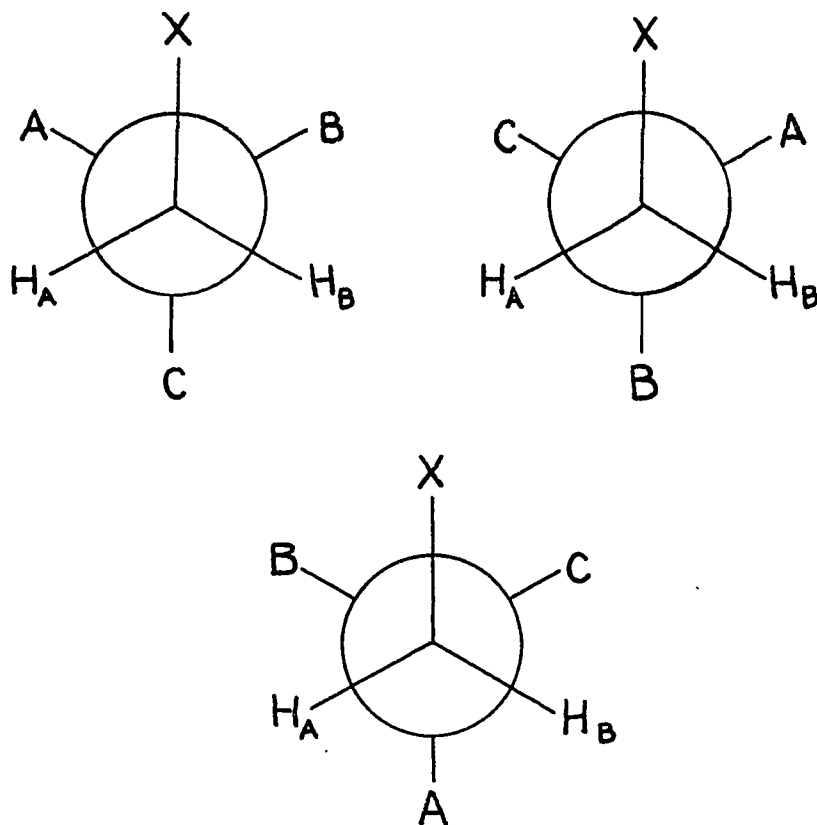


Figure 6. Three stable conformations in 1,1,1,2-tetra-substituted ethane.

It would then seem that, under conditions of rapid rotation and equal population, the chemical shifts of  $H_A$  and  $H_B$  would average to approximately the same value. This would mean that the intrinsic asymmetry contribution should be near zero. The values measured by Gutowsky and Raban would seem to support this reasoning. However, Raban has calculated a value of 55 c.p.s. for the intrinsic asymmetry non-equivalence in  $CF_2Br-CHBrCl$ . Raban further points out that the value of  $CF_2Br=CFBrCl$  is near zero because of fortuitous cancellation of large terms of opposite signs.

These results then indicate that two nuclei such as the ones in Fig. 6 which appear to have similar environments can still have very different chemical shifts, and thus in some cases, the intrinsic asymmetry contribution to the non-equivalence can be substantial.

Although intrinsic asymmetry has been shown to be important in the above cases, the careful studies made by Roberts and co-workers (43) clearly show that non-equivalence is due primarily to conformational preferences in compounds of the general formula  $Ph-CH_2-O-CHR'R''$ . These authors found that the most important single factor in determining the magnitude of the chemical shift difference was the conformation of the methylene group with respect to the directly bonded phenyl ring.

The biggest non-equivalence occurred when the preferred conformation was such that one methylene proton was situated in the plane of the phenyl ring and the second one was appreciably out of this plane. The magnetic anisotropy of the phenyl ring was held responsible for the major contribution to magnetic non-equivalence.

In a series of homologous ethers, they also showed that the magnitude of the chemical shift difference depends upon the distance between the diastereotopic nuclei and the center of asymmetry. The chemical shift difference usually decreases as the distance is increased. However, a sudden increase in the chemical shift occurred when two non-equivalent methyl groups were five bonds removed from the center of asymmetry. When the number of bonds was increased further, the non-equivalence decreased to zero. This observation would indicate that a six-membered ring conformation of the isopropyl group with respect to the asymmetric center may be populated to a significant extent, in accordance with the Newman "rule of six" (44).

Magnetic non-equivalence is also solvent and temperature dependent. It has been related to the changes in population of the different conformers with a change in the dielectric constant of the solvent or a change in temperature. However, similar changes with solvents have been observed also in olefins (45) where no conformational changes are possible. It would then seem likely that magnetic properties of solvents may produce chemical shift changes which may override those caused by differences in rotational equilibria.

8. Correlation of chemical shifts with the electronic properties of the molecule.

Although it is generally accepted that the chemical shift is dependent on the electronic properties of the molecule, there does not seem to be any general agreement as to the exact nature of this dependence.

Several factors have been proposed that can influence the shielding of a hydrogen nucleus in a molecule. Attempts have been made to relate shieldings to specific substituent properties such as electronegativity or dipole moment, as well as to correlate them with more general expressions like the Hammett  $\sigma$  constant of the substituent which reflects its ability to affect the electronic density at one particular site of the molecule (46-49).

In the absence of effects from bulk diamagnetic susceptibility and intermolecular interactions, the main factors to consider in the shielding of an hydrogen nucleus are: a) intramolecular electric field effects; b) inductive or conjugative properties of the substituent; c) neighbouring magnetic anisotropic effects; and d) Van der Waal's interactions.

In the case of hydrogen nuclei in alkanes, Dailey and Cavanaugh (48) have suggested an additional deshielding factor referred to as the "C-C bond shift". It is not considered to be a C-C bond anisotropic effect.

The origin is somewhat obscure, but it has been suggested that when a C-C bond replaces a C-H bond there could be an appreciable change in the electronic excitation energy, which increases the paramagnetic contribution to the shielding (3).

One point one should make clear here is that the above factors to consider in the shielding of an hydrogen nucleus are so much interrelated and intermingled that one cannot establish a clear line of separation between one factor and the other.

a) Intramolecular electric field effects.

This is the effect arising from an electric field created by the presence of a permanent dipole moment in the molecule, like a C-X bond and is not being transmitted by inductive or resonance effects in the chemical sense.

The effect of an electric field arising from a permanent dipole in the molecule on a particular proton is given by the relation:

$$E = \frac{\mu(1 + 3 \cos^2 \theta)^{\frac{1}{2}}}{r^3}$$

where  $\mu$  is the electric dipole moment giving rise to the field (usually considered to be that of the C-X group),  $r$  is the distance between the locus of the dipole and the proton, and  $\theta$  is the angle between  $r$  and  $\mu$ . The component along the C-H bond  $E_z$  is given by

$$E_z = E \cos \varphi$$

where  $\varphi$  is the angle between the vector  $E$  and the C-C bond.

Buckingham (51) has shown that the change in the proton screening constant of an X-H bond subjected to an electrical field E is approximately given by:

$$\Delta\sigma_E = -2 \times 10^{-12} E_z - 10^{-18} E^2$$

A field along the X-H bond draws the electrons in the enriched region between the nuclei away from the proton, thereby causing its resonance to occur at lower magnetic field strengths, while a field in the H-X direction leads to resonance at higher fields.

Buckingham also found that the electric field produced by the polarization of neighboring solvent molecules may also be important and lead to a solvent shift related to the dielectric constant of the solvent. Musher (52) has proposed a relationship slightly different from the one by Buckingham:

$$\sigma_E = -2.19 \times 10^{-12} E_z - 7.3 \times 10^{-19} E^2$$

b) Inductive or conjugative properties of the system.

This effect involves the diamagnetic shielding of the nucleus by the electron cloud in which it resides. Neighboring electro-negative groups or groups with free electron pairs will influence the electron cloud via inductive or resonance effects through the bonds and thus cause variations in this term.

c) Neighbour magnetic anisotropic effect.

This effect arises when a nucleus is near to a magnetically anisotropic center in the molecule. Such a center can be formed by a neighboring atom, group or bond having different values for the transverse ( $\chi_T$ ) and longitudinal ( $\chi_L$ ) components of its magnetic susceptibility tensor, (e.g. aromatic rings, C=O, -C≡C- and C-X bonds). Whether the hydrogen nucleus is shielded or deshielded depends on the relative values of the susceptibility components of the adjacent system and on the molecular geometry.

The neighbour magnetic anisotropic effect is expressed by a relation due to McConnell (53),

$$\sigma_M = \sum_g \left[ \frac{\Delta\chi_g (1 - 3\cos^2 \theta_g)}{3r_g^3} \right]$$

where  $\Delta\chi_g$  is the anisotropy in the magnetic susceptibility of the gth bond,  $r_g$  is the distance between the proton and that bond, and  $\theta_g$  is the angle between  $r_g$  and the bond axis.

d) Van der Waals forces.

These arise from a steric interaction in the equilibrium configuration of the substituent with the nearby proton. This causes a distortion in the electron cloud of the hydrogen (as the electrons are attracted by the nuclei of the substituent group) and causes a low field shift of the proton signal (54).

The above two factors b) and c) have been successfully employed to account for a vast amount of chemical shift data, yet they have not always proved adequate (49,55-57).

Numerous papers have appeared trying to relate the chemical shift to specific properties of the substituent in the molecule such as electronegativity (20,22,50,58-60). The Hammett  $\sigma$  constants and their variations have been widely used for explaining the chemical shifts variations with substituents on an aromatic ring. In general, excellent linear correlations have been found between both proton and fluorine chemical shifts and  $\sigma$ . The Hammett  $\sigma$  constants are mainly associated with the inductive and conjugative effects, although there is no general agreement as to which factors are affecting the chemical shift.

For example, since Hammett constants are obtained from meta and para-substituted benzoic acids, they should, therefore, not be strictly applicable to monosubstituted derivatives in which a linear correlation exists (62, 63). Furthermore, Hammett constants are derived from thermodynamic or kinetic data and would be expected to be related to the change in electron distribution on conversion of A to B or to some transition state complex rather than that in the unperturbed ground-state molecule. It should also be considered that contributions to the shielding of hydrogen and carbon nuclei need not necessarily have their origin in the electron density around the nuclei. For example, diamagnetic anisotropies and paramagnetic contributions are possible and these will not show a correlation with chemical reactivity parameters.

The studies of the effect of substituents on the chemical shifts of hydrogens have been mainly concerned with atoms attached directly to aromatic rings. It has been only recently, that the work has been extended to consider the substituents effects on the chemical shifts of hydrogens in the side chain of aromatic systems.

Jackman (64) reported the chemical shifts of some para substituted toluenes, and stated that only the more powerful electron-withdrawing substituents significantly alter the resonance frequency of the methyl group.

Williamson and co-workers (65) found a linear correlation between the Hammett constant and the  $\alpha$  (methylene) and  $\beta$  (methyl) protons in ethyl benzenes and in the  $\alpha$  (methyne) and  $\beta$  (methylene) protons in para-substituted phenylhexachloro bicyclo [2.2.1.] heptene. The  $\rho$  value for the  $\alpha$  protons in both systems was the same (-0.22). The value for the  $\beta$  protons was also the same in both systems (-0.11). The change in the  $\rho$  value going from the  $\alpha$  to the  $\beta$  protons indicates, as expected, that the effect of substituent decreases as the number of intervening bonds increases. The fact that the values for the  $\alpha$  and  $\beta$  protons in the two systems are the same shows that the ability of the substituent to donate and withdraw electrons from these groups is the same in both the freely rotating ethylbenzenes and the rigid protons of the bicyclic system.

In their studies of a series of aromatic aldehydes, Klinck and Stothers (66) found a rough correlation between the chemical shift of the formyl proton and the corresponding Hammett  $\sigma$  constant.

Paterson and Tipman (56), studying some p-substituted phenols, found that the hydroxyl proton chemical shift at infinite dilution in carbon tetrachloride was almost independent of the ring substituent. However, when the studies were done in dimethyl sulfoxide, a linear correlation was found between the chemical shift of the phenolic hydroxyl within  $\sigma^-$ . In this case, because of solvent interaction, (no concentration dependence was observed), the range of hydroxyl resonances was much larger (161.4 c.p.s.) than the one observed in dilution work in carbon tetrachloride (4.8 c.p.s.) (67). Heathcock (68) in studying a much larger series of p-substituted anisoles, found a reasonable good correlation between the methyl resonance and the corresponding Hammett  $\sigma$  constant.

Cook and Danyluk (57) have found that the acetylenic proton chemical shifts for a series of para-substituted phenyl acetylenes give a good linear correlation with a combination of inductive and resonance  $\sigma$  constants.

More recently, Wittstruck and Trachenberg (49) from a study of a series of meta and para-substituted styrenes, ethylbenzenes, dihydrocinnamic acids and cis and trans cinnamic acids concluded that variations in their chemical shifts are caused mainly by inductive and resonance effects rather than by electric and magnetic field effects.

Data on the chemical shifts of the trans and cis cinnamic acids, when compared with ethyl benzene and styrenes, reveals that the trans cinnamic acids show marked conjugation when substituted with electron releasing groups, and that the side chains in the cis-compounds are sufficiently twisted out of coplanarity with the phenyl ring as to markedly dampen conjugation. In the dihydro-cinnamic acids, the electronic effects can be effectively transmitted from the phenyl ring to the  $\beta$ -carbonyl group through the solvent.

Gurudata, Stothers and Talman (69) studied the effect of substituents on the chemical shifts of the vinyl protons of some substituted styrenes. They found good correlation between the Hammett  $\sigma$  constant and the  $\alpha$  and  $\beta$  protons chemical shifts, in meta and para substituted compounds. Linear correlations were also found when the chemical shifts for the two  $\beta$  protons were plotted against the  $^{13}\text{C}$  chemical shifts of the  $\beta$  carbon atom. The best correlation was with the  $\beta$  proton trans to the phenyl ring. No correlation appeared to be between the  $\alpha$  proton and the  $\alpha$  carbon shieldings.

Dewar and co-workers (73) in a series of papers have published their work on the elucidation of the mechanisms involved in the transmission of electronic effects.

According to them, the main contributions to the effect of substituents in aromatic systems are the field and resonance effects. The field effect of a substituent attached at atom  $i$  on a side chain attached at atom  $j$  is given approximately by  $F/r_{ij}$ ,  $F$  being a measure of the field set up by the substituent and  $r_{ij}$  the distance between atoms  $i$  and  $j$ . Since the authors assumed the  $\sigma$ -inductive effect to be unimportant, and also considered only cases where there is no mutual conjugation between the substituent and the reaction center, the only factors to consider were the  $\pi$ -inductive and resonance effects. These two effects vary in approximately the same way with the orientation of a given substituent, the net effect being given approximately by one of the expressions:  $Mq_{ij}$  or  $-M\pi_{ij}$ , where  $\pi_{ij}$  is the atom-atom polarizability of atoms  $i$  and  $j$ ,  $q_{ij}$  is the formal charge at position  $j$  produced by attaching the group  $-\text{CH}_2^-$  at position  $i$  and  $M$  or  $M'$  is a measure of the combined  $\pi$ -inductive-resonance effect of the substituent. The overall  $\sigma$  constant is then given by

$$\sigma_{ij} = F/r_{ij} + Mq_{ij} \quad \text{or} \quad \sigma_{ij} = F'/r_{ij} - M' \pi_{ij}$$

The signs in the above equations are chosen so that  $M$ ,  $M'$  for a given substituent should have similar signs. The constants  $F$ ,  $M$ , or  $F'$ ,  $M'$  can be found for a given substituent from  $\sigma_m^-$  and  $\sigma_p^-$  for benzene, and the  $\sigma_{ij}^-$  for any other system can then be calculated.

The quantities  $q_{ij}$  have been tabulated for different systems (70). The atom-atom polarizabilities  $\pi_{ij}$  are troublesome to calculate.

Very good agreement is obtained when the calculated  $\sigma_{ij}$  are plotted against the experimental  $\sigma$  values. Dewar and co-workers used these calculated values  $\sigma_{ij}$  to study the substituent effect on the fluorine chemical shift in substituted 3'- and 4'-fluoro-biphenyls and 3'' substituted 4-fluoroterphenyls. (This method of correlation of  $\sigma_{ij}$  with the property being studied is called the FM method).

Studies of the effect of substituents on the fluorine chemical shift in substituted 1- and 2- fluoronaphthalenes showed that the results could be better interpreted in terms of a modified FM treatment where the major contribution to the field effect is supposed to arise from lengthwise polarization of the C-F bond, so that its magnitude depends on the vector potential of the field rather than the scalar potential (71, 72).

The results found in the fluorine nuclear magnetic resonance studies have to be modified, if extended to the case of the hydrogen atom. The order in the variations of the proton chemical shifts caused by the effect of substituents are about 20 times less than in the fluorine atom, so that long range magnetic interactions are much more important in the case of hydrogen than in the case of fluorine. It is because of this that in the case of fluorine long range magnetic interactions can be neglected.

In a subsequent study, trying to establish the importance of the field effect, a series of substituted fluorinated decalins and steroids were prepared. The results suggested that in the case of saturated systems, the effect of substituents on the chemical shift are stereochemical rather than electronic, being due to the conformational distortion of the saturated skeleton (73).

In general, the results obtained on the effect of substituents on the atoms attached to the aromatic ring can be extended to the atoms in the side chain as shown by Marcus, Reynolds and Miller (74). Based on a study of over 25 families of the type  $R-C_6H_4-T-H$ , the normal fall-off factor in  $\rho$  for the group  $T=0,1,2$  and 3 atoms is approximately 2-3/atom in carbon tetrachloride. For example, in the families of compounds studied, the  $\rho$  values decreased in the order of .60, .21, and .11. This fall-off is in the range of the one found for many rate and equilibrium studies (75), as well as in the studies on ethylbenzenes by Williamson (65). It is interesting to note that some  $\sigma_I$  values, based on n.m.r. fluorine chemical shifts in the fluorobenzenes, decreased by approximately the same factor when a methylene group was interposed between the substituent and the ring (76). When T could conjugate with the benzene ring which was the case for  $T=O, N,$  and  $C\equiv C$ , the electronic communication between the substituted R and the terminal proton was enhanced, oxygen appeared to be a far better conductor of electronic effects on proton magnetic shielding than any other group examined.

When compared with sulfur, it was found that in a conjugative role as an acceptor or an acceptor-donor of negative charge, sulfur is a better transmitter than oxygen, but as a conjugative donor, sulfur is worse than oxygen. Similar studies on the transmission of electronic effects have been also carried out in saturated systems (77, 78).

9. Studies applied to systems containing the sulfide, sulfoxide and sulfone groups.

Very few workers have studied the effect of substituents on the chemical shift of protons vicinal to a sulfide, sulfoxide or sulfone group. F. Taddei studied the effect of the sulfide, sulfoxide and sulfone groups in the chemical shifts of protons in the system  $\text{Ph-SO}_n\text{-R}$  (79), R being methyl, ethyl, isopropyl and t-butyl groups (79).

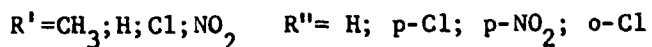
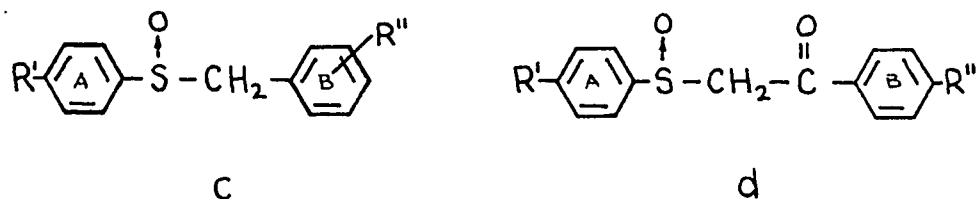
In the aliphatic groups, as found previously in the saturated system  $\text{R-SO}_n\text{-R}'$  (80) the chemical shift of the  $\alpha$  protons decrease in the order  $-\text{S}-, -\text{SO}-, -\text{SO}_2$ , in qualitative agreement with the electronic effects of these groups. Furthermore, while in the aliphatic series  $\text{R-SO}_n\text{-R}'$ , it was observed that the shift of methyl, methylene and methene hydrogens in  $\text{R}'$  are not influenced by R, when R is a phenyl ring, this does no longer holds. For instance, the  $\tau$  value of the  $\alpha$  methyl group moves to lower field relative to the corresponding aliphatic derivatives (0.38 p.p.m. for sulfides; 0.10 p.p.m. for sulfoxide and 0.07 p.p.m. for sulfones).

The same group of workers in an attempt to determine the effect of conjugative interactions of the S, SO and SO<sub>2</sub> groups with aromatic systems prepared a series of p-substituted alkylphenyl sulfides, sulfoxides and sulfones and studied them by n.m.r. (alkyl = CH<sub>3</sub>; C<sub>2</sub>H<sub>5</sub>; i-C<sub>3</sub>H<sub>7</sub>; t-C<sub>4</sub>H<sub>9</sub>). Good linear relations were found between the Hammett  $\sigma$  constant and the different protons in the  $\alpha$  carbon of the alkyl group (81). The  $\rho$  values for the methyl series, which gave the best results were: -0.17; -0.11; -0.18, for sulfide, sulfoxide and sulfone respectively.

As mentioned previously, Finegold (36) reported the 'abnormal' splitting of the methylenic absorption in diethyl sulfite which Kaplan and Roberts (82) analysed and explained as an ABC<sub>3</sub> system. Oki and Iwamura (83) reported that dibenzyl sulfite which has no other magnetic nuclei to interact with methylene protons, gave rise to AB type quartets. These authors found a correlation between the magnitude of J<sub>Gem</sub> and  $\sigma$  for a series of p-substituted derivatives but gave no data regarding chemical shifts.

From these works, the origin of magnetic non-equivalence of methylene protons in sulfites was well established. The works of Nishio (84, 85) were directed to establish the origin of non-equivalence in the case of sulfoxides, as well as the effect of substituents on the chemical shift of the methylene protons vicinal to this group.

He studied the n.m.r. spectra of a series of sulfoxides of the type:



The substituent effects in the benzyl and benzoyl groups have a bigger effect on the coupling constant and magnetic non-equivalence of these protons than the substituents on the phenyl ring.

The magnitude of magnetic non-equivalence is markedly dependent on the substituent on the benzyl group.

For example, phenyl benzyl, phenyl p-chlorobenzyl, phenyl o-chlorobenzyl sulfoxides exhibited very small chemical shift differences between two protons in  $\text{CDCl}_3$ . On the other hand, substituted phenyl p-nitrobenzyl sulfoxides, which contain a p-nitro group on the B phenyl ring exhibited large chemical shift differences (9.4- 15.2 c.p.s.) in the same solvent. In contrast, the compounds which contain a p-nitro group on the A-phenyl ring gave a singlet. Phenyl phenacyl and phenyl p-bromophenacyl sulfoxides exhibited large chemical shift differences in the same solvent (8.3-16.7 c.p.s.)

Regarding the substituent  $R'$  in structures c and d, no appreciable relationship was found between the substituent  $R'$  and geminal coupling constants. ( $R' = \text{CH}_3, \text{H}, \text{Cl}, \text{NO}_2$ ). However, an interesting relationship between the chemical shift of the methylene protons and the substituent  $R'$  was observed for  $R'' = \text{Cl}, \text{NO}_2$ , in structures c and d in various solvents.

It is noteworthy that the chemical shift in the compounds with structure c increases with the increasing electronegativity of the substituent  $R'$ . In contrast in compounds with structure d, the chemical shift decreases as the electron withdrawing power of  $R'$  increases.

A closer inspection of the independent chemical shifts of the methylene protons showed that the two protons have different sensitivities to the substituent  $R'$  in compounds with structures c and d.

In the case of compounds with structure d, the chemical shift of the proton which gives rise to a peak in a lower field ( $\nu'_A$ ) is more sensitive to the substituent. On the contrary in compounds with structure c, the proton in a higher field ( $\nu'_B$ ) is more sensitive to the substituent.

Nishio expressed his results by plotting chemical shifts of each proton as a function of the mean value of chemical shifts. In order to compare his results with those of the current study, Hammett plots of chemical shift against  $\sigma$  constants were prepared from his data. The calculated  $\rho$  values for the low and high field methylene signals, respectively, are -0.02 and -0.28 for c ( $R''=NO_2$ ) and -0.28 and 0.00 for d ( $R''=H$ ). Nishio (85) proposed that the difference in sensitivity in the methylene protons has a conformational effect as its origin. It is very likely that the conformations in Fig. 7 are unequally populated and that the conformation which possesses two bulky groups in a trans relation such as e exists in predominance.

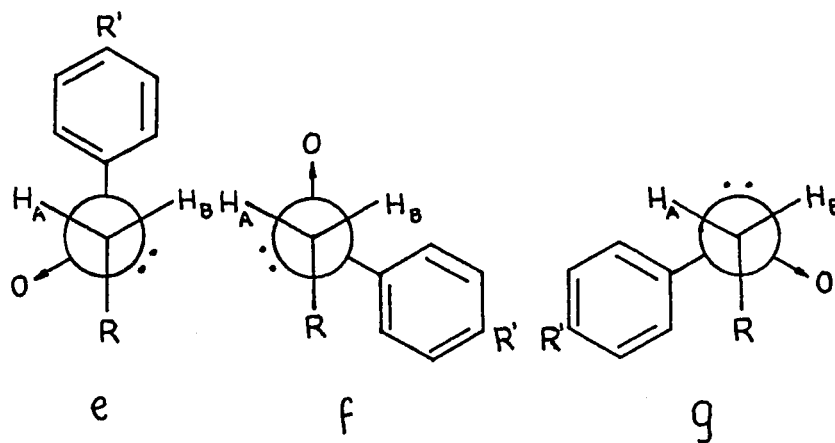


Figure 7. Three stable conformations in substituted benzyl-phenyl sulfoxide.

Two explanations could then account for this difference in influence of R' on the two methylene protons. One, as claimed before by Taddei (80) is based on the anisotropy of the phenyl ring that would deshield one proton more than the other. The other explanation, more likely, is that the proton which is more sensitive to the change of electronegativity of substituent R' is that which is in the trans position to the unshared electron pair on sulfur.

As discussed by Hamlow et.al. (86), a partial participation of the lone pair in a  $\sigma^*_{C-H_A}$  orbital is possible and such a participation allows some overlap between  $\sigma^*$  and lone pair orbitals to generate some double bond character between C and S. Since such an interaction can be expected only in the direction of H<sub>A</sub> (trans to the lone pair on sulfur atom), it is possible that the substituent R' affects these protons to a different degree.

EXPERIMENTAL

cis-2,3-Dichloro-1,4-dioxane (II)

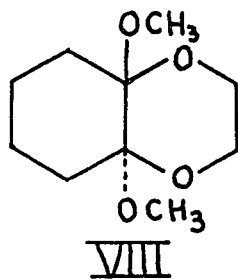
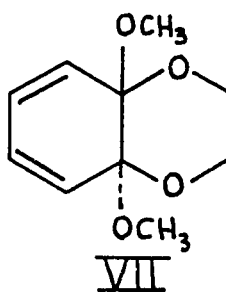
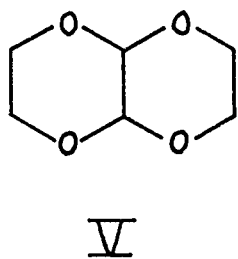
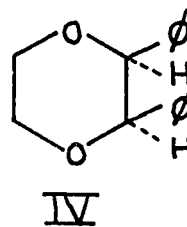
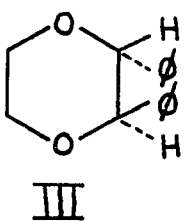
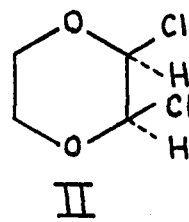
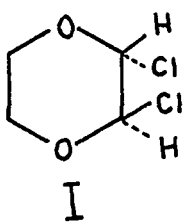
This compound was prepared by passing chlorine through a solution of p-dioxane in carbon tetrachloride at reflux temperature according to the procedure of Summerbell and Berger (87). After several recrystallizations from pentane-ether, the compound melted from 52-53° (lit. 53°) (87).

cis-2,3-Diphenyl-1,4-dioxane (IV)

The method of Stumpf (88) reacting phenyl magnesium bromide with trans-2,3-dichloro dioxane was used to prepare a mixture of diastereomeric 2,3-diphenyl-1,4-dioxanes. The products were separated by chromatography. The minor product, the cis isomer, after several recrystallizations from ethyl acetate melted at 132-134° (lit. 133-134°) (88).

Naphthodioxane (V)

This compound was prepared reacting 2,3-dichloro-1,4-dioxane with ethylene glycol in benzene according to the procedure of Summerbell and Lunk (89). After recrystallization from benzene and sublimation, the solid melted at 138-139° (lit. 133-136°) (89).



4a,8a-Dimethoxy-4a,8a-dihydro-1,4-benzodioxan(VII)

This compound was prepared by the electrochemical procedure and apparatus of Weinberg (90), passing an electric current through a basic solution of benzodioxane in methanol. The crude product was recrystallized from water to give a white solid which, after sublimation, melted at 90.0-91.0° (lit. 88.5-89.5°) (90).

4a,8a-Dimethoxy-4a,5,6,7,8,8a-hexahydro-1,4-benzodioxan(VIII)

Compound VII was shaken with palladium on charcoal (10%) in ethanol under an atmosphere of hydrogen until 2M equivalents of hydrogen were absorbed. The product, after removal of catalyst and solvent, was recrystallized from petroleum ether (b.p.60-80°) to give a 60% yield of a solid, m.p. 85.0-85.5° (90).

2,3-Dihydrofuran:

This compound was obtained by the isomerization of 2,5-dihydrofuran in basic medium according to the procedure of Paul, Fluchaire and Collardeau (91). The product was purified by distillation to give 73% yield of a liquid, b.p. 58° (lit. 55°) (91). Its n.m.r. spectrum did not show the presence of impurities.

2,2,2-Trifluoroethyl-2-tetrahydrothiaphuranylether:

A solution of 2,2,2-trifluoroethanol in 12 mls. of freshly distilled 2,3-dihydrofuran was cooled in an ice bath. 5 mg of p-toluenesulfonic acid was added to the cooled solution and the mixture was stirred for five hours during which time it warmed to room temperature. The reaction mixture was diluted with ether, washed with dilute sodium carbonate solution and water. The organic phase was dried over anhydrous magnesium sulfate. The drying agent was filtered off and the filtrate distilled at atmospheric pressure. The liquid which distilled over at 90-105<sup>o</sup> was collected and examined by nuclear magnetic resonance. The spectrum showed a peak at  $\tau$  8.80 attributable to impurities. All attempts to purify further the compound were unsuccessful and no elementary analysis was taken.

Tetrahydrothiapyran:

This compound was prepared according to the procedure used to prepare tetrahydrothiophene (92) by condensation of 1,5-dibromopentane with sodium sulfide. The liquid obtained distilled over at 130-140<sup>o</sup> and did not show any impurity when examined by n.m.r. (lit. 141<sup>o</sup>) (93).

Tetrahydrothiapyran-1-oxide:

The compound was prepared in 80% yield by the oxidation of tetrahydrothiapyran with hydrogen peroxide in absence of solvent, according to the procedure of Tarbell and Weaver (94). The product was purified by distillation (bp. 115-118<sup>o</sup>) and on standing in the desiccator solidified to a glassy mass.

2,3-Dihydrothiapyran:

This compound was prepared by heating a solution of tetrahydrothiapyran-1-oxide and benzoic anhydride at reflux temperature for 14 hours according to the procedure of Parham et. al. (95). The product was distilled to give 50% yield of the pure compound, b.p. 42-46° at 38 mm. (lit. 66° at 57mm.) (95).

2,2,2-Trifluoroethyl-2-Tetrahydrothiapyranyl ether:

A solution of 2.0 g of 2,2,2-trifluoroethanol and 1.0 g. of 2,3-dihydrothiapyran in 50 ml. benzene was cooled in an ice bath. Two drops of hydrochloric acid in ether were added to the cooled solution and the mixture warmed to room temperature. The reaction mixture was diluted with ether, and then washed with 5% sodium carbonate solution and water. The aqueous washings were extracted with ether and the combined organic phases were dried over anhydrous sodium sulfate. The drying agent was filtered off and the filtrate distilled at atmospheric pressure. The liquid which distilled over at 140-150° was collected and examined by nuclear magnetic resonance. The spectrum showed no peaks attributable to impurities. The yield was 50%.

p-Aminobenzyl phenyl sulfide:

This compound was prepared according to the procedure of Lau and Grillot (96) by adding aniline to a solution of thiophenol and formaldehyde in ethanol. After recrystallization from ethanol in 60% yield, the compound melted at 75.0-76.0° (lit. 74-75°). (96).

p-Aminobenzyl phenyl sulfoxide:

Procedure a.- A solution of 0.5 of p-aminobenzyl phenyl sulfide in 50 ml methanol was cooled in an ice bath. 0.5 g of sodium metaperiodate in 50 ml methanol was added dropwise. The mixture was stirred overnight and the precipitated sodium iodate removed by filtration. Part of the methanol was removed under reduced pressure and 100 ml. of chloroform was added. This solution was washed with water in order to eliminate any traces of sodium iodate. The extract was dried over anhydrous magnesium sulfate and the solvent was removed. Recrystallization from ethanol afforded 0.32 g of light yellow needles m.p. 154-156°. This compound is very easily oxidized, turning dark orange after standing for a few days in air.

Procedure b.- To a solution of 0.5 g of p-nitrobenzyl phenyl sulfoxide in 100 ml methanol was added 50 mg of palladium on charcoal. The compound was reduced in the Parr hydrogenator at 15 psi. for 1 hour, the catalyst removed by filtration and the solvent evaporated at reduced pressure. Recrystallization of the material from ethanol gave the expected product in 20% yield m.p. 155-156°.

Anal. calc'd for  $C_{13}H_{13}ONS$ : C, 67.5; H, 5.7; N, 6.0;

Found: C, 67.0; H, 5.6; N; 5.13.

Para-aminobenzyl phenyl sulfone:

This compound was prepared by condensation of benzene-sulfinic acid, aniline and formaldehyde in an acidic solution of ethanol according to the procedure of Pollak and Grillot (97) in 90% yield. The product was isolated as a solid m.p.  $172-176^{\circ}$  (lit.  $170-176^{\circ}$ ) (97).

Partially deuterated p-nitrobenzyl phenyl sulfoxide:

To a solution of 0.50 g of p-nitrobenzyl phenyl sulfoxide in 10 ml deuterated chloroform was added 10 ml of deuterium oxide. After addition of 1 ml of 0.1% solution of NaOD in deuterium oxide, the mixture was shaken overnight. The reaction was followed by n.m.r. until there was approximately 50% exchange by deuterium of one of the protons of the methylene group ( $\sim 16$  hr). 50 ml of chloroform were added and the aqueous layer separated. The organic layer was washed with water and after solvent evaporation the solid was crystallized twice from ethanol, m.p.  $160^{\circ}$ .

Partially deuterated p-aminobenzyl phenyl sulfoxide:

A solution of 0.84 g of partially deuterated p-nitrobenzyl phenyl sulfoxide in 20 ml of glacial acetic acid was cooled in an ice bath with a magnetic stirrer. 4.2 g of carefully grinded hydrated stannous chloride dissolved in 7.5 ml of 3N HCl was added dropwise. During the addition, the temperature raised to  $8^{\circ}$ . After stirring for five hours, during which time the temperature was kept below  $20^{\circ}$ ,

50 ml of water was added and the solution filtered. The filtrate was poured over cracked ice and neutralized with 10% NaOH. After extraction with chloroform, washing with water and drying over anhydrous sodium sulfate, the solvent was removed under reduced pressure and the solid material was crystallized twice from methanol. The compound melted at 153°.

-----

The n.m.r. spectra were recorded on a Varian DA-60 spectrometer equipped with external lock. Two of the compounds were examined on a Varian HA-100 spectrometer. The experimental line positions were determined from the average of at least six traces, usually ten, with a standard deviation in all like positions being less than 0.2 c.p.s. and usually less than 0.1 c.p.s.

Solute concentration was usually 10-20%(w/v) for all measurements except for those on the sulfides and sulfones where dilute solutions were used (0.2M). In the case of sulfoxides, 0.3M solutions were used.

The deuterium spin-decoupling experiment was performed with the aid of an N.M.R. Specialties SD-60 Spin Decoupler.

The calculations of the line positions in the theoretical spectra were carried out on an IBM 1620 computer for the Frequent IV-A program. More accurate calculations were obtained from calculations on an IBM 360, model 50 computer using the LAOCOON II program.

The spectra measured at temperatures above and below room temperatures were taken using a probe assembly which has been described previously (98). In the case of the p-nitro and p-amino benzyl phenyl sulfoxides, the experiments were carried out using the built-in accessory of the HA-100 spectrometer.

RESULTS AND DISCUSSION

1. Determination of the configuration and conformation of  
2,3-Dichloro-1,4-dioxane. m.p. 52° (II)

Two different products are obtained in the photochlorination of p-dioxane depending on the reaction temperature. When the reaction is accomplished by chlorinating dioxane at reflux temperature, which varies from 100° to 150° as higher boiling products are formed, the main product is one isomer of 2,3-dichloro-p-dioxane m.p. 31° (I) (99,100). When the chlorination is carried out in carbon tetrachloride solution, a mixture of 65% of I and 35% of another isomer of 2,3-dichlorodioxane m.p. 52° is obtained (compound II) (89). The main function of the solvent is to maintain a moderate reaction temperature since the same results were obtained when dioxane was chlorinated without solvent at temperatures about 75°. When the reaction was carried out at temperatures above 110°, compound II was converted into I. This conversion can also be carried out by the action of aluminum or thionyl chloride.

Considerable confusion arose concerning the configuration and conformation of isomer II. Summerbell and Lunk assigned the cis configuration to it based on the fact that it is less stable than isomer I and by the fact that I was proved to be trans by the demonstration that it was capable of kinetic resolution into one enantiomer (99).

Later, Altona, Romers and Havinga (101) verified the assignment of the trans configuration to isomer I and established the configuration to be diaxial through X-ray analysis, infrared spectra and dipole moment studies. The dipole moment of II was in agreement with the cis configuration. Later, Caspi et. al. from the n.m.r. spectrum of isomer II concluded that its configuration was trans and that its conformation was a rigid eclipsed boat with the oxygen occupying the bowsprit positions (102). Its n.m.r. shows a single peak at  $4.3\tau$  for the hydrogens at  $C_2$  and  $C_3$  and an  $A_2B_2$  pattern for the hydrogens at  $C_5$  and  $C_6$ . From the appearance of the multiplet along with the single peak at  $4.3\tau$ , they thought the spectrum seemed to be due to a rigid boat conformation but failed to realize that a mobile molecule consisting of a pair of rapidly interconverting chairs conformations would also give rise to the observed spectrum. Unfortunately, their findings were accepted in part by Chen and Le Fèvre (103) who measured the dipole moments, polarization and polarizability of I and II. Because they accepted Caspi's conclusion that isomer II possessed a rigid conformation, they were forced by elimination to assign the trans diequatorial conformation to it.

If assignment of either the cis boat conformation or the trans diequatorial conformation were correct, then some of the fundamental energetic concepts in conformational analysis would be invalidated. For this reason, a rigorous analysis of the  $A_2E_2$  absorption pattern of isomer II was undertaken in an attempt to clarify the existing discrepancies.

The nuclear magnetic resonance spectrum of a 15% solution of isomer II in chloroform was measured. Fig. 8a shows the low-field half of the  $A_2B_2$  absorption. The analysis of this pattern was achieved in the standard manner as described in the introduction using the Frequent IV program. Assignment of the lines to specific transitions was relatively straightforward, since the spectrum closely resembled that solved by Abraham for 2-methyl-1,3-dioxolane (104). The parameters K, L, M, N and  $\delta$  were adjusted until agreement between calculated and observed line positions was obtained to within 0.15 c.p.s. (Fig. 8b). To check the parameters a spectrum was taken of a 50% solution (w/v) of isomer II in benzene, and again obtained agreement to within 0.15 c.p.s. between the observed line positions and those calculated from the same values of K, L, M and N and an adjusted value for  $\delta$ . From the parameters, the coupling constants that appear in Table 8 were found. The coupling constants relations have already been described in the introduction.



Figure 8. The low field half of the  $-\text{OCH}_2\text{CH}_2\text{O}-$  absorption of compound II: (a) the experimental spectrum; (b) the calculated spectrum.

Table 8. Coupling constants and chemical shifts obtained in the analysis of compounds containing the 1,4-dioxane system (a).

	$\nu_{AB}$	J <sub>A</sub>	J <sub>B</sub>	J	J'	Ref.
<u>cis</u> -2,3-Dichloro-1,4-dioxane (II)	22.95(b)	3.1	3.1	5.45	-12.25	This work
	21.6	3.2	3.2	6.3	-12.2	Ref. 104
	22.9(c)	3.20	3.21	6.35	-12.1	Ref. 33
<u>trans</u> -2,3-Dichloro-1,4-dioxane (I)	39.7	12.37	0.59	3.28	-12.15	Ref. 33
<u>cis</u> -2,3-Diphenyl-1,4-dioxane (IV)	15.8	2.8	2.9	5.4	-11.65	This work
	17.1	3.0	3.0	6.4	-11.9	Ref. 101
Naphthodioxane (V)	32.8	2.8	2.8	5.4	-11.7	This work
	32.7	2.9	2.9	6.3	-11.8	Ref. 101
4a,8a-Dimethoxy-4a,5,6,7,8,8a-hexahydro-1,4-benzodioxan(VII)	43.9	12.0	1.0	4.3	-11.20	This work(d)
	44.0	11.8	0.9	4.1	-11.8	
4a,8a-Dimethoxy-4a,5,6,7,8,8a-hexahydro-1,4-benzodioxan (VIII)	45.0	12.4	0.8	3.8	-11.2	This work

(a) Values obtained in CDCl<sub>3</sub>.

(b) The chemical shift value in benzene is 31.1 c.p.s.

(c) Values obtained in CCl<sub>4</sub>.

(d) Two sets of values were obtained from the iterative calculations for this compound.

In Fig. 9, all reasonable configurations for isomer II are shown. If the compound were cis and in a rigid chair conformation, we would expect two signals for the protons labelled X and Y in case h. We would also expect an ABCD pattern for the four hydrogens on carbons 5 and 6. Since neither expectation is fulfilled, we can eliminate structure h.

If the compound is trans and has its chlorines in either the rigid diaxial or the rigid diequatorial conformation, we would expect an  $A_2B_2$  absorption pattern for the 5 and 6 hydrogens. But in this  $A_2B_2$  system,  $J_A$  and  $J_B$  should have widely different magnitudes, one typical of diaxial protons and the other typical of diequatorial protons. Since  $J_A = J_B$  as found in the analysis, this case i is eliminated.

Should the compound possess the trans configuration and be rapidly interconverting between the diaxial and diequatorial conformations, there would likely be an unequal population of the two conformations. In this case,  $J_A$  would not equal  $J_B$ , and so this possibility is eliminated. If the two conformations were of equal stability, we would observe coupling constants which are an average of the two contributing structures. This would require  $J_A = J_B = (J_{60} + J_{180})/2$  (observed value 3.1 c.p.s.)  $J = J_{gem}$ , and  $J' = J_{60}$  (observed value 6.45 c.p.s.), where the subscripts represent  $\phi$ , the dihedral angle between the interacting protons.

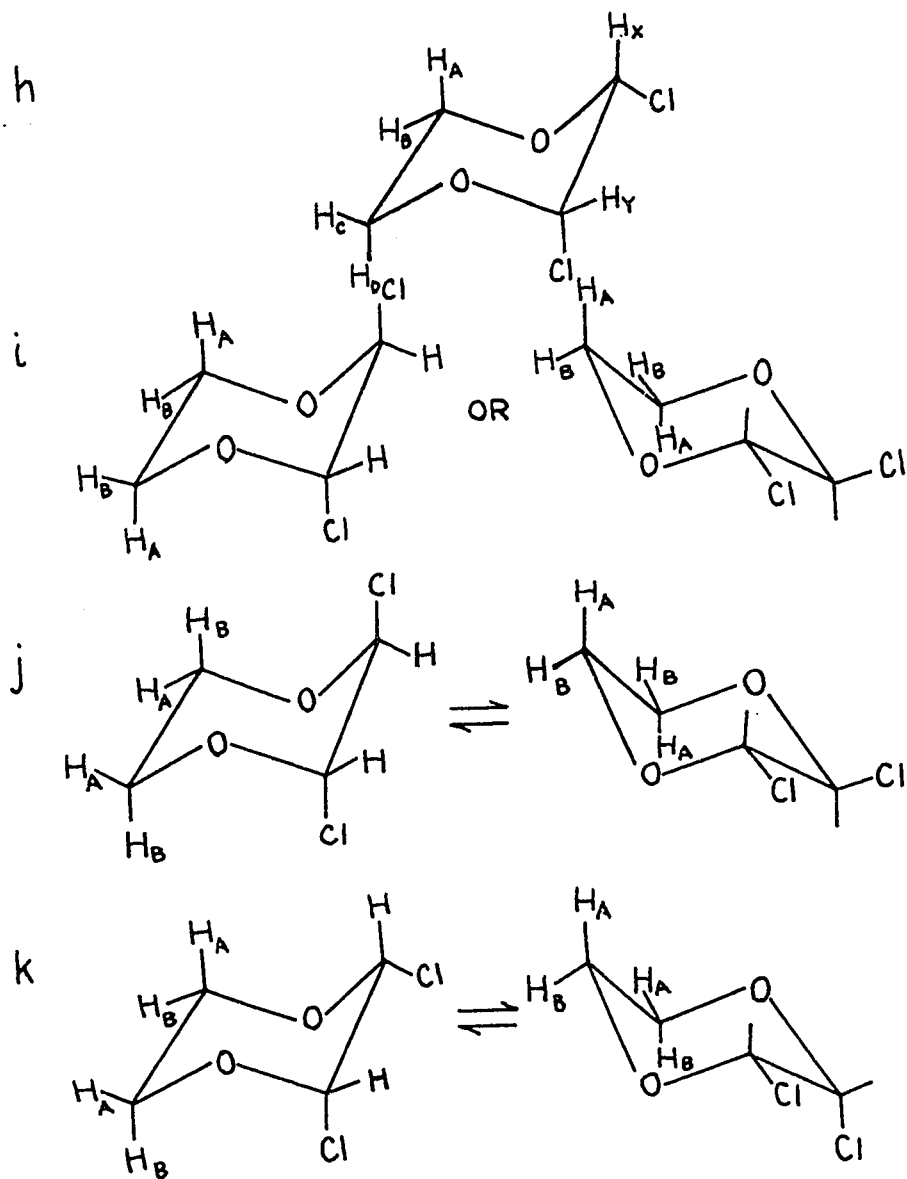


Figure 9. The four considered representations for 2,3-dichloro-1,4-dioxane, m.p. 52°.

The experimental results would then require that  $J_{60}$  be more than twice as large as  $(J_{60} + J_{180})/2$ . This completely revokes the Karplus relation between  $J_{vic}$  and  $\phi$ . Although the relation is far from quantitative, it is completely reliable in predicting  $J_{180} > J_{60}$ . Thus, case i is eliminated.

In case k, the observed parameters compare favorably with those encountered in similar six-membered rings. The best model for comparison found in the literature is the 1,3-dioxane system (Fig.10),

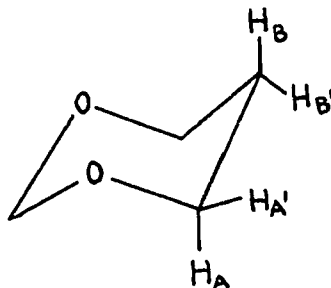


Figure 10. The chair form of 1,3-dioxane showing the four protons whose coupling constants have been determined.

whose analysis gave the following parameters (105):

$$J_{60} = J_{AB'} = 3.8 \text{ c.p.s.}; \quad (J_{60} + J_{180})/2 = J_{AB'} + J_{AB})/2 = 6.7 \text{ c.p.s.};$$

$$J_{AA'} = -11.0 \text{ c.p.s.}$$

(a better model in this case might be  $\text{CH}_3\text{-CH(OH)-CH}_2\text{-OH}$ , in which

$$J_{gem} = -11.9 \text{ c.p.s.}) \text{ (106).}$$

$$\text{In dioxane } J_{60} = 2.7 \text{ c.p.s. and } (J_{60} + J_{180})/2 = 6.1 \text{ c.p.s. (107).}$$

In view of the good agreement between the coupling constants for isomer II and those predicted from the cis configuration for interconverting chairs, any consideration of the relatively high energy boat conformations is entirely unwarranted. It is, therefore, concluded that isomer II has the cis configuration and undergoes rapid chair-chair interconversion at room temperature (108).

2. Determination of the configuration and conformation of 2,3-Diphenyl-1,4-dioxane m. p. 136<sup>o</sup> (IV)

As in the case of the 2,3-dichloro-1,4-dioxanes, considerable confusion existed regarding both the configuration and the conformation of the two isomeric 2,3-diphenyl-1,4-dioxanes. By reacting 2,3-dichloro-1,4-dioxane with phenyl magnesium bromide Christ and Summerbell (109) obtained for the first time the isomer of 2,3-diphenyl-1,4-dioxane with a m. p. of 49<sup>o</sup> (III). Later, Summerbell and Berger (87) were able to separate by chromatography the 136<sup>o</sup> isomer (IV) from the residual oil in the preparation of III. The compound was also obtained from the catalytic reduction of 2,3-diphenyl-para-dioxene.

The n.m.r. spectrum of III at room temperature (Fig. 11) consists of two lines for the dioxane ring protons. The peak at 5.22  $\tau$  is assigned to the protons at carbons 2 and 3 of the dioxane ring and the peak at 5.58  $\tau$  to the remaining protons at carbons 5 and 6. The intensities of the signals agree with this assignment.

The finding of only one unsplit peak for the protons at carbons 5 and 6 indicates that the molecule is inverting rapidly, and hence the 5.22 peak represents the average position between axial and equatorial extremes. This was the conclusion that Caspi, Wittstruck and Piatak arrived at after considering the n.m.r. spectra of this isomer III (102).

After considering the n.m.r. spectra of isomer IV (Fig.12), these authors arrived at the conclusion that the compound was the cis isomer and that its conformation was a rigid boat with the oxygens at the "bow" and "stern" positions. The n.m.r. spectrum shows a series of fourteen peaks centered at 6.14  $\tau$  for the protons at carbon 5 and 6 and a single, unsplit peak at 4.88  $\tau$  for the protons at carbons 2 and 3. They did not observe any change in the spectrum with a change in temperature in the range 55<sup>o</sup> to -19<sup>o</sup>. The main argument they had for assuming that the compound had a rigid conformation was the findings of Altona, Romers and Havinga (101) that the dipole moment of trans-2,3-dibromo and trans-2,3-dichloro-1,4-dioxane did not change with a change in the dielectric constant of the solvent suggesting a rigid conformation for these compounds. From there, the authors assumed that other substituted dioxanes will also adopt a preferred conformation.

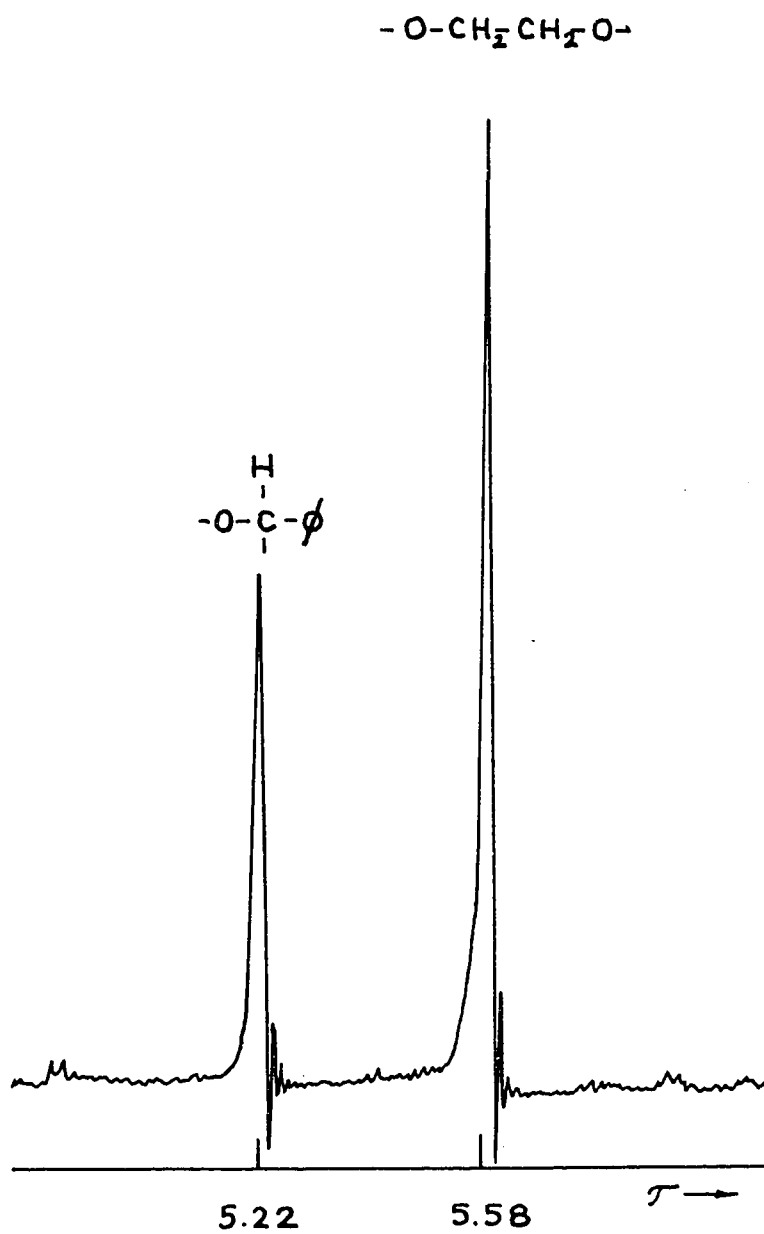


Figure 11. The partial n.m.r. spectrum of trans-2,3-diphenyl-1,4-dioxane (III) measured in CDCl<sub>3</sub>.

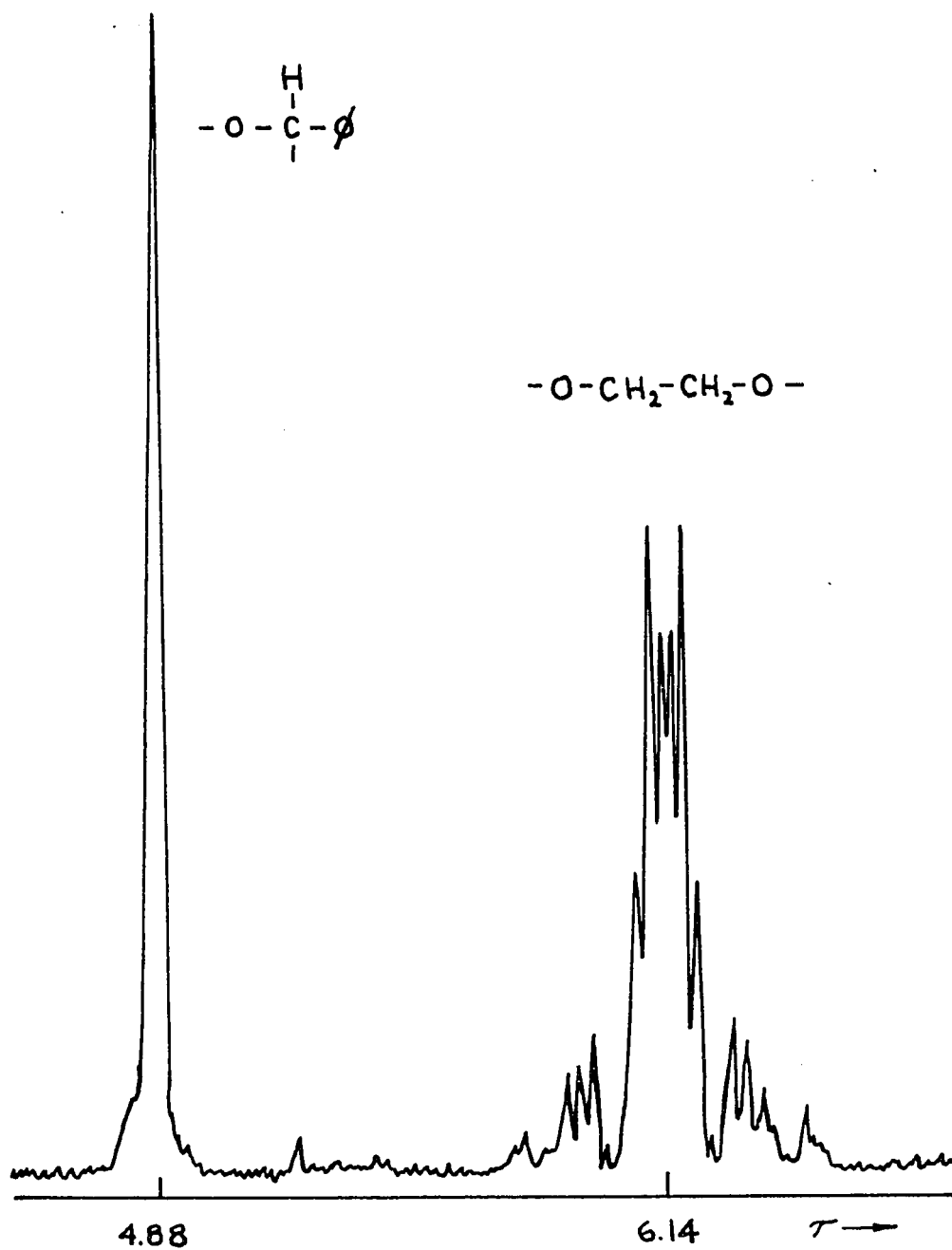


Figure 12. The partial n.m.r. spectrum of *cis*-2,3-diphenyl-1,4-dioxane (IV) measured in CDCl<sub>3</sub>.

According to Chen and Le Fèvre (103), the measured dipole moment of 0.65 D excluded the possibility that the ring might have a boat form which according to them should exhibit a moment of not less than 1.5 D if  $\mu_{\text{C-Ph}}$  is 0.4 D. Because they assumed also that the molecule was rigid based on the single peak observed for the protons at carbons 2 and 3 in its n.m.r. spectrum, they proposed that this isomer is the trans isomer contrary to the previous assignment.

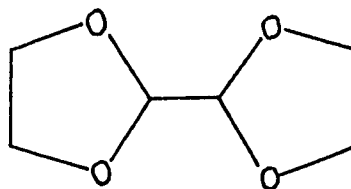
It was with the purpose of clarifying the existing discrepancies that an analysis of the  $A_2B_2$  multiplet observed in the n.m.r. spectrum was carried out in detail. The procedure was the same as the one used for analysis of compound II. The results are shown in Table 8.

In order to check the accuracy of this analysis, the spectrum of II was also measured at 100 M.c.p.s. and compared it with that calculated from the coupling constants in Table 8 and the adjusted chemical shifts. All line positions agreed to within 0.2 c.p.s. The fact that  $J_A$  is found to be equal to  $J_B$  provides conclusive evidence that 2,3-diphenyl 1,4-dioxane m.p. 133° has the cis configuration and is rapidly interconverting between chairs conformations at room temperature (110).

More recently, Hussey (111) has confirmed by chemical means the configuration of this compound. 2,3-Bis(4-bromo-phenyl)-1,4-dioxane and its 4-chloro counterpart were converted to 2,3-diphenyl-1,4-dioxane m.p. 49° and to 2,3-bis (4-carboxyphenyl)-1,4-dioxane. The partial resolution of the later constituted unequivocal proof of the trans configuration of the lower melting isomer III.

3. Determination of the configuration and conformation of Naphto-dioxane (hexahydro-p-dioxino(2,3-b)-p-Dioxin) (V)

Compound V and a lower melting point isomer VI were isolated by Boeseken et.al. (112) by fractional crystallization



VI

of the reaction mixture from trans-2,3-dichlorodioxan and ethylene glycol. On the basis of dipole moment measurements, the trans-structure was assigned to V ( $\mu=0.72$  D) and the cis-structure, picture as two boat forms, to VI ( $\mu=1.9$  D). Compound VI was later studied by X-ray analysis (113) and found to be 2,2'-bis-1,3-dioxolane. Interestingly, a similar mixture of V and VI is obtained from cis-2,3-dichlorodioxane and ethylene glycol (89). As with the previous compounds discussed, several assignments appear in the literature regarding the configuration and conformation of this compound (103). From its n.m.r. spectra, dipole moment and a single Fourier projection of its mercuric chloride complex (113), the trans configuration was assigned to it. We redetermined the n.m.r. spectrum of V in deuteriochloroform which is shown in Fig. 13.

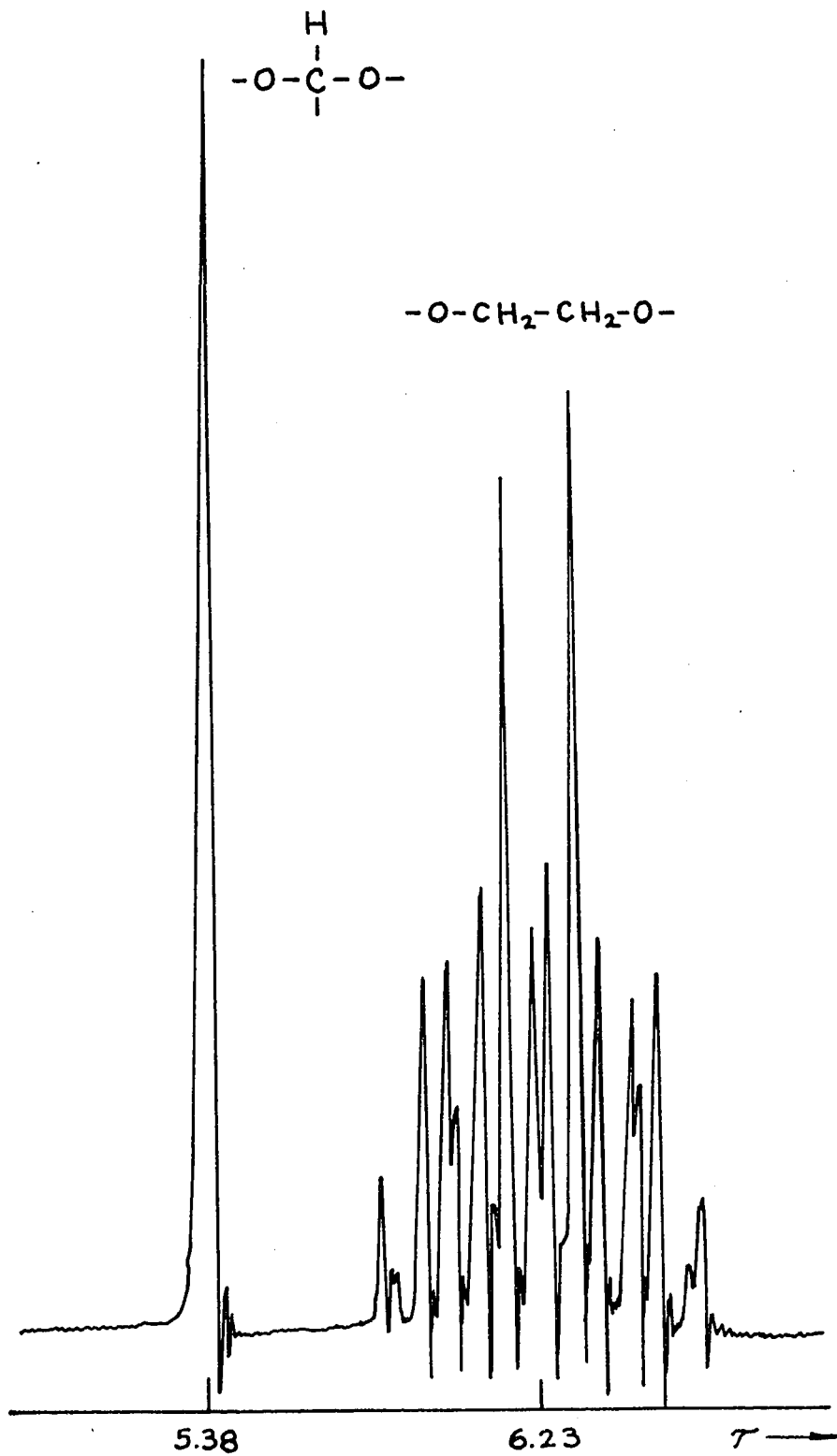


Figure 13. N.m.r. spectrum of Naphthodioxane (V) measured in  $\text{CDCl}_3$ .

It consists of two peaks, a sharp singlet at 5.38  $\tau$  and a multiplet centered at 6.23  $\tau$ . This multiplet appears as a typical  $A_2B_2$  pattern arising from the  $-O-CH_2-CH_2-O-$  portion of the molecule. All line positions in the multiplet were accurately measured from the spectra of a 6%(w/v) solution of V in benzene. The determination of the chemical shifts and coupling constants was then carried out by the standard  $A_2B_2$  method of analysis, as described in the introduction.

For the calculations the Frequent IV program was used followed by the more refined Laocoon II program. The agreement between the calculated and experimental line positions was comparable for either program and was less than 0.12 c.p.s. for each transition. Table 8 lists the parameters obtained from the analysis along with those found independently by Altona and Havinga. As a final check on the parameters, a spectrum at 100 M.c.p.s. was taken and compared with the calculated one at the same frequency. All line positions agreed to within 0.2 c.p.s. It can be seen from Table 8 that the two vicinal coupling constants  $J_A$  and  $J_B$  are equal. This result is possible only if V possesses the cis configuration and undergoes a rapid chair-chair interconversion at room temperature, as shown in Fig. 14.

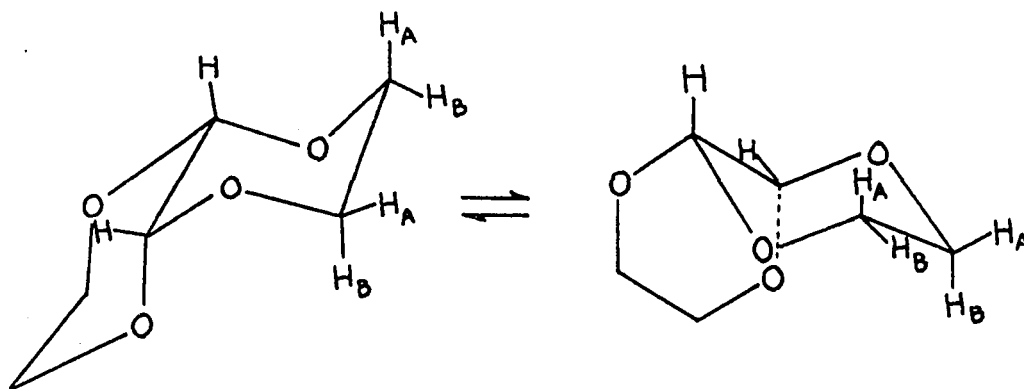


Figure 14. Chair-chair conformations for Naphthodioxane (V).

To confirm this conclusion, the behaviour of the n.m.r. spectrum of V, as the temperature was lowered, was examined. When a solution of V in a mixture of methylene chloride and carbon disulfide was cooled, the  $A_2B_2$  pattern began to show significant line broadening at  $-30^\circ$ . At  $-76^\circ$  the pattern appeared as a complex multiplet. At  $-104^\circ$  further change to an unsymmetrical absorption pattern consisting of two peaks (intensity ratio 3:1) was observed. No further change was seen when the solution was cooled to  $-117^\circ$ , at which temperature crystallization occurred. These changes are recorded in Fig. 15.

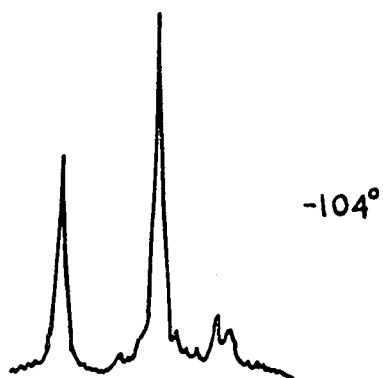
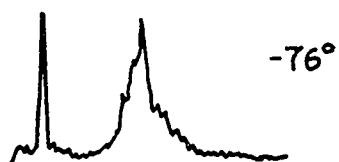
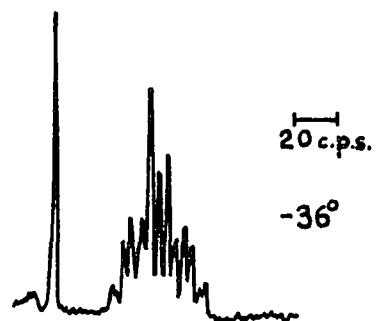


Figure 15. The temperature dependence of the  $A_2B_2$  absorption pattern in the n.m.r. spectrum of naphthodioxane.

The 3:1 ratio of peaks seen at  $-104^{\circ}$  is interpreted as representing the ABCD spectrum of one conformational isomer of the cis compound in which three of the four protons have similar chemical shifts. The lack of well resolved lines at this temperature is likely due to the decreased resolution at such a low temperature. The width at half height of the tetramethylsilane standard was slightly less than 2 c.p.s. in the same solution. These spectral changes can only be accounted for if V has the cis configuration. The rigid trans isomer would not be expected to show any significant change in its  $A_2B_2$  pattern when the temperature is lowered (110).

4. Determination of the configuration and conformation of 4a-8a-Dimethoxy-4a,8a-dihydro-1,4-benzodioxan (VII) and 4a,8a-Dimethoxy-4a,5,6,7,8,8a-hexahydro-1,4-benzodioxan (VIII)

In 1963, Belleau and Weinberg (114) reported the discovery of an electrochemical method of methoxylation of aromatic ethers. By use of this method, it was found that hitherto unattainable quinone ketals could be prepared in a good yield. When a solution of benzodioxane in methanol was electrolyzed, with potassium hydroxide as an electrolyte, a 31% yield of a solid, m.p.  $88.5-89.5^{\circ}$ , was obtained. Based on combustion analysis and spectroscopic data, the compound was assigned structure VII~~II~~ (90).

Reductive hydrolysis of VII with zinc and hydrochloric acid gave pyrocatechol; this is consistent with the assigned structure. Catalytic hydrogenation of VII produced the tetrahydro derivative VIII. The determination of the configuration of the methoxyl groups in these two compounds is of particular interest, because this knowledge could provide evidence concerning the mechanism of the methoxylation reaction.

The n.m.r. spectrum of VIII (Fig. 16) (10% w/v in  $\text{CCl}_4$ ) showed absorption at 4.22  $\tau$  (six protons) consistent with methoxyl absorption, and a four proton multiplet centered at 6.35  $\tau$  which is assigned to the  $-\text{O}-\text{CH}_2-\text{CH}_2-\text{O}-$  portion of the dioxane ring. This multiplet is typical of an  $\text{A}_2\text{B}_2$  system.

As before, from the analysis of this pattern, four coupling constants and the chemical shift between the A and B protons are obtained. It is the vicinal coupling constants  $J_A$  and  $J_B$  which provide the information necessary for the determination of the stereochemistry at the ring junction. In the trans isomer, the molecule would be prevented from undergoing chair-chair interconversions by the decalin type of ring junction. Thus, this isomer would most probably have the conformation shown in Fig. 17a whereas the cis isomer would be expected to be a rapidly interconverting pair of chair conformations as shown by 17b. The major difference in the coupling constants for these two configurations is that in the trans isomer  $J_A \neq J_B$ , the experimental line positions for the analysis were measured from the spectra taken in deuteriochloroform.

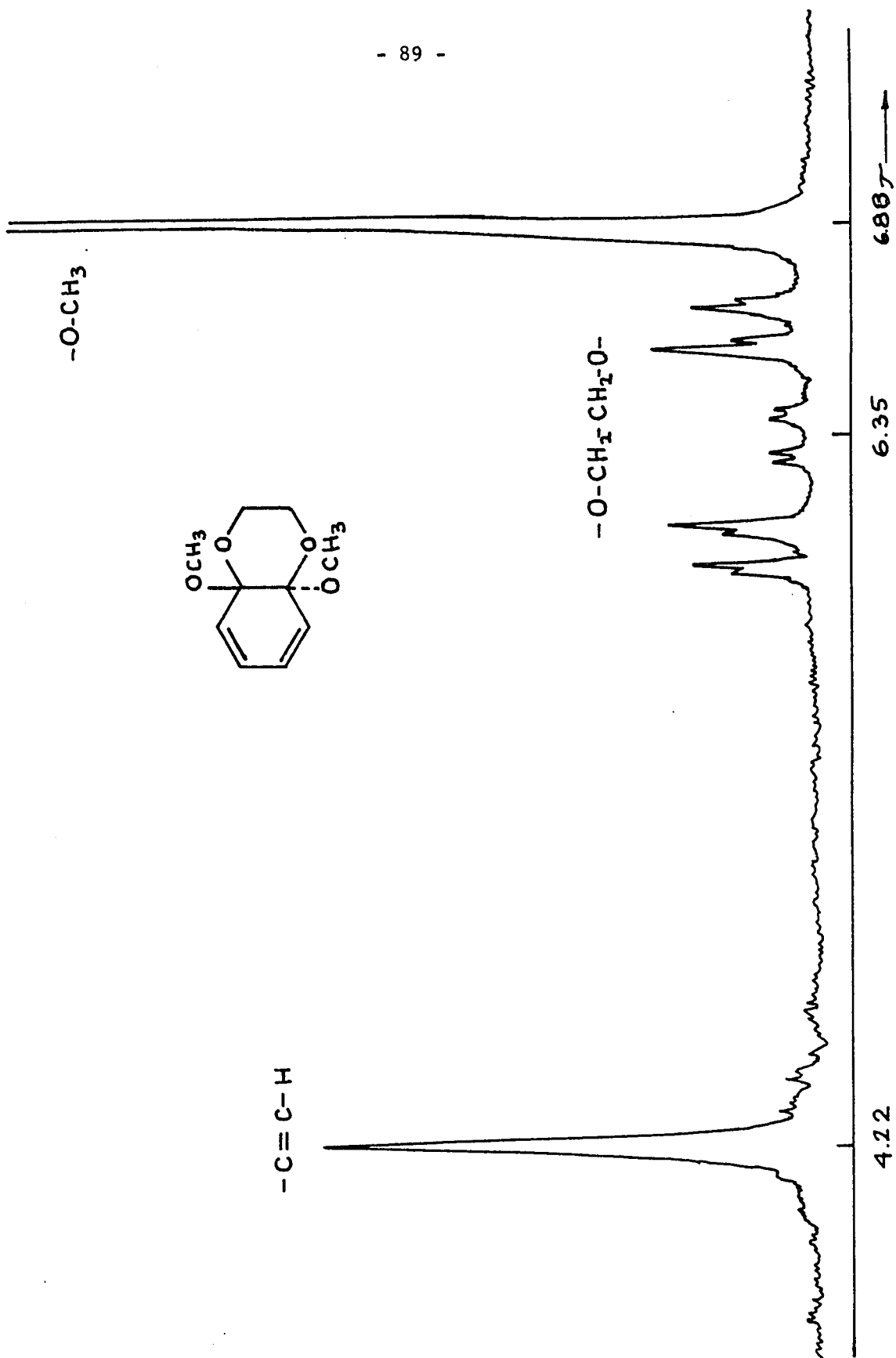


Figure 16. The n.m.r. spectrum of 4a,8a-dimethoxy-4a,8a-dihydro-1,4-benzodioxan (VII)

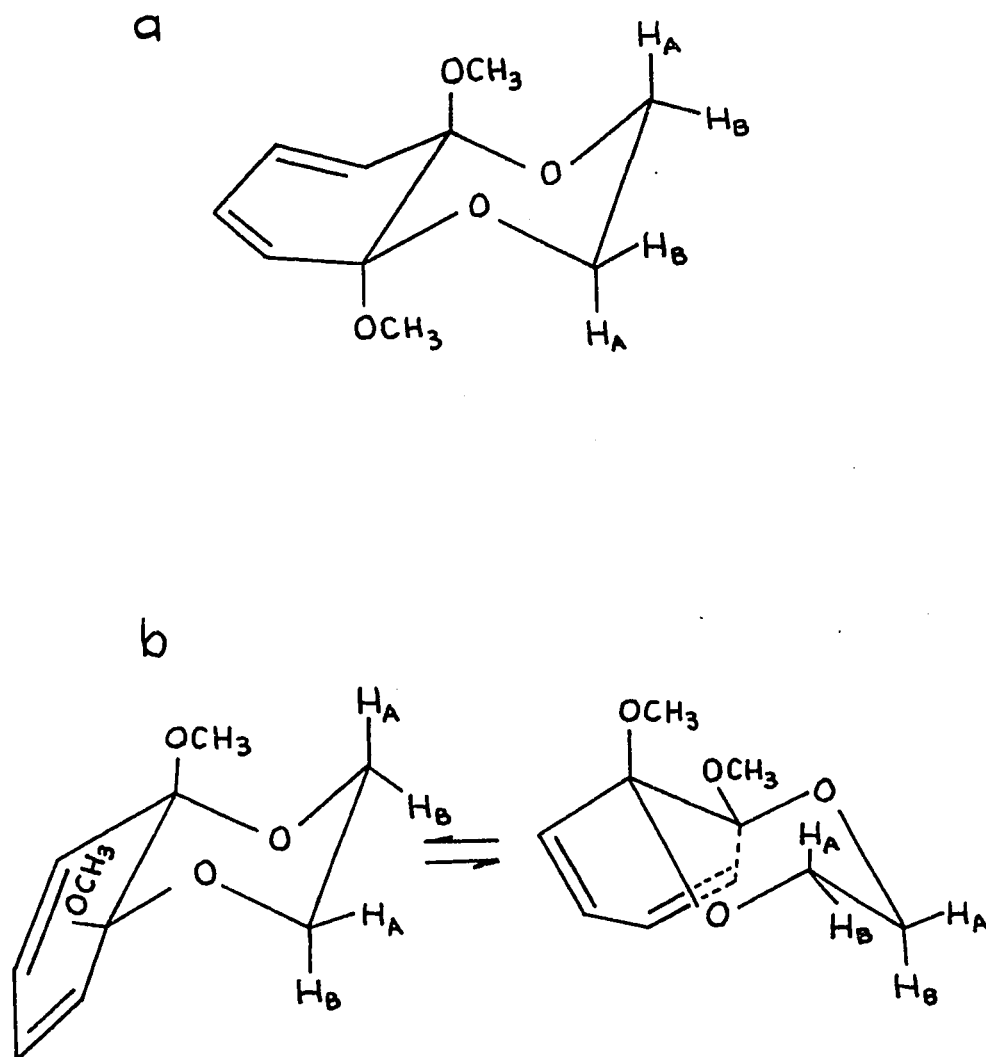


Figure 17 (a) The possible conformation for trans-4a,8a-dimethoxy-4a,8a-dihydro-1,4-benzodioxan(b). The possible conformations for cis-4a,8a-dimethoxy-4a,8a-dihydro-1,4-benzodioxan.

For the analysis, the programs used were the Frequent IV and the more refined Laocoon II. The results of the analysis are given in Table 8.

There is some doubt about which of the two sets of parameters obtained from the Laocoon program gives the best fit with the experimental data for VII. This ambiguity is due to the lack of resolution of the closely spaced lines. Fig. 18 shows the experimental spectrum of VII along with the two calculated spectra. In the figure, only the low-field half of the  $A_2B_2$  pattern is shown, because the methoxyl absorption obscures a large portion of the rest of the spectrum. The first set of parameters gives slightly better agreement among the line positions and is, therefore, preferred. The second set cannot, however, be rejected conclusively, since the experimental accuracy of the line positions and the deviations between the calculated and experimental line positions are still of a comparable order of magnitude (0.4 c.p.s.). Fortunately, a decision is not essential to the arguments regarding stereochemistry. It is seen that in each case  $J_A = 12$  and  $J_B = 1$  c.p.s. It is inconceivable that the isomer with the cis ring fusion could give rise to such different values for  $J_A$  and  $J_B$ . Furthermore, the observed values are very similar to those found by Jung for the trans isomer of 2,3-dichloro-1,4-dioxane. He reported that  $J_A = 12.3$  and  $J_B = 0.6$  c.p.s. (33). It is, therefore, concluded that VII possess the trans configuration.

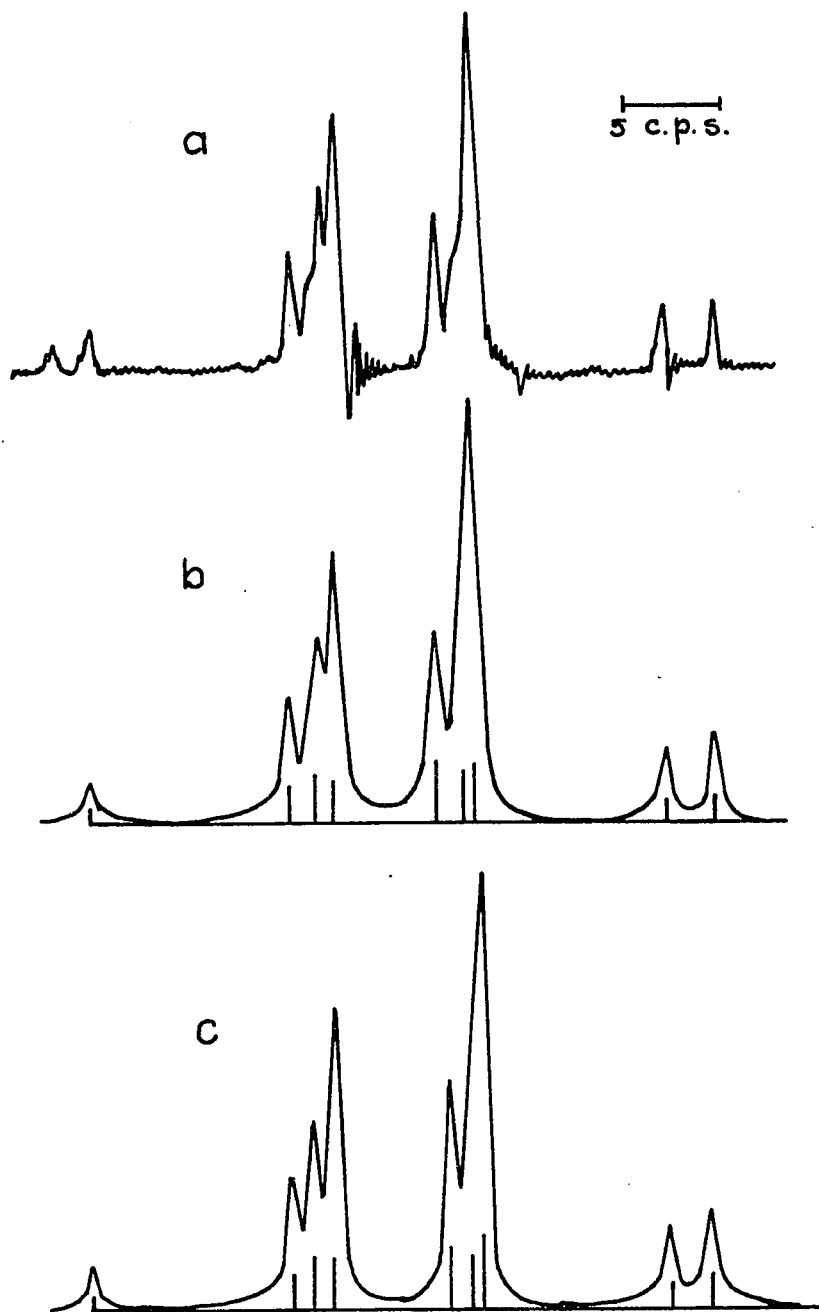


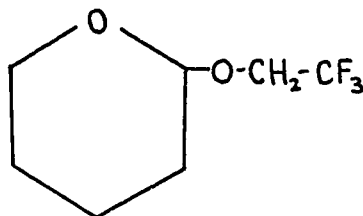
Figure 18. The low-field half of the  $\text{OCH}_2\text{CH}_2\text{O}$  absorption of compound VII: (a) the experimental spectrum (the small peak of lowest field is thought to be an impurity because of its variable intensity); (b) the spectrum calculated from the parameters of assignment A, Table 8; and (c) the spectrum calculated from the parameters of assignment B, Table 8.

The m.m.r. spectrum of compound VIII (10% w/v in  $\text{CCl}_4$ ) showed a sharp peak at 6.86  $\tau$  ( six protons ) typical of methoxyl absorption, a broad multiplet at 8.5  $\tau$ (eight protons) assigned to the cyclohexane ring protons, and a four-proton multiplet centered at 6.40 $\tau$  which is the  $A_2B_2$  absorption pattern of the protons in the dioxane ring. Again, the line positions in the  $A_2B_2$  pattern were determined from spectra measured in deuteriochloroform. Analysis of this pattern by the Frequent IV and Laocoon II programs gave the results shown in Table 8. Again, it is seen that  $J_A = 12$  and  $J_B = 1$  c.p.s., a result which is consistent only with a trans configuration for the methoxyl groups.

Table 8 shows that the values of the coupling constants in II, IV, V and VII, VIII do not differ much. The maximum deviation in all the cases are within 0.2 c.p.s. The small differences might be due to solvent effects or differences in the strain of the rings. One would have expected that the coupling constants in II, IV and V might have shown more pronounced differences. That this is not the case is indicative that at room temperature there is equal population of the interconverting chairs in the three cases and that other factors like differences in the ring strains or anisotropies of the part of the molecule not directly involved in the  $A_2B_2$  system have very little effect on the coupling constants (115).

5. Study of the non-equivalence of  $J_{AX}$  and  $J_{BX}$  in 2-(2,2,2-trifluoroethoxy)-tetrahydropyran.

In connection with another problem, R.R. Fraser and P. Hanbury (116) prepared the tetrahydropyranyl ether of 2,2,2-trifluoroethanol (IX). The proton magnetic resonance spectrum



IX

of this compound exhibited a surprising and unique feature. From the analysis of the  $ABX_3$  pattern produced by the trifluoroethyl group, it was found that the vicinal proton-fluorine coupling constants  $J_{AX}$  and  $J_{BX}$  were not equal. The parameters are shown in Table 9. The spectrum was also taken in several solvents and at different temperatures. In all the cases  $J_{AX} \neq J_{BX}$ . It was also apparent that the variation in coupling constants with changes in solvent or temperature was quite small.

Table 9. Coupling constants and chemical shifts in compounds with the  $ABX_3$  absorption pattern.

	$J_{AB}$	$J_{BX}$	$J_{AB}$	$\nu\delta_{AB}$	$J_A J_B$
2,2,2-Trifluoroethyl-2-tetrahydropyranyl ether (IX) (a)	9.13	8.77	-12.53	8.84	.36
2,2,2-trifluoroethyl-2-tetrahydrofuranyl ether (X)	9.32	8.86	-12.54	7.16	.46
2,2,2-trifluoroethyl-2-tetrahydrothiapyranyl ether (XI)	9.24	8.67	-12.25	21.00	.57

(a) P. Hanbury, M.Sc. Thesis, University of Ottawa, Ottawa, Canada, 1967.

The authors then examined the spectrum of the tetrahydropyranyl ether of ethanol to see if the vicinal proton-proton coupling constants in the ethyl group of this compound would also be non-equivalent. The ethyl group gives rise to an  $ABC_3$  spectrum. Unfortunately, the analysis of such a pattern is too complex to allow the detection of asymmetry of the same magnitude as observed in IX. The two vicinal coupling constants were then determined from the deuterium irradiated spectra of the racemic mixture of the tetrahydropyranyl ether of  $\alpha$ -deuterioethanol. The values of the two coupling constants  $J_{CH_3-CH}$  in this case were 7.18 and 7.19 c.p.s.

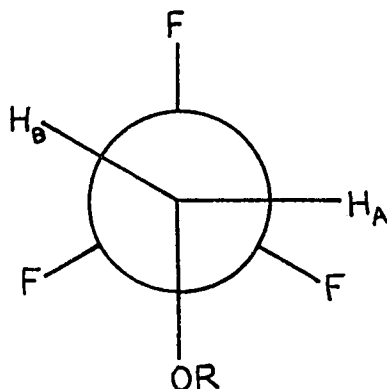
Thus it appears that vicinal proton-fluorine coupling constants are more sensitive than vicinal proton-proton coupling constants to variation in bonding as has been illustrated by different authors (117-120). Although it might also be that the greater electronegativity of the  $\text{CF}_3$  group over the  $\text{CH}_3$  group may be responsible for the appearance of non-equivalent coupling constants in the trifluoroethanol derivative only.

The magnetic non-equivalence observed in the case of IX belong to the type where both chemical shifts and coupling constants are involved. However, in this case the non-equivalence cannot be explained as readily as in the examples discussed in the introduction since there is no rigid structure; in this case there is free rotation of the trifluoroethyl group. This type of non-equivalence is without precedence. It cannot be explained on the basis of the simple Karplus relationship and some other explanation must be sought.

It is well known a fact that the coupling between nuclei occurs primarily through the bonding electrons, but there is some evidence that coupling between protons and fluorine nuclei sometimes occurs through space (121-122). The examples reported are when the H and F nuclei are separated by five bonds and in this way it is possible for the atoms to lie close to one another by way of a six-membered ring.

Vicinal H-F coupling constants have also been shown to be strongly dependent upon the dihedral angle  $\phi$  (120, 123, 124), but in this case the  $\text{CF}_3$  group is rotating rapidly on the n.m.r. time scale. This rapid rotation averages out the environment around each fluorine atom, making all fluorine atoms equivalent in the chemical shift sense. The only structural feature that could account for the non-equivalent couplings would be some non-equivalence between the  $\text{C-H}_A$  and  $\text{C-H}_B$  bonds.

This difference could be a result of different dihedral angles between  $\text{H}_A$  and the three fluorines compared with those between  $\text{H}_B$  and the three fluorines as shown in the Newman projection formula.



Alternatively, differences in the bond lengths, H-C-C bond angles, or bond hybridizations, all of which can affect the coupling constant, could be responsible for the non-equivalent coupling. Differences in bond length in  $\text{ClF}_3$  gives rise to a spectrum with two different chemical shifts for the fluorine atoms (125).

The reasons for the difference between the  $\text{C-H}_A$  and  $\text{C-H}_B$  bonds in IX could arise from an interaction between the oxygen in the ring and  $\text{H}_A$  and  $\text{H}_B$ . In Fig. 19, the most favorable conformation for IX is shown.

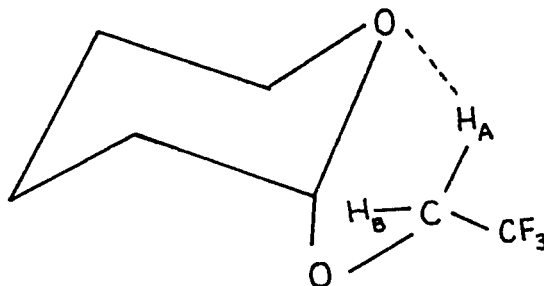


Figure 19. The most favorable conformation of 2(2,2,2-trifluoroethoxy)-tetrahydropyran.

The  $\text{CF}_3\text{CHO}$  group has the axial position because of the anomeric effect (126). The narrow half band width of the signal for the anomeric proton at  $\tau$  5.2. is direct evidence for the axial  $\text{CF}_3\text{CH}_2\text{O}$ - group. The remaining bonds in this group are assumed to occupy the staggered conformation in which the bulkiest substituents are trans to one another. In this conformation one of the methylene protons is quite close to the oxygen atom of the ring. It may be that there is some  $\text{O}\cdots\text{H}_A$  interaction which leads to a change in the  $\text{C-H}_A$  bond, thus making the  $\text{C-H}_A$  and  $\text{C-H}_B$  bonds non-equivalent. It is interesting to note that this  $\text{O}\cdots\text{H}$  interaction is also an important factor in producing the anomeric effect.

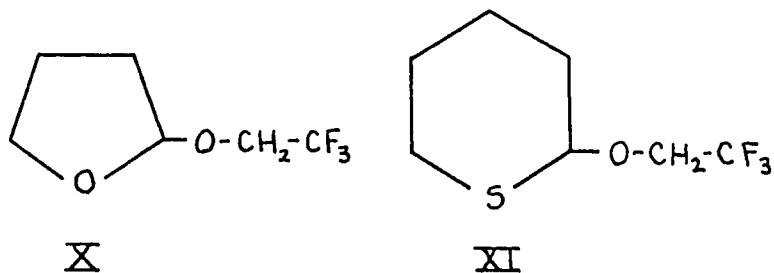
It was hoped that temperature dependent studies would confirm the above rationalizations in that they require a decrease in non-equivalent coupling constants with increasing temperature. A brief study of temperature dependence of  $J_{AX}$  and  $J_{BX}$  was conducted on compound IX (Table 10), but no change in coupling constants could be detected beyond the experimental error. If the differences in coupling constants could be increased by a change in structure then such a test could be conducted.

Table 10. N.M.R. Parameters of 2(2,2,2-trifluoroethoxy)-  
Tetrahydropyran. Variation with temperature.

Solvent	T(°C)	$J_{H_A-F}$ (cps)	$J_{H_B-F}$ (cps)	J(cps)*	$\% \delta_{AB}$ (cps)
CDCl <sub>3</sub>	-38	9.07	8.77	0.30	9.8
	28	9.13	8.77	0.36	8.8
CH <sub>2</sub> Cl <sub>2</sub>	-43	9.35	8.63	0.72	10.1
	-28	9.21	8.87	0.34	10.1
	28	9.14	8.89	0.25	9.1
	60	9.01	8.77	0.24	9.0
	98	9.12	8.76	0.36	8.5
Benzene	28	9.15	8.92	0.23	15.0
Acetone	28	9.33	9.12	0.21	6.6

\* All data in this table is accurate to within 0.1 c.p.s. except for the spectral measurements at -43° in CH<sub>2</sub>Cl<sub>2</sub>, where the accuracy is only 0.3 c.p.s. due to line broadening.

In an attempt to obtain evidence bearing upon the above speculations the structurally related compounds X and XI were prepared.



The n.m.r. spectra of X and XI, measured in deuterochloroform are reproduced in Fig. 20 and 21. The complex absorption pattern centered at  $\tau$  6.17 and  $\tau$  6.10 respectively represents the methylene protons of the trifluoroethyl groups. The patterns consist of 16 lines and are the AB part of an  $\text{ABX}_3$  spectrum. This portion of the spectra are reproduced on an enlarged scale in Figures 22a and 23a. In X the signals for the two protons on the 6 carbon atom of the tetrahydrofuran ring also appear in the same region as the AB pattern, but these signals are very broad and do not interfere significantly with the sharper 16 line pattern.

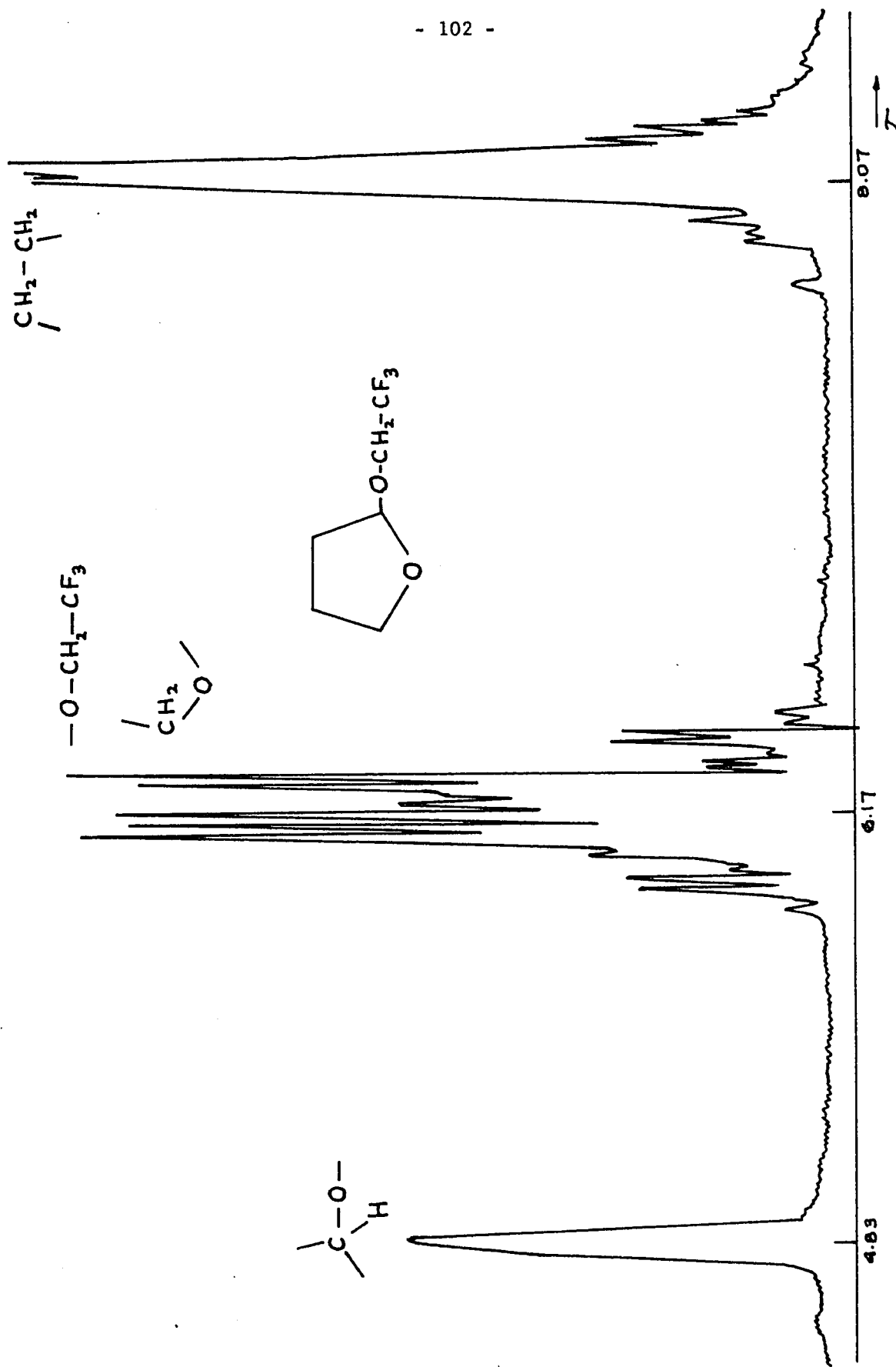


Figure 20. The n.m.r. spectrum of 2,2,2-trifluoroethyl-2-tetrahydrofuranylether (X).

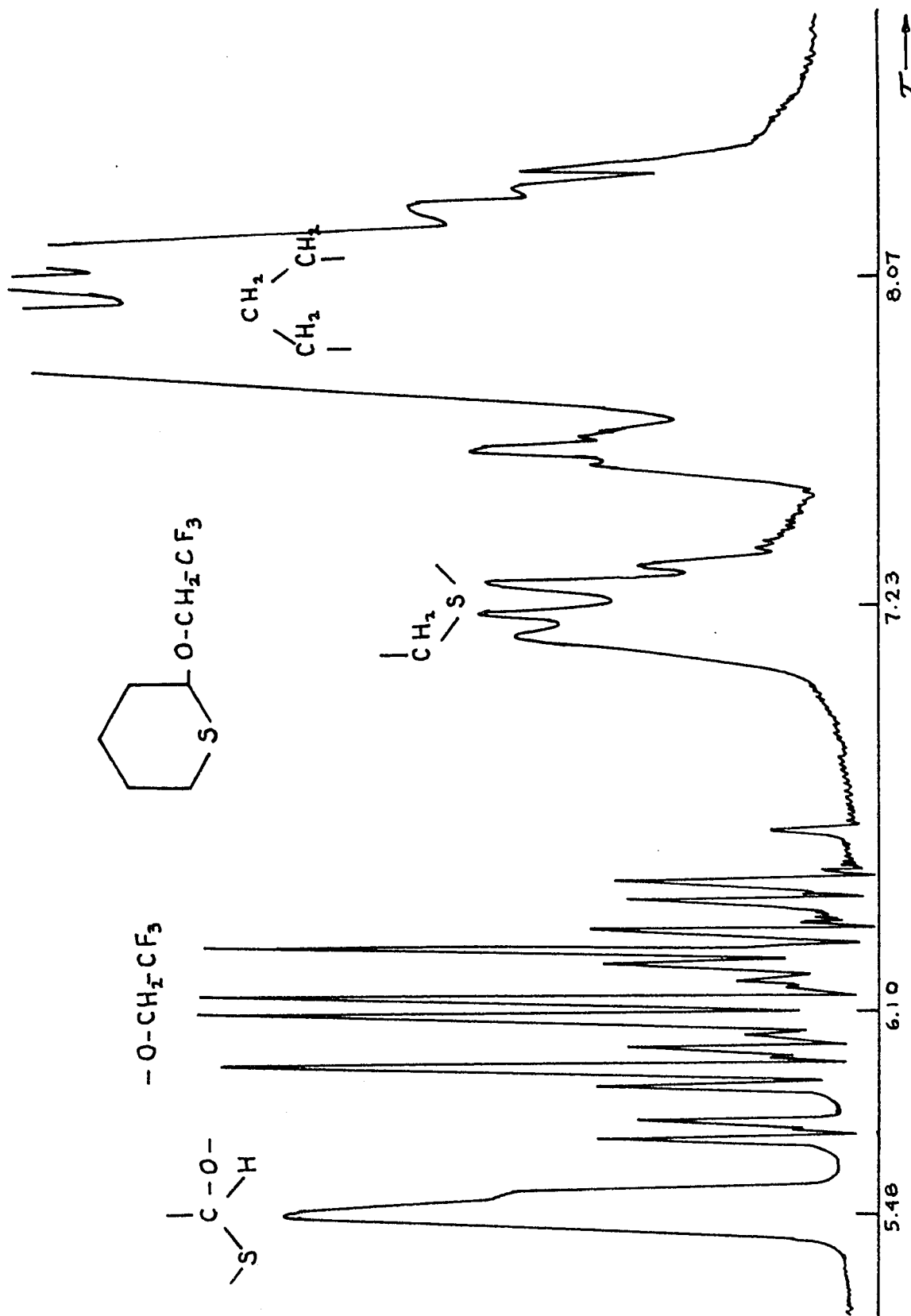


Figure 21. N.m.r. spectrum of 2,2,2-trifluoroethyl-2-tetrahydrothiopyranylether.

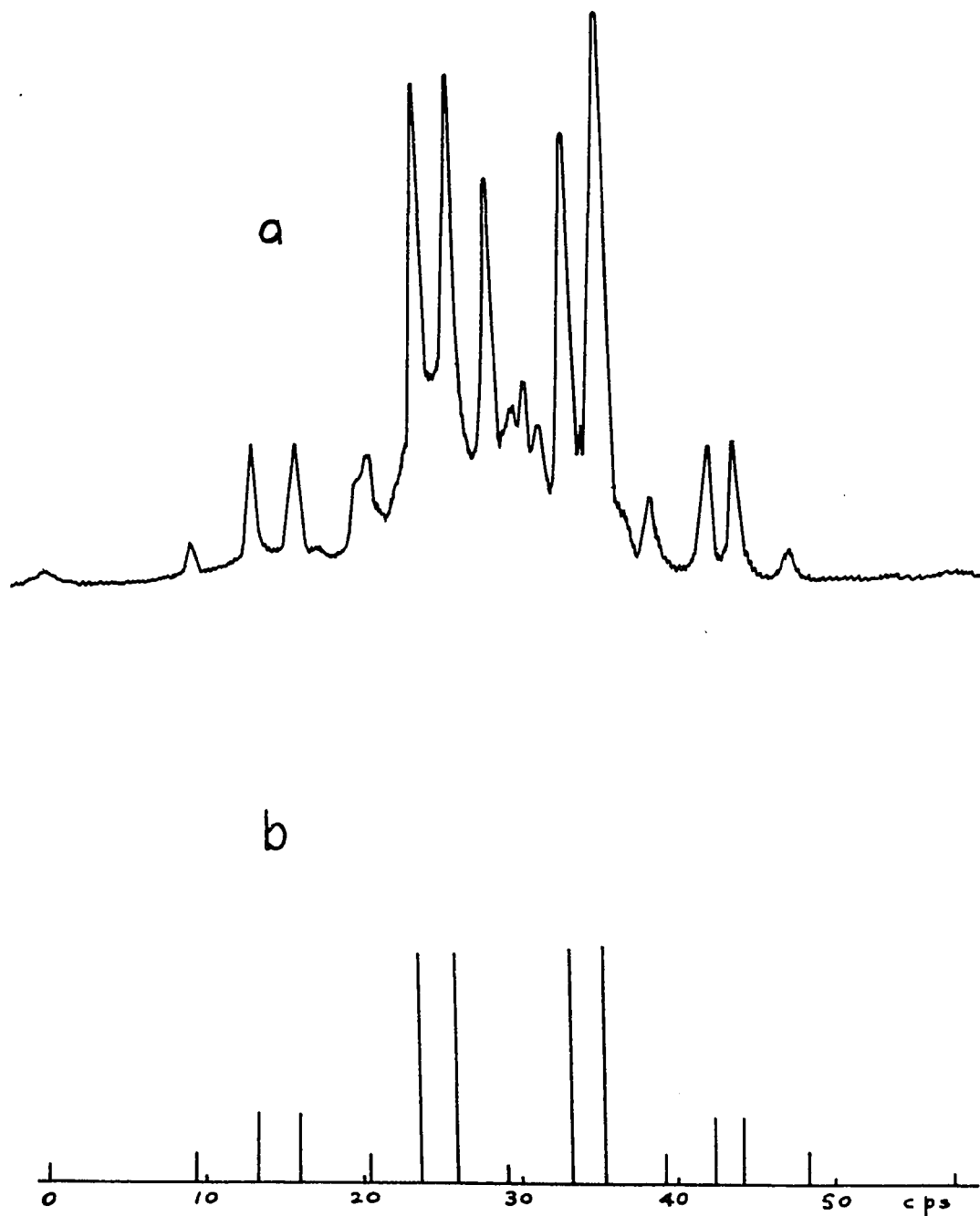


Figure 22. N.m.r. spectrum of the diastereomeric methylene protons in 2,2,2-trifluoroethyl-2-tetrahydrofuranylether (a) experimental (b) calculated.

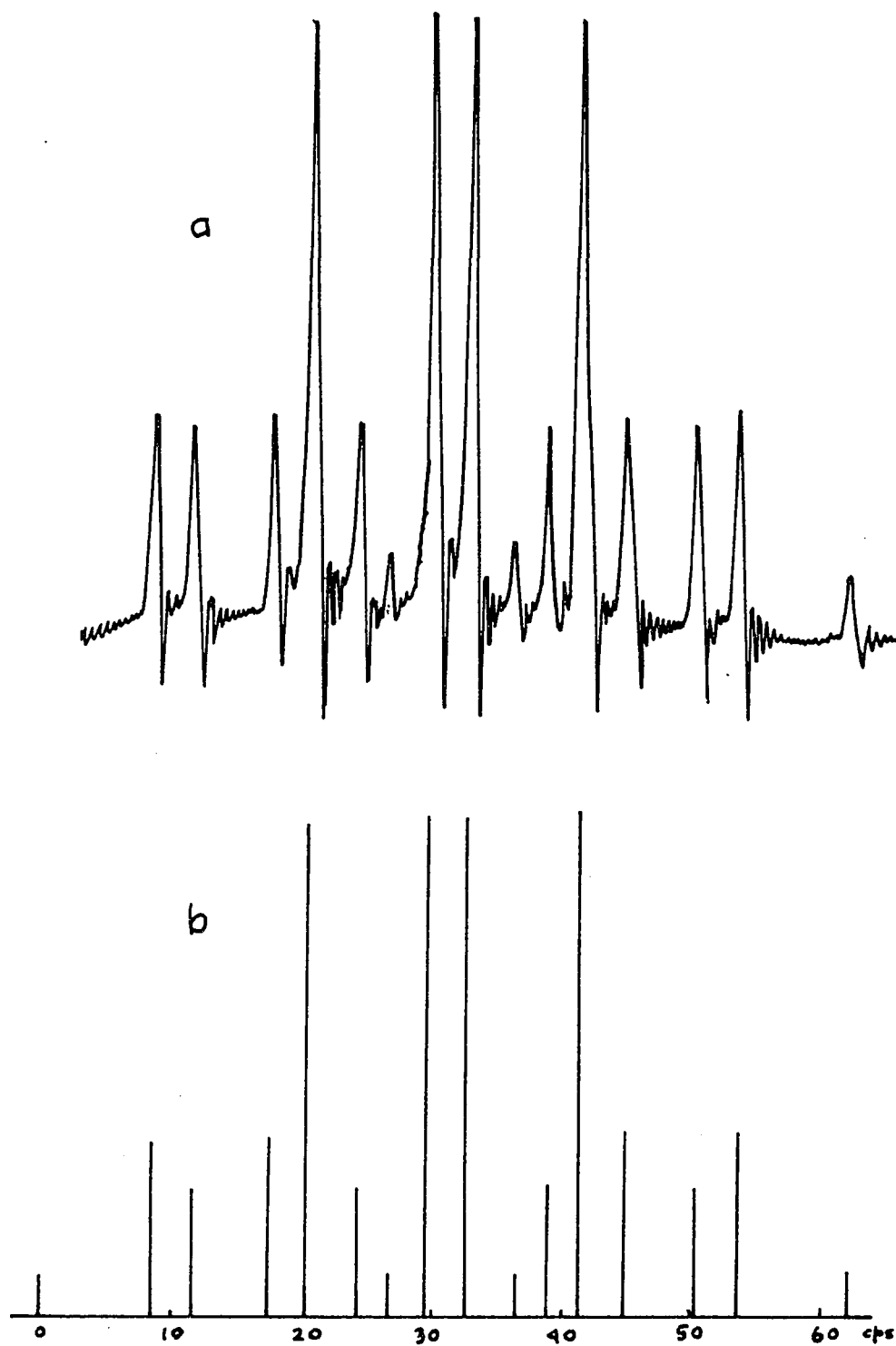


Figure 23. N.m.r. spectrum of the diastereomeric methylene protons in 2,2,2-trifluoroethyl-2-tetrahydrothiapyranylether (XI) (a) experimental (b) calculated.

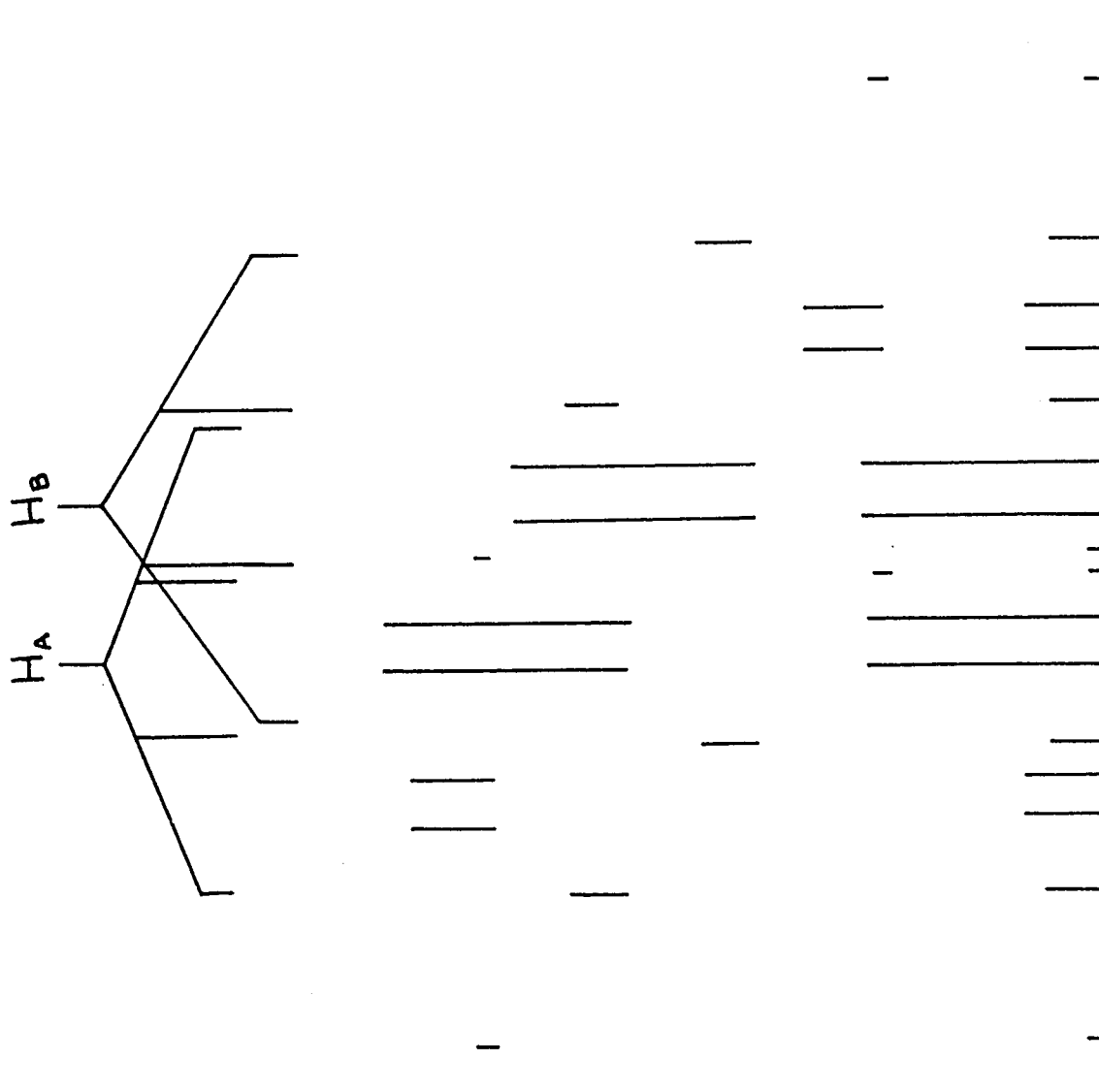


Figure 24. Example of the splittings resulting from coupling of an AB<sub>3</sub> grouping.

In XI the corresponding signals for the ring protons appear at  $\tau$  5.38; away from the AB pattern. As in the case of X the analysis of the  $ABX_3$  patterns showed that the vicinal fluorine-proton coupling constants  $J_{AX}$  and  $J_{BX}$  had different magnitudes. The analysis of the sixteen line pattern was carried out according to the method of Pople and Shaefer (15). Fig. 24 illustrates the splitting of the signal for protons A and B of the methylene group, caused by coupling of these protons with the fluorines of the trifluoromethyl group. Both the A and B proton signals are split into a quartet by the three fluorine nuclei. The spacings between the lines of quartet A and quartet B are equal to  $J_{AX}$  and  $J_{BX}$  respectively. The first line of the A quartet and the first line of the B quartet are then split into an AB quartet because of the coupling between the A and B protons. Three other quartets result in the same way from splitting of the second line of the A quartet and the second line of the B quartet, and so for the third and fourth lines.  $J_{AX}$  and  $J_{BX}$  can then be calculated from the analysis of the four observed quartets. Non-equivalence of  $J_{AX}$  and  $J_{BX}$  is reflected in the observed spectrum by a gradual decrease in the magnitude of the spacing between the two inner lines of each quartet, going in the upfield direction.

The parameters obtained from the analysis of compounds X and XI are shown in Table 9 along with the results for compound IX.

The  $ABX_3$  analysis cannot provide information about the relative signs of  $J_{AX}$  and  $J_{AB}$ . It does show that  $J_{AX}$  and  $J_{BX}$  have the same signs. The latter two are assigned a positive sign on the basis of similar examples in the literature (127). The parameters quoted in Table 9 were then used to calculate a theoretical pattern of the  $ABX_3$  splittings. The results are shown in Figures 22b and 23b. The theoretical line positions agreed to within 0.2 c.p.s. with the corresponding experimental ones.

From the small variations in coupling constants that appear in the trifluoroethyl ethers no firm conclusion can be drawn regarding the reasons for the difference in vicinal coupling constants nor is the difference large enough to allow information to be obtained from further variable temperature studies. One would have expected that if hydrogen bonding is one of the determining factors in the difference between  $J_{AX}$  and  $J_{BX}$  then a larger difference in these coupling constants along with a larger difference in the geminal coupling constant  $J_{AB}$  would have been shown in compounds X and XI. The reasons for that would have been a neighbouring diamagnetic anisotropic effect (128) and or a difference in the angle that the sulfur or oxygen non bonding molecular orbitals form with the  $H_A-H_B$  plane (129).

6. Effects of substituents on the chemical shift of benzylic protons.

In this part of the work, the chemical shifts of the methylene protons in a series of benzyl phenyl sulfides, sulfoxides and sulfones were measured. These series had different substituents in the para position of the benzyl ring and the effect of these substituents on the chemical shifts of the methylene protons was examined.

All the spectra were taken at low concentrations (0.1-0.3 M) to avoid any intermolecular effect. As an example, the n.m.r. spectrum of para-nitro benzyl phenyl sulfoxide is shown in Fig. 25. The other benzyl phenyl sulfoxides in the series have basically the same type of spectrum.  $J_{AB}$  was measured directly from the AB quartet which in the spectrum in Fig. 25 is centered at  $\tau$  5.92. The sulfides and sulfones showed only a singlet for this group.

The  $\rho$  values obtained from the plot of the Hammett  $\sigma$  constants vs. the  $\tau$  values for the methylene protons appear in Table 11. In the same Table appear also data obtained by Dr. Fraser for other series. These are included to allow the reader to assess the overall picture of this relationship.

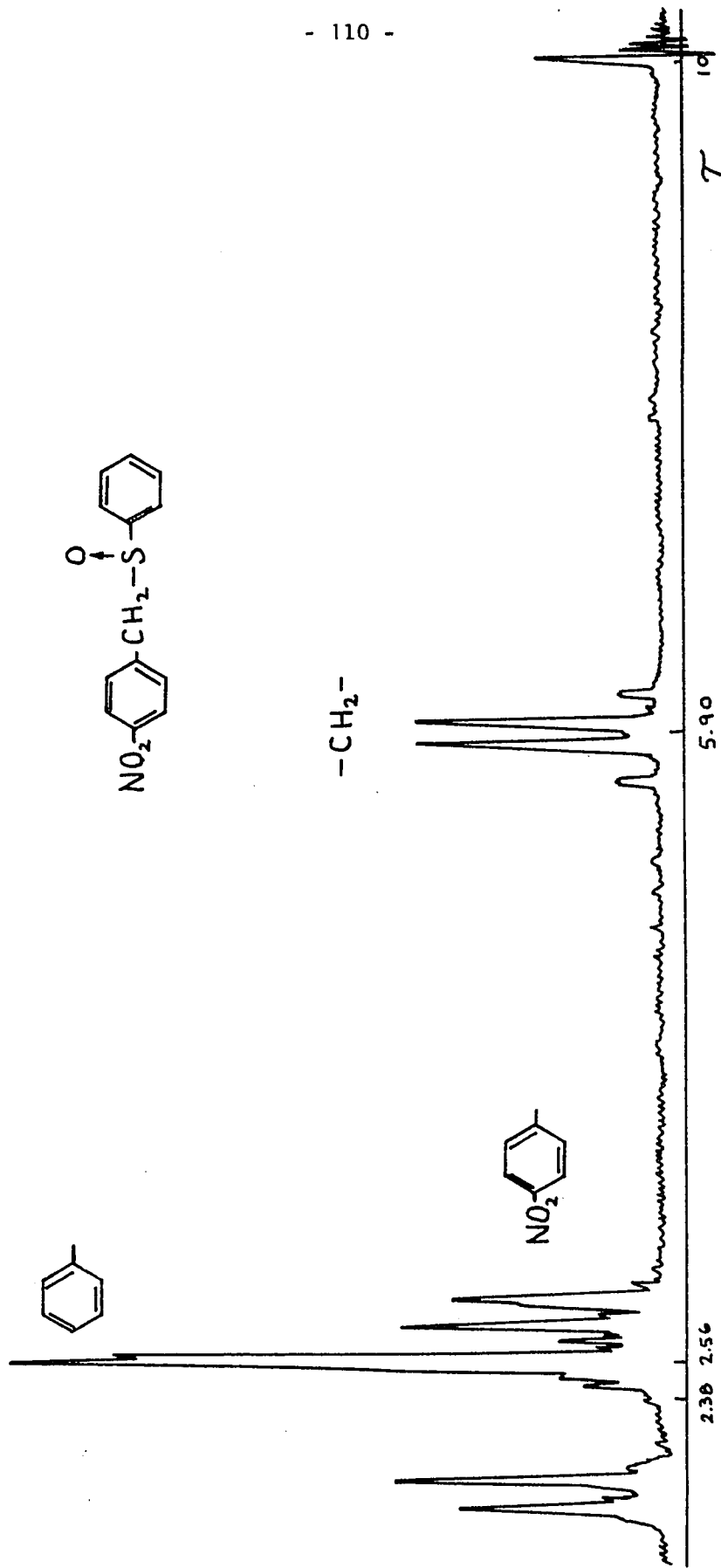
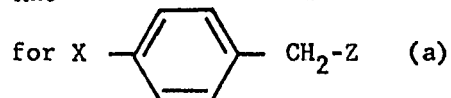


Figure 25. N.m.r. spectrum of p-nitrobenzyl phenyl sulfoxide.

The chemical shift assignments of the A and B protons in para-nitro-benzyl phenyl sulfoxide are reversed in the para-amino benzyl phenyl sulfoxide. That this was the case, was shown by the selective partial deuteration of the methylene group in the para-nitro sulfoxide and subsequent reduction with stannous chloride in 0.3 M hydrochloric acid to the partially deuterated para-amino sulfoxide (130). Several other methods and conditions were tried for the above reduction. When more concentrated hydrochloric acid was employed the sulfoxide group was also reduced to the sulfide. When calcium chloride and zinc dust was used, only para-amino benzyl phenyl sulfide was obtained (131). The method using zinc dust and acetic acid yielded a mixture of reduction products from which the desired material could not be isolated (132.)

Fig. 26 shows the n.m.r. spectrum of the partially deuterated para-nitro-benzyl phenyl sulfoxide and its reduction product, the para-amino derivative. In the figure is also included the deuterium irradiated spectra for the two compounds.

Table 11. Rho values of substituent chemical shift-Hammett plots



Z	$-\rho$	Van der Waal's radius	Electro-negativity	Standard error(b)	N(c)
H	0.20	1.2	2.1	1.0	8
CN	0.20	-	2.5	0.6	7
CH <sub>3</sub>	0.22	-	2.5	0.9	7
COOH	0.19	-	2.5	0.8	4
OH	0.21	1.4	3.5	1.7	6
OCH <sub>3</sub>	0.15	1.4	3.5	1.4	6
OTHP	0.16; 0.15	1.4	3.5	1.1	8
Cl	0.11	1.8	3.0	0.8	5
SCH <sub>3</sub>	0.10	1.85	2.5	0.8	4
SC <sub>6</sub> H <sub>5</sub>	0.08	1.85	2.5	1.4	5
SOCH <sub>3</sub>	0.10; 0.14	1.85	2.5	1.3	5
SOC <sub>6</sub> H <sub>5</sub>	0.00; 0.20	1.85	2.5	1.4	5
SO <sub>2</sub> CH <sub>3</sub>	0.16	1.85	2.5	0.9	5
SO <sub>2</sub> C <sub>6</sub> H <sub>5</sub>	0.16	1.85	2.5	1.4	5
Br	0.02	1.95	2.8	1.0	5

(a) Reference 133.

(b) The standard error of estimate is given in units of c.p.s.

(c) N represents the number of compounds studied in each series.

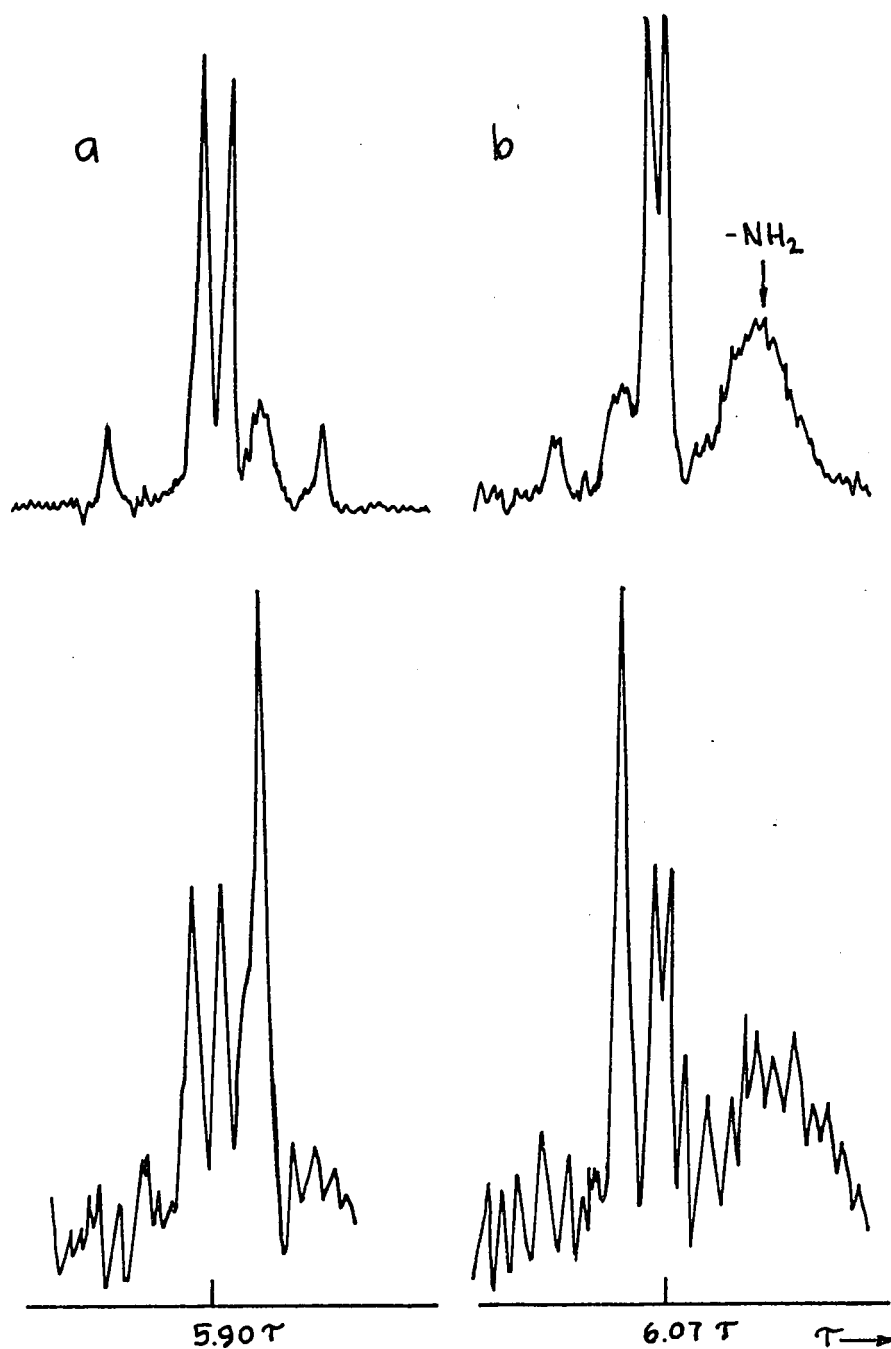


Figure 26. a) Non-irradiated and irradiated n.m.r. spectra of the methylene group in the partially deuterated p-nitrobenzyl phenyl sulfoxide.

b) Non-irradiated and irradiated n.m.r. spectra of the methylene group in the partially deuterated p-aminobenzyl phenyl sulfoxide.

The spectrum for the partially deuterated para-nitro compound shows a broad peak on the high field side of the methylene quartet. This broad peak corresponds to the hydrogen signal of the stereoselectively mono-deuterated compound and is broadened by coupling to the deuterium atom. (The spectra are a mixture of undeuterated and mono-deuterated compounds). In the spectrum of the deuterated para-amino compound this broad signal appears on the low field side of the quartet. In order to see better this shift of the broad signal the sample was irradiated at the resonance frequency of deuterium; in this way the H-D coupling is eliminated and the hydrogen signal appears now as a sharper peak.

In Fig. 27 the Hammett plots of  $\sigma$  constants vs.  $\tau$  values are shown for the sulfoxide series. This plot is typical of the degree of correlation found in all series. In each series the point for chlorine deviates the most and lies above the best straight line by 1-3 c.p.s. In all the series the slope of the best straight line,  $\rho$ , is negative.

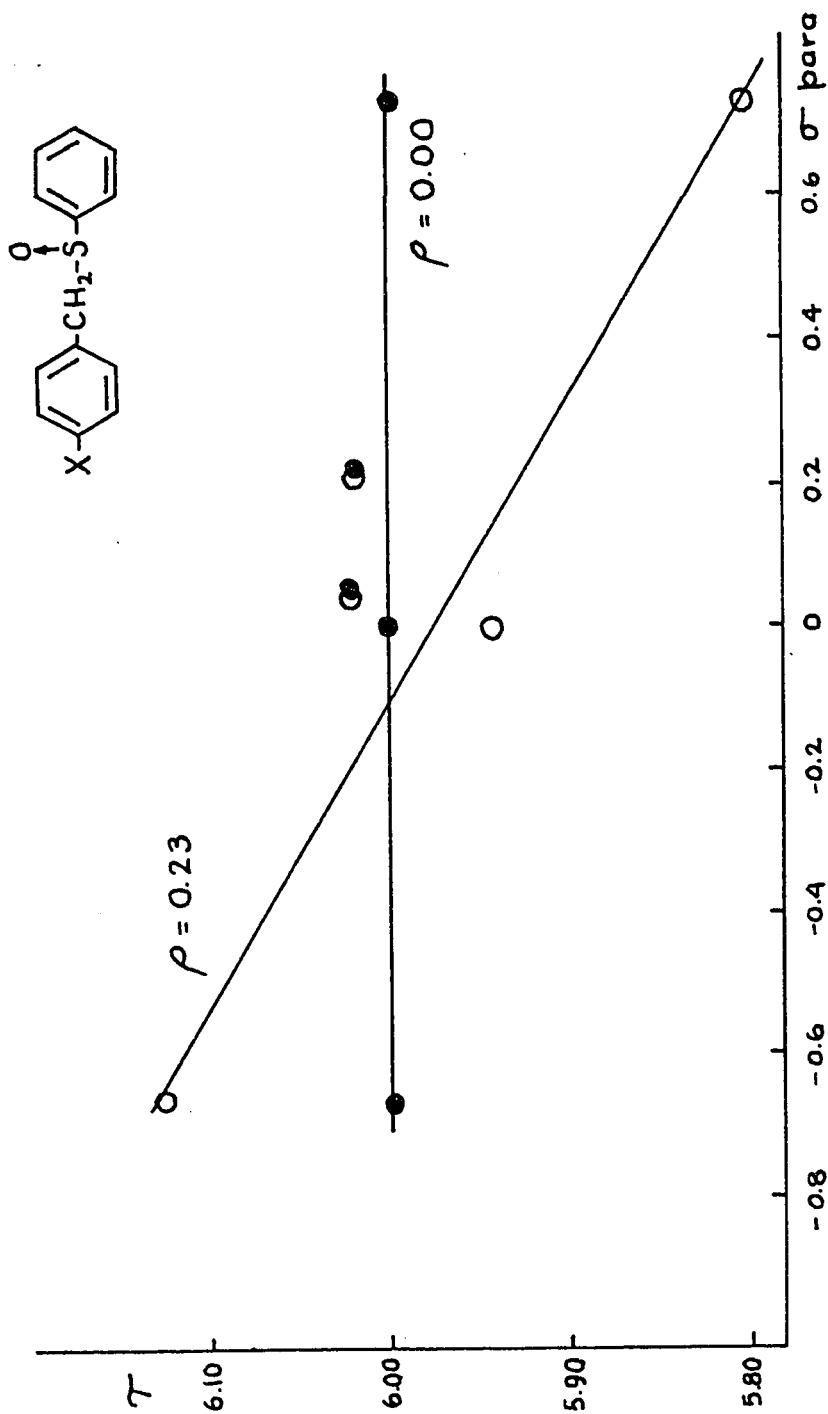
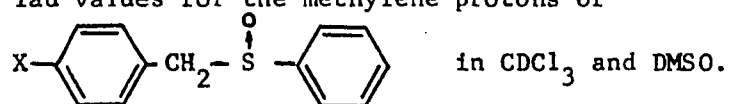


Figure 27. A. Hammett plot of the benzylic proton shifts of para-substituted benzyl phenyl sulfoxides.

The compounds included in Table 11 have the general formula  $X-C_6H_5-CH_2-Z$ . It can be seen that  $\rho$  varies widely (0.22 to 0.00) as the nature of Z is altered. If we accept the premise that any para substituent affects only the  $\pi$  electron distribution of the benzene ring, then the variation in  $\rho$  must be due to the variation in Z. The most important properties of Z which change from series to series, electronegativity and size, are also listed in Table 11. Consider the electronegativity of the atom attached to the methylene group. There is no relation between the electronegativity of this atom and the changes in  $\rho$ . But there is a reasonable parallel between  $\rho$  and the size of Z; the sulfones being the only exception. This indicates that  $\rho$  depends to a large extent on the conformation of the methylene group with respect to the benzene ring.

This conclusion is most strikingly supported by the data for the sulfoxides. When the spectra are run in deuterio-chloroform the value for the  $H_A$  proton is 0.23 and the value for the  $H_B$  proton is 0.00. This indicates that the  $H_B$  proton is not affected at all by the substituent. This could be more clearly seen from the values of the chemical shifts in Table 12. While the chemical shift of  $H_B$  remains almost constant, the chemical shift of  $H_A$  changes with the substituent.

Table 12. Tau values for the methylene protons of



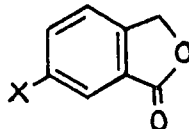
X	$\text{CDCl}_3$		DMSO	
	$\tau_A$	$\tau_B$	$\tau_A$	$\tau_B$
$\text{NH}_2$	6.12	5.99	5.99	6.11
Cl	6.02	6.02	5.70	5.92
F	6.02	6.02	5.72	5.94
H	5.94	6.00	5.75	5.93
$\text{NO}_2$	5.80	5.99	5.48	5.48

The most probable conformation for this sulfoxide has the bulky phenyl rings trans and the larger oxygen atom located further from the ortho position of the benzene ring than the electron pair. As a result, the diastereotropic protons are placed differently with respect to the plane of the adjacent benzene ring. If the substituent effect is largest when the C-H bond of a benzylic proton is perpendicular to the plane of the benzene ring and a minimal when parallel to it then, the difference in the  $\rho$  value for the two methylene protons could be explained (133.)

As a way to confirm this hypothesis, the spectra of para-nitro and para-amino benzyl phenyl sulfoxide were also taken at 90°. With an increase in temperature there will be a change in the population of the different conformers (considering that this temperature is sufficiently high to reduce the population of the most stable conformer) and consequently a change in the  $\rho$  value for the sulfoxides should be observed. The changes in  $\rho$  were from 0.23 to 0.20 and from 0.00 to 0.02 for H<sub>A</sub> and H<sub>B</sub> respectively from 29° to 90°.C. These results are in qualitative accord with expectations based on the consideration of a pair of conformational isomers.

When the chemical shifts for the same sulfoxide series are measured in dimethyl sulfoxide, the  $\rho$  values are 0.36 and 0.26 for the H<sub>A</sub> and H<sub>B</sub> protons respectively. It would not be likely that a change in conformation produced by a change in solvent would lead to such a difference in the  $\rho$  value in the two solvents. Probably the solvent also affects  $\rho$  by a specific interaction. Support for this idea is provided by the work of Mr. R. Renaud who examined the solvent effect on  $\rho$  in a rigid system. The results are shown in Table 13.

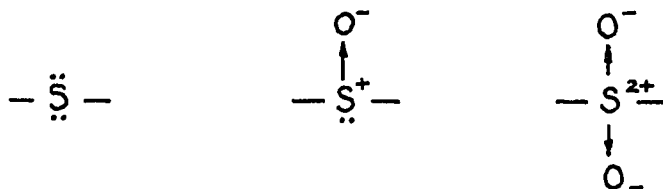
Table 13. Variation of the  $\rho$  value with the solvent of the methylene group in



Solvent	$\epsilon$	$\rho$
$\text{CDCl}_3$	0.18	5.1
$(\text{CH}_2\text{-Cl})_2$	0.18	10.5
Acetone	0.28	21.4
Acetonitrile	0.20	38.8
Dimethylsulfoxide	0.24	47.0

Specially in the case of sulfide, sulfoxide and sulfone, the electronegativity of the group rather than the electronegativity of only the sulfur atom should probably be considered. Taddei and Maccagnani have measured the electronegativity of the phenyl sulfide, phenyl sulfoxide and phenyl sulfone groups, following a method similar to Dailey and Schooley (60) based on chemical shift data. The electronegativity values, reported in the Mulliken's scale, are 8.45, 8.76, and 9.45 respectively (81). The values in the corresponding alkyl sulfide, sulfoxide and sulfone are 7.60, 8.42, and 9.14 respectively (79).

The more likely electron distribution in the three groups are:



The sulfoxide and sulfone groups have semipolar bonds in which the oxygen is bonded to sulfur by only a single pair of shared electrons, both having come from sulfur. Since this involves a net loss of an electron by sulfur and a net gain by oxygen, the ionic charges on the sulfur atom in the three groups is therefore different. This difference in positive charge on the sulfur atom could account for the differences in  $\rho$  in sulfide, sulfoxides and sulfones if we consider that the effect is transmitted by inductive effect through the sigma C-S bond. The electron density at the carbon atom in the methylene group would then be different in the three series. The same argument could be applied to the other series in Table 11.

In summary, it seems that besides the conformational preference in the series, the electronegativity of the Z group might have also some influence on  $\rho$  at least in the case of the sulfides, sulfoxides and sulfones and that perhaps some intermolecular effect can explain also the fact that only a small change in  $\rho$  was observed with a change in temperature in the sulfoxides and that the value of  $\rho$  differs widely in deuteriochloroform and dimethyl sulfoxide, also in the sulfoxide series.

CLAIMS FOR ORIGINAL WORK

1. The determination by n.m.r. spectroscopy of the configuration and conformation of the following compounds has been accomplished:
  - a) 2,3-dichloro-1,4-dioxane, m.p. 52°.
  - b) 2,3-diphenyl-1,4-dioxane, m.p. 132°.
  - c) Naphthodioxane.
  - d) 4a,8a-Dimethoxy-4a,8a-dihydro-1,4-benzodioxan.
  - e) 4a,8a-Dimethoxy-4a,5,6,7,8,8a-hexa-hydro-1,4-benzodioxane.
  
2. The synthesis and analysis of the ABX<sub>3</sub> portion in the n.m.r. spectra of: 2,2,2-trifluoroethyl-2-tetrahydrofuranlyl ether and 2,2,2-trifluoroethyl-2-tetrahydrothiapyranlyl ether has been carried out.
  
3. The effect of the substituent on the chemical shift of the methylene group in para-substituted benzylphenyl sulfides, sulfoxides and sulfones was determined. Good linear correlations were found between these shifts and the Hammett  $\sigma$  constants of the substituents. The variation in the  $\rho$  value going from one series to another was attributed to a variation in conformation around the bond between the benzene ring and the methylene group.
  
4. The synthesis of para-aminobenzyl phenyl sulfoxide was accomplished.

BIBLIOGRAPHY

1. J.A. Pople, W.G. Schneider, and H.J. Bernstein, "High Resolution Nuclear Magnetic Resonance", McGraw-Hill Book Co., New York, 1959.
2. P.L. Corio, "Structure of High-Resolution N.M.R. Spectra", Academic Press, New York, 1966.
3. J.W. Emsley, J. Feeney, and L.H. Sutcliffe, "High Resolution Nuclear Magnetic Resonance Spectroscopy", Pergamon Press, 1965, Vol. I.
4. H.J. Bernstein, J.A. Pople and W.G. Schneider, Can. J. Chem., 35, 65 (1957).
5. P. Diehl and J.A. Pople, Molecular Physics, 3, 557 (1960).
6. B. Dischler, Angew Chemie, Int. Ed., 5, 623 (1966).
7. D.M. Grant, R.C. Hirst and H.S. Gutowsky, J. Chem. Phys. 38, 470 (1963).
8. R.C. Hirst and D.M. Grant, J. Chem. Phys., 40, 1909 (1964).
9. P.L. Corio, Chem. Revs., 60, 363 (1960).
10. B. Dischler and Englert, Z. Naturforsch., 16a, 1180 (1961).
11. R.W. Fessenden and J.S. Waugh, J. Chem. Phys., 30, 944 (1959).
12. L. Cohen and N. Sheppard, Proc. Roy. Soc., 252A, 488 (1959).
13. F.S. Mortimer, J. Mol. Spectrosc., 3, 335 (1959).
14. H.S. Gutowsky, C.H. Holm, A. Saika, G.A. Williams, J. Am. Chem. Soc., 79, 4596 (1957).
15. J.A. Pople and T. Schaefer., Mol. Phys., 3, 547 (1960).
16. E.C. Eliel, "Stereochemistry of Carbon Compounds", McGraw-Hill, New York, 1962.
17. N.C. Franklin and H. Feltkamp, Angew Chemie, Int. Ed. 4, 774 (1965).

18. M. Karplus, J. Chem. Phys., 30, 11 (1959).
19. M. Karplus, J. Am. Chem. Soc., 85, 2870 (1963).
20. T. Schaefer, Can. J. Chem., 40, 1 (1962).
21. C.N. Banwell and N. Sheppard, Discuss. Faraday Soc., 39, 118 (1962).
22. K.L. Williamson, J. Am. Chem. Soc., 85, 516 (1963).
23. P. Laszlo and P. von R. Schleyer, J. Am. Chem. Soc., 85, 2709 (1963).
24. O.L. Chapman, J. Am. Chem. Soc., 85, 2014 (1963).
25. G.V. Smith and H. Kriloff, J. Am. Chem. Soc., 85, 2016 (1963).
26. P. Lagzlo and P. von R. Schleyer, J. Am. Chem. Soc., 85, 2017 (1963).
27. F.A.L. Anet, J. Am. Chem. Soc., 84, 1053 (1962).
28. D.H. Williams and N.S. Bhacca, J. Am. Chem. Soc., 86, 2742 (1964).
29. J. Delman, C. Barbier, J. Chem. Phys., 41, 1103 (1964).
30. H. Feltkamp, N.C. Franklin, M. Hanack and K.W. Heinz, Tetrahedron Letters, 1964, 3535.
31. H. Feltkamp and N.C. Franklin, Tetrahedron, 21; 1541 (1965).
32. H. Booth, Tetrahedron Letters, 1965, 441.
33. D. Jung, Chem. Ber., 99, 566 (1966).
34. C. Altona and C. Romers, Acta Cryst., 16, 1225 (1963).
35. P.R. Schaefer, D.R. Davis, M. Vogel, K. Nagaran and J.D. Roberts, Proc. Natl. Acad. Sc. U.S., 47, 49 (1961).
36. H.S. Finegold, Proc. Chem. Soc., 1960, 283.

37. T.D. Coyle and F.G.A. Stone, J. Am. Chem. Soc., 83, 4138 (1961).
38. K. Mislow, A.L. Ternay and J.T. Melillo; J. Am. Chem. Soc., 85, 2329 (1963).
39. D.R. Davis and J.D. Roberts, J. Am. Chem. Soc., 84, 2252 (1962).
40. D.R. Davis, R.P. Lutz and J.D. Roberts, J. Am. Chem. Soc., 83, 246 (1961).
41. H.S. Gutowsky, J. Chem. Phys., 37, 2196 (1962).
42. M. Raban, Tetrahedron Letters, 1966, 3105.
43. G.M. Whitesides, J.J. Grocki, D. Holtz, H. Steinberg, and J.D. Roberts, J. Am. Chem. Soc., 87, 1058 (1965).
44. M.S. Newman, "Steric Effects in Organic Chemistry". M.S. Newman, Ed. John Wiley and Sons Inc., New York. 1956. Chap. 4.
45. E.I. Snyder, J. Am. Chem. Soc., 85, 2624 (1963).
46. R.O. Kan, J. Am. Chem. Soc., 86, 5180 (1964).
47. S.H. Marcus, W.F. Reynolds and S.J. Miller, J. Org. Chem., 31, 1872 (1966).
48. M.J.S. Dewar and A.P. Marchand, J. Am. Chem. Soc., 88, 3318 (1966).
49. A. Wittstruck and E.N. Trachtenberg, J. Am. Chem. Soc., 89, 3803 (1967).
50. J.R. Cavanaugh and B.P. Dailey, J. Chem. Phys., 34, 1099 (1961).
51. A.D. Buckingham, Can. J. Chem., 38, 300 (1960).
52. J.I. Musher, J. Chem. Phys., 37, 34 (1962).
53. H.M. McConnell, J. Chem. Phys., 27, 226 (1957).
54. T. Shaefer, W.F. Reynolds, and T. Yonemoto, Can. J. Chem., 41, 2969 (1963).
55. R.R. Fraser, Can. J. Chem., 38, 2226 (1960).

56. W.G. Paterson and N.R. Tipman, *Can. J. Chem.*, 40, 2122 (1962).
57. C.D. Cook and S.S. Danyluk, *Tetrahedron*, 19, 177 (1963).
58. J.N. Shoorley, *J. Chem. Phys.*, 21, 1899 (1953).
59. L.H. Meyer, A. Saika and H.S. Gutowsky, *J. Am. Chem. Soc.*, 75, 4567 (1953).
60. B.P. Dailey and J.N. Schoolery, *J. Am. Chem. Soc.*, 77, 3977 (1955).
61. H. Spiesecke and W.G. Schneider, *J. Chem. Phys.*, 35, 731 (1961).
62. P.L. Corio and B.P. Dailey, *J. Am. Chem. Soc.*, 78, 3043 (1956).
63. A.A. Bothner-By and R.E. Glick, *J. Am. Chem. Soc.*, 78, 1071 (1956).
64. L.M. Jackman, "Applications of Nuclear Magnetic Resonance Spectroscopy in Organic Chemistry". Pergamon Press, New York. 1959. p. 58.
65. K.L. Williamson, N.C. Jacobus and K.T. Soucy, *J. Am. Chem. Soc.*, 86, 4021 (1964).
66. R.E. Klinck and J.B. Stothers, *Can. J. Chem.*, 40, 1071 (1962).
67. R.J. Ouellette, *Can. J. Chem.*, 43, 707 (1965).
68. C. Heathcock, *Can. J. Chem.*, 40, 1865 (1962).
69. Gurudata, J.B. Stothers, and J.D. Talman, *Can. J. Chem.*, 45, 731 (1967).
70. H. C. Longuet-Higgins, *J. Chem. Phys.*, 18, 283 (1950).
71. M.J.S. Dewar and D.P. Marchand, *J. Am. Chem. Soc.*, 88, 3318 (1966).
72. M.J.S. Dewar and Y. Talceuchi, *J. Am. Chem. Soc.*, 89, 390 (1967).
73. M.J.S. Dewar and Squires, *J. Am. Chem. Soc.*, 90, 210 (1968).
74. S.H. Marcus, W.F. Reynolds, and S.I. Miller, *J. Org. Chem.*, 31, 1872 (1966).
75. P.R. Wells, *Chem. Rev.*, 63, 171 (1963).

76. R.W. Taft, E. Price, I.R. Fox, J.C. Lewis, K.K. Anderson, and G.T. Davis, *J. Am. Chem. Soc.*, 85, 709, 3146 (1963).
77. W. Hofman, L. Stefaniak, T. Urbanski, and M. Witanowski, *J. Am. Chem. Soc.*, 86, 554 (1964).
78. J.R. Van Wazer, and D. Grant, *J. Am. Chem. Soc.*, 86, 1450 (1964).
79. F. Taddei, *Boll. Sc. Fac. Chim. Jud. Bologna*, 23, 273 (1965).
80. P. Biscarini, F. Taddei, C. Zauli, *Boll. Sci. Fac. Chim. Ind. Bologna*, 21, 169 (1963).
81. G. Maccagnani and F. Taddei, *Boll. Sci. Fac. Chim. Ind. Bologna*, 23, 381 (1965).
82. F. Kaplan and J.D. Roberts, *J. Am. Chem. Soc.*, 83, 4668 (1961).
83. M. Oki, H. Iwamura, *Bull. Chem. Soc., Japan*, 35, 1428 (1962).
84. M. Nishio and T. Ito, *Chem. Pharm. Bull. (Japan)*, 13, 1392 (1965).
85. M. Nishio, *Chem. Pharm. Bull. (Japan)*, 15, 1669 (1967).
86. H. Hamlow, S. Okuda, N. Nakagawa, *Tetrahedron Letters*, 1964, 2553.
87. R.K. Summerbell and D.R. Berger, *J. Am. Chem. Soc.*, 81, 637 (1959).
88. W. Stumpf, *Z. Electrochem.*, 57, 690 (1953).
89. R.K. Summerbell and H.E. Lunk, *J. Am. Chem. Soc.*, 79, 4802 (1957).
90. N.L. Weinberg, Ph.D. Thesis, University of Ottawa, Canada, 1963.
91. R. Paul, M. Fluchaire and G. Collardeau, *Bull. Soc. Chim. France*, 1950, 668.
92. *Org. Synthesis, Coll. Vol. 4*, 892 (1956).
93. R.F. Naylor, *J. Chem. Soc.*, 1947, 1106.
94. D.S. Tarbell and C. Weaver, *J. Am. Chem. Soc.*, 63, 2939 (1941).
95. W.E. Parham, L. Christensen, S.H. Groen and R.M. Dodson, *J. Org. Chem.*, 29, 2211 (1964).

96. P.T.S. Lau and G.F. Grillot, J. Org. Chem., 28, 2765 (1963).
97. J.E. Pollak and G.F. Grillot, J. Org. Chem., 32, 3105 (1967).
98. F.A.L. Anet, J. Am. Chem. Soc., 86, 458 (1964).
99. R.R. Umhoefer, Ph.D. Dissertations, Northwestern University, 1948.
100. G.R. Lappin, Ph.D. Dissertations, Northwestern University, 1946.
101. C. Altona, C. Romers and E. Havinga, Tetrahedron Letters, 10, 16 (1959).
102. E. Caspi, Th. A. Wittstruck and D.M. Piatak, J. Org. Chem., 27, 3183 (1962).
103. C.Y. Chen and R.J.W. Le Fèvre, J. Chem. Soc., 1965, 558.
104. R.J. Abraham, J. Chem. Soc., 1965, 256.
105. C. Barbier, J. Delman and J. Rauf, Tetrahedron Letters, 45, 3339 (1964).
106. Varian Nuclear Magnetic Resonance Spectra Catalog. 1962. p. 45.
107. N. Sheppard and J. Turner, Proc. Roy. Soc. London, 252A, 206 (1961).
108. R.R. Fraser and C. Reyes-Zamora, Can. J. Chem., 43, 3445 (1965).
109. R. Christ and R.K. Summerbell, J. Am. Chem. Soc., 55, 4547 (1933).
110. R.R. Fraser and C. Reyes-Zamora, Can. J. Chem. 45, 1012 (1967).
111. R.K. Summerbell, B.S. Sokolski, J.P. Bays, D.J. Godfrey and A.S. Hussey, J. Org. Chem., 1967, 946.
112. J. Boeslenc, F. Tellegen and P.C. Henriguez, Rec. Trav. Chim., 54, 733 (1935).
113. S. Furberg and O. Hassel, Acta Chem. Scand., 10, 136 (1956).
114. B. Belleau and N.L. Weinberg, J. Am. Chem. Soc., 85, 2525 (1963).

115. R.R. Fraser and C. Reyes-Zamora, *Can. J. Chem.*, 45, 929 (1967).
116. R.R. Fraser and P. Hanbury, *Can. J. Chem.*, 45, 1485 (1967).
117. S.L. Manatt, *J. Am. Chem. Soc.*, 88, 1323 (1966).
118. W.H. Pirkle, *J. Am. Chem. Soc.*, 88, 1837 (1966).
119. J.T. Gerig and J.D. Roberts, *J. Am. Chem. Soc.*, 88, 2791 (1966).
120. K.L. Williamson, V.F. Li, F.H. Hall and S. Swager, *J. Am. Chem. Soc.*, 88, 5678 (1966).
121. A.A. Bothner-By. "Advances in Magnetic Resonance". Ed. J.S. Waugh. Academic Press, New York - 1965.
122. P.C. Myhre, J.W. Edmonds and J.D. Krueger, *J. Am. Chem. Soc.*, 88, 2459 (1966).
123. J. Abraham, L. Lavallo and K.G.R. Pachler, *Mol. Phys.*, 11, 471 (1966).
124. A. Peake and L.F. Thomas, *Trans. Faraday Soc.*, 62, 2980 (1966).
125. D.F. Smith, *J. Chem. Phys.*, 21, 609 (1953).
126. R.U. Lemieux. "Rearrangements and Isomerizations in Carbohydrate Chemistry" in *Molecular Rearrangements*. P. de Mayo Ed. Interscience Publishers Inc., New York. 1964. p. 726, 735.
127. E.L. Machor and C. McLean, *J. Chem. Phys.*, 44, 64 (1966).
128. H. Spieseke and J.N. Schneider, *J. Chem. Phys.*, 35, 722 (1961).
129. Y. Allingham, R.C. Cookson, T.A. Crabb, *Tetrahedron*, 24, 1989 (1968).
130. R.K. Brown, R.G. Christiansen, and R.B. Sandin, *J. Am. Chem. Soc.*, 70, 1748 (1948).
131. J.R. Sampey and E.E. Reid, *J. Am. Chem. Soc.*, 69, 712 (1947).
132. *Org. Synthesis*, Coll. Vol. 3, 73 (1955).
133. R.R. Fraser, Gurudata, C. Reyes-Zamora, and R.B. Swingle, *Can. J. Chem.*, 46, 1595 (1968).
134. E. Altma, E. Havinga *Tetrahedron* 22 2275 (1966).